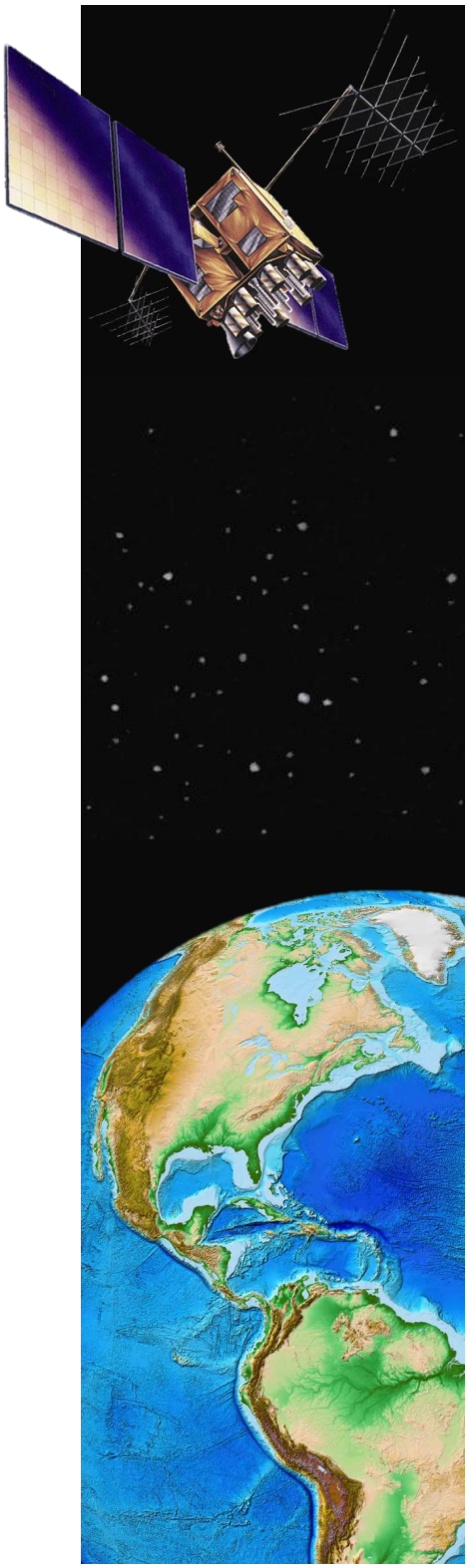

An Analysis of Global Positioning System (GPS) Standard Positioning Service Performance for 2019

May 14, 2020

Space and Geophysics Laboratory
Applied Research Laboratories
The University of Texas at Austin
P.O. Box 8029
Austin, TX 78713-8029

Brent A. Renfro,
Miquela Stein,
Emery B. Reed,
James Morales,
Eduardo J. Villalba

Contract: NAVSEA Contract N00024-17-D-6421
Task Order: 5101192
Technical Report: TR-SGL-20-02

This Page Added for Document Spacing

Executive Summary

Applied Research Laboratories, The University of Texas at Austin (ARL:UT) examined the performance of the Global Positioning System (GPS) throughout 2019 for the U.S. Space Force Space and Missile Systems Center PNT Mission Integration office (ZAC-PNT). This report is based upon work supported by ZAC-PNT through Naval Sea Systems Command Contract N00024-17-D-6421, task order 5101192, "GPS Data Collection and Performance Analysis."

Performance is defined by the 2008 Standard Positioning Service (SPS) Performance Standard (SPS PS) [1]. The performance standard provides the U.S. government's assertions regarding the expected performance of GPS. This report does not address all of the assertions in the performance standards. This report covers those assertions which can be verified by anyone with knowledge of standard GPS data analysis practices, familiarity with the relevant signal specification, and access to a GPS data archive.

The assertions evaluated include those of accuracy, integrity, continuity, and availability of the GPS signal-in-space (SIS) along with the assertions on accuracy of positioning and time transfer. Chapter 1 is an introduction to the report. Chapter 2 contains a tabular summary of the results for each assertions. Chapter 3 presents details on the analysis associated with each assertion. Chapter 4 details additional findings of the performance analysis.

All the SPS PS assertions examined in this report were met in 2019.

Contents

List of Figures

List of Tables

Chapter 1

Introduction

Applied Research Laboratories, The University of Texas at Austin (ARL:UT)[1] examined the performance of the Global Positioning System (GPS) throughout 2019 for the U.S. Space Force Space and Missile Systems Center PNT Mission Integration office (ZAC-PNT). This report is based upon work supported by ZAC-PNT through Naval Sea Systems Command Contract N00024-17-D-6421, task order 5101192, "GPS Data Collection and Performance Analysis."

Performance is assessed relative to selected assertions in the 2008 Standard Positioning Service (SPS) Performance Standard (SPS PS) [1]. (Hereafter the term SPS PS, or SPSPS08, is used when referring to the 2008 SPS PS.) Chapter 2 contains a tabular summary of performance stated in terms of the metrics provided in the performance standard. Chapter 3 presents a more detailed explanation of the analysis conducted in evaluating each assertion. The assertions are presented in the order of appearance in the performance standards. Chapter 4 details additional findings of the performance analysis.

The performance standards define the services delivered through the L1 C/A-code signal. The metrics are limited to the signal-in-space (SIS) and do not address atmospheric errors, receiver errors, or errors due to the user environment (e.g. multipath errors, terrain masking, and foliage). This report addresses assertions in the SPS PS that can be verified by anyone with knowledge of standard GPS data analysis practices, familiarity with the relevant signal specification [2], and access to a GPS data archive (such as that available via the International Global Navigation Satellite System (GNSS) Service (IGS)) [3]. The assertions examined include those related to coverage, accuracy, continuity, availability, and position domain standards.

[1] *A complete list of abbreviations found in this document is provided in Appendix G.*

The majority of the assertions related to user range error (URE) values are evaluated by comparison of the space vehicle (SV) clock and position representations as computed from the broadcast GPS legacy navigation (LNAV) message data against the SV truth clock and position data as provided by a precise orbit calculated after the time of interest. The URE process requires both broadcast clock and position data (BCP) and truth clock and position data (TCP). The process by which the URE values are calculated is described in Appendix B. The orbit information in the GPS LNAV message are referenced to the GPS L1/L2 P(Y)-code antenna phase center. As a result, the derived URE values represent those experienced by a dual-frequency user. These are scaled to SPS-equivalent values by a process described in Appendix F.

Observation data from tracking stations were used to cross-check the URE values and to evaluate non-URE assertions. Examples of the latter application include the areas of Continuity (Section 3.4), Availability (Section 3.5), and Position/Time Availability (Section 3.6). In these cases, data from two networks are used. The two networks considered were the National Geospatial-Intelligence Agency (NGA) Monitor Station Network (MSN) [4] and a subset of the tracking stations that contribute to the IGS. The geographic distribution of these stations is shown in Figure 1.1. The selection of these sets of stations ensure continuous simultaneous observation of all space vehicles by multiple stations. The assertions focus on SIS performance, which is not directly observable from ground tracking locations. To mitigate this problem, this performance review uses ionospherically-corrected dual-frequency observation data as opposed to L1 C/A-only observations.

Navigation message data used in this report were collected from the NGA MSN. The collection and selection of navigation message data are described in general terms in Appendix B.2.

Several metrics in the performance standards are stated in terms of either the Baseline 24 constellation, which consists of six orbital planes and four slots per plane, or the Expandable 24 constellation, in which three of the 24 slots may be occupied by two SVs. Currently, there are more than 32 GPS SVs on-orbit. Of the SVs on-orbit, 27 are located in the Expandable 24 constellation. The SVs in excess of those located in defined slots are assigned to locations in various planes in accordance with operational considerations.

The majority of the metrics in this report are evaluated on either a per-SV basis or for the full constellation. The metrics associated with continuity and availability are defined with respect to the slot definitions.

Each of the GPS SVs are identified by pseudo-random noise ID (PRN) and by space vehicle number (SVN). PRN IDs are assigned to SVs for periods of time. A given SV may be assigned different PRNs at different times during its operational life. The SVN represents the permanent unique identifier for the vehicle under discussion. As the number of active SVs has increased to nearly the total available, PRNs are now being used by multiple SVs within a given year (but by no more than one SV at a time). In general, we list the SVN first and the PRN second because the SVN is the unique identifier of the two. The SVN-to-PRN relationships were provided by the GPS Master

Control Station (MCS). Other useful summaries of this information may be found on the U.S. Coast Guard Navigation Center website [5] and the U.S. Naval Observatory (USNO) website [6]. See Appendix C for a summary of the SVN-to-PRN mapping for 2019.

The authors acknowledge and appreciate the effort of several ARL:UT staff members who reviewed these results. For 2019 this included Scott Sellers, Taben Malik, and David Rainwater.

Karl Kovach of The Aerospace Corporation provided valuable assistance in interpreting the SPSPS08 assertions. John Lavrakas of Advanced Research Corporation and P.J. Mendicki of The Aerospace Corporation have long been interested in GPS performance metrics and have provided valuable comments on the final draft. However, the results presented in this report are derived by ARL:UT, and any errors in this report are the responsibility of ARL:UT.

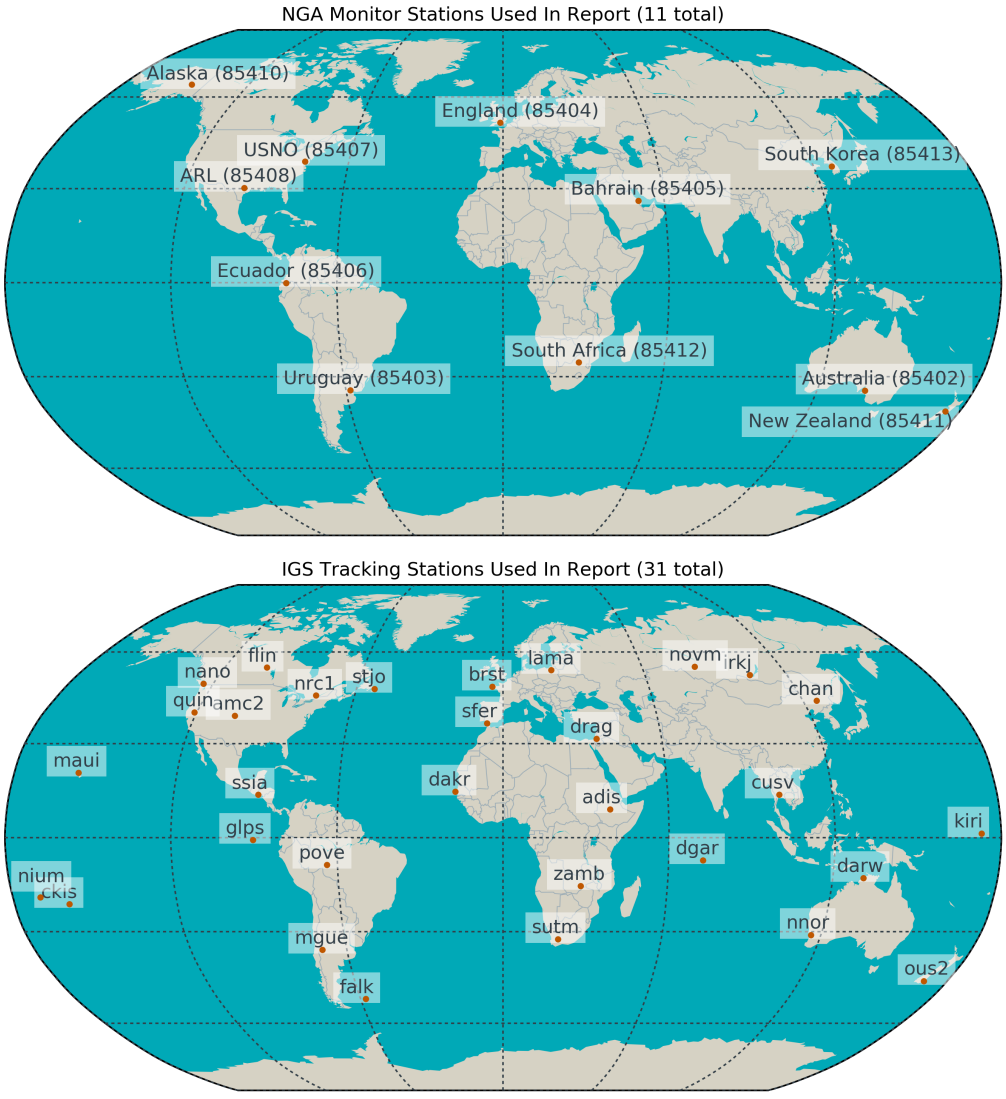

Figure 1.1: Maps of the Network of Stations Used in this Report

Chapter 2

Summary of Results

Table 2.1 provides a summary of the assertions defined in the performance standards. The table is annotated to show which assertions are evaluated in this report and the status of each assertion.

Of the assertions evaluated, all were met in 2019.

Details regarding each result may be found in Chapter 3. All abbreviations used in Table 2.1 may be found in Appendix G.

Table 2.1: Summary of SPS PS Metrics Examined for 2019

SPSPS08 Section	**SPS PS Assertion**	**2019 Status**	**Report Section**
3.3.1 SIS Per-Satellite Coverage	100% Coverage of Terrestrial Service Volume	not eval.	3.1.1
3.3.2 SIS Constellation Coverage	100% Coverage of Terrestrial Service Volume	✔	3.1.2
3.4.1 SIS URE Accuracy	$\leq$ 7.8 m 95% Global average URE during normal operations over all AODs	✔	3.2.1
	$\leq$ 12.8 m 95% Global average URE during normal operations at any AOD	✔	3.2.2
	$\leq$ 6.0 m 95% Global average URE during normal operations at zero AOD	✔	3.2.3
	$\leq$ 30 m 99.94% Global average URE during normal operations	✔	3.2.4
	$\leq$ 30 m 99.79% Worst case single point average URE during normal operations	✔	
	$\leq$ 388 m 95% Global average URE after 14 days without upload	not eval.	3.2.5
3.4.2 SIS URRE Accuracy	$\leq$ 0.006 m/s 95% Global average at any AOD	✔	3.2.6
3.4.3 SIS URAE Accuracy	$\leq$ 0.002 m/s^2 95% Global average at any AOD	✔	3.2.7
3.4.4 SIS UTCOE Accuracy	$\leq$ 40 nsec 95% Global average at any AOD	✔	3.2.8
3.5.1 SIS Instantaneous URE Integrity	$\leq 1X10^{-5}$ Probability over any hour of exceeding the NTE tolerance without a timely alert	✔	3.3.1
3.5.4 SIS Instantaneous UTCOE Integrity	$\leq 1X10^{-5}$ Probability over any hour of exceeding the NTE tolerance without a timely alert	✔	3.3.2
3.6.1 SIS Continuity - Unscheduled Failure Interruptions	$\geq$ 0.9998 Probability over any hour of not losing the SPS SIS availability from the slot due to unscheduled interruption	✔	3.4.1
3.6.3 Status and Problem Reporting	Appropriate NANU issue at least 48 hours prior to a scheduled event	✔	3.4.2.1
3.7.1 SIS Per-Slot Availability	$\geq$ 0.957 Probability that (a.) a slot in the baseline 24-slot will be occupied by a satellite broadcasting a healthy SPS SIS, or (b.) a slot in the expanded configuration will be occupied by a pair of satellites each broadcasting a healthy SIS	✔	3.5.1
3.7.2 SIS Constellation Availability	$\geq$ 0.98 Probability that at least 21 slots out of the 24 slots will be occupied by a satellite (or pair of satellites for expanded slots) broadcasting a healthy SIS	✔	3.5.2
	$\geq$ 0.99999 Probability that at least 20 slots out of the 24 slots will be occupied by a satellite (or pair of satellites for expanded slots) broadcasting a healthy SIS	✔	
3.7.3 Operational Satellite Counts	$\geq$ 0.95 Probability that the constellation will have at least 24 operational satellites regardless of whether those operational satellites are located in slots or not	✔	3.5.3
3.8.1 PDOP Availability	$\geq$ 98% Global PDOP of 6 or less	✔	3.6.1.1
	$\geq$ 88% Worst site PDOP of 6 or less	✔	
3.8.2 Position Service Availability	$\geq$ 99% Horizontal, average location	✔	3.6.2
	$\geq$ 99% Vertical, average location	✔	
	$\geq$ 90% Horizontal, worst-case location	✔	
	$\geq$ 90% Vertical, worst-case location	✔	
3.8.3 Position/Time Service Accuracy	$\leq$ 9 m 95% Horizontal, global average	✔	3.6.3
	$\leq$ 15 m 95% Vertical, global average	✔	
	$\leq$ 17 m 95% Horizontal, worst site	✔	
	$\leq$ 37 m 95% Vertical, worst site	✔	
	$\leq$ 40 nsec time transfer error 95% of the time	✔	3.6.4

✔ Met

not eval. See report text for more information

Chapter 3

Discussion of Performance Standard Metrics and Results

While Chapter 2 summarizes the status of the SPSPS08 metrics for 2019, the statistics and trends reported in this chapter provide both additional information and support for those conclusions.

3.1 SIS Coverage

3.1.1 Per-Satellite Coverage

SIS per-satellite coverage is asserted in Section 3.3.1 of the SPSPS08. The following standard is provided (from Table 3.3-1).

- *"100% Coverage of Terrestrial Service Volume"*

This means that the direction of the Earth coverage beam of each GPS SV will be managed such that the beam will cover the Terrestrial Service volume visible to that SV providing at least the minimum required received power. This assertion is not evaluated at this time. Within the control segment, the operators have various tools to enable them to monitor and control SV pointing. Monitoring this assertion external to the control segment will require both SV-specific antenna gain pattern information and calibrated power observations. The potential for evaluation may be examined in future reports.

3.1.2 Constellation Coverage

SIS constellation coverage is asserted in Section 3.3.2 of the SPSPS08. The following standard is provided (from Table 3.3-2).

- *"100% Coverage of Terrestrial Service Volume"*

This assertion is interpreted to mean that a user will have at least four SVs transmitting a healthy or marginal signal visible at any moment. This is evaluated as part of the examination of DOP (see Section 3.6). The condition was true throughout 2019. As a result, the assertion is considered verified for 2019.

3.2 SIS Accuracy

SIS URE accuracy is asserted in Section 3.4 of the SPSPS08. The following standards (from Tables 3.4-1 through 3.4-4 in the SPS PS) are considered in this report:

- *"≤ 7.8 m 95% Global Average URE during Normal Operations over all AODs"*
- *"≤ 12.8 m 95% Global Average URE during Normal Operations at any AOD"*
- *"≤ 6.0 m 95% Global Average URE during Normal Operations at Zero AOD"*
- *"≤ 30 m 99.94% Global Average URE during Normal Operations"*
- *"≤ 30 m 99.79% Worst Case Single Point Average URE during Normal Operations"*
- *"≤ 388 m 95% Global Average URE after 14 days without upload"*
- *"≤ 0.006 m/s 95% Global Average URRE over any 3-second interval during Normal Operations at Any AOD"*
- *"≤ 0.002 m/s^2 95% Global Average URAE over any 3-second interval during Normal Operations at Any AOD"*
- *"≤ 40 nsec 95% Global Average UTCOE during Normal Operations at Any AOD"*

SIS accuracy values are only included in the statistics when the SV is healthy. Throughout this report, an SV is considered healthy based on the definition in SPS PS Section 2.3.2.

The URE statistics presented in this report are based on a comparison of the BCP against the TCP (see also Appendix B). This is a useful approach, but one that has specific limitations, the most significant being that the TCP may not capture the effect of individual discontinuities or large effects over short time scales (e.g. a frequency step or clock run-off). Nonetheless, this approach is appropriate given the 30 day period of averaging implemented in determining URE compared to brief (less than an hour) periods of the rare discontinuities. Briefly, this approach allows the computation of URE without direct reference to observations from any particular ground sites, though the TCP carries an implicit network dependency based on the set of ground stations used to derive the precise orbits from which the TCP is derived.

In the case of this report, the BCP and TCP are both referenced to the ionosphere-free linear combination of the L1/L2 P(Y)-code signal. As a result, the resulting URE values are best characterized as Precise Positioning Service (PPS) dual-frequency URE values. The SPS results are derived from the PPS dual-frequency results by a process described in Appendix F.

Throughout this section and the next, there are references to several distinct SIS URE expressions. Each of these SIS URE expressions means something slightly different. It is important to pay careful attention to the particular SIS URE expression being used in each case to avoid misinterpreting the associated URE numbers.

Appendix C of the SPSPS08 provides two algorithms for computing SIS URE: *Instantaneous SIS URE*, which express the URE at a given moment along a specific line of sight; and *root mean square (RMS) SIS URE*, which expresses URE on a statistical basis across the field of view of the SV at a given moment. When BCP and TCP are used to estimate range residual along a satellite-to-receiver line-of-sight vector at a given instant in time, the result is an "Instantaneous SIS URE". Some of the primary differences between instantaneous basis SIS UREs and statistical basis SIS UREs are given below.

Table 3.1: Characteristics of SIS URE Methods

Instantaneous Basis SIS URE	**Statistical Basis SIS URE**
Always algebraically signed (±) number	Never algebraically signed
Never a statistical qualifier	Always a statistical qualifier (RMS, 95%, etc.)
Specific to a particular time and place	Statistic over span of times, or places, or both
Next section (Section 3.3)	This section (Section 3.2)

Throughout this section, there are references to the "Instantaneous RMS SIS URE." This is a statistical basis SIS URE (note the "RMS" statistical qualifier), where the measurement quantity is the Instantaneous SIS URE, and the span of the statistic covers that one particular point ("instant") in time across a large range of spatial points. This is effectively the evaluation of the Instantaneous SIS URE across every spatial point in the area of the service volume visible to the SV at that particular instant in time. Put another way; consider the signal from a given SV at a given point in time. That signal intersects the surface of the Earth over an area, and at each point in that area there is a unique Instantaneous SIS URE value based on geometric relationship between the SV and the point of interest. In the name "Instantaneous RMS SIS URE," the "Instantaneous" means that no time averaging occurs. The "RMS" refers to taking the RMS of all the individual Instantaneous SIS URE values across the area visible to the SV for a single time. This concept is explained in SPSPS08 Section A.4.11, and the relevant equation is presented in Appendix B.1.2 of this report.

3.2.1 URE Over All AOD

The performance standard URE metric that is most closely related to a user's observations is the calculation of the 95th percentile Global Average URE over all ages of data (AODs). This is associated with the SPSPS08 Section 3.4 metric:

- *"$\leq$ 7.8 m 95% Global Average URE during Normal Operations over all AODs"*

This metric can be decomposed into several pieces to better understand the process, as follows:

- *7.8 m* - This is the limit against which to test.
- *95%* - This is the statistical measure applied to the data. In this case, there are a sufficiently large number of samples to allow direct sorting of the results across time and selection of the 95th percentile.
- *Global Average URE* - This is another term for the Instantaneous RMS SIS URE, a statistical quantity representing the average URE across the area of the service volume visible to the SV at a given point in time. The expression used to compute this quantity is provided in Appendix B.1.2.
- *during Normal Operations* - This is a constraint related to normal vs. extended mode operations. See IS-GPS-200 20.3.4.4 [2] and Section 4.4.
- *over all AODs* - This constraint means that the Global Average URE is considered at each evaluation time regardless of the AOD at the evaluation time. A more detailed explanation of the AOD and how this quantity is computed can be found in Section 4.2.

In addition, the following general statements in Section 3.4 of SPSPS08 have a bearing on this calculation:

- These statistics are "per SV" - that is, they apply to the signal from each satellite, not for averages across the constellation.
- *"The ergodic period contains the minimum number of samples such that the sample statistic is representative of the population statistic. Under a one-upload-per-day scenario, for example, the traditional approximation of the URE ergodic period is 30 days."* (SPSPS08 Section 3.4, Note 2)

The statistics are computed over monthly periods, not daily. Monthly periods approximate the suggested 30 day period while conforming to a familiar time scale and avoiding the complication that a year is not evenly divisible by 30. We have computed the monthly statistic regardless of the number of days of availability in each month but

have identified SV-months with fewer than 25 days of availability to note any SV-month with significantly less data than expected.

Table 3.2 contains the monthly 95th percentile values of the RMS SIS URE based on the assumptions and constraints described above. For each SV, the worst value across the year is marked in red. In all cases, no values exceed 7.8 m, and so this requirement is met for 2019.

Figure 3.1 provides a summary of these results for the entire constellation.

A number of points are evident from Table 3.2 and Figure 3.1:

1. All SVs meet the performance assertion of the SPSPS08, even when only the worst performing month is considered. Even the worst value for each SV (indicated by the upper extent of the range bars) is more than factor of 2 smaller than the threshold.
2. For most of the SVs, the value of the 95th percentile SIS URE metric is relatively stable over the course of the year, as indicated by relatively small range bars.
3. The "best" SVs are those which cluster at the 1.0 m level and whose range variation is small.
4. The values for SVN 65/PRN 24 and SVN 72/PRN 8 are noticeably different than the other Block IIF SVs. These are the only Block IIF SVs operating on a Cesium frequency standard.
5. There are no values for SVN 34/PRN 18 for November and December as the SV was decommissioned in October (see Table 3.9).

Table 3.2: Monthly 95th Percentile Values of SIS RMS URE for All SVs in Meters

SVN	PRN	Block	Jan	Feb	Mar	Apr	May	Jun	Jul	Aug	Sep	Oct	Nov	Dec	2019
34	18	IIA	1.64	1.96	2.24	2.05	1.68	1.75	1.49	1.92	1.87	2.06	–	–	1.89
41	14	IIR	1.07	1.57	1.23	1.08	1.00	1.06	1.02	1.06	0.97	1.03	1.10	0.93	1.07
43	13	IIR	1.54	1.40	1.21	1.30	1.38	1.38	1.16	1.15	1.19	1.35	1.29	1.20	1.27
44	28	IIR	2.38	2.38	2.48	2.22	2.42	2.41	2.27	2.36	2.00	2.08	2.44	2.24	2.33
45	21	IIR	1.09	1.03	1.00	0.99	1.00	1.08	1.20	0.98	0.93	1.02	1.01	1.03	1.02
46	11	IIR	1.09	1.34	1.16	1.11	1.04	1.24	1.35	1.08	1.02	1.08	1.11	1.19	1.16
47	22	IIR	0.96	0.99	0.92	0.95	0.89	0.97	0.97	0.98	0.93	0.92	0.92	0.94	0.95
48	7	IIR-M	1.19	1.22	1.22	1.15	1.19	1.27	1.27	1.25	1.25	1.20	1.21	1.20	1.22
50	5	IIR-M	0.94	0.97	0.94	0.93	0.97	0.99	1.00	0.99	1.08	0.95	0.91	0.92	0.97
51	20	IIR	0.97	1.09	0.94	0.96	1.00	0.94	0.99	1.00	0.93	0.93	0.97	0.93	0.97
52	31	IIR-M	1.22	1.31	1.19	1.15	1.13	1.17	1.25	1.26	1.16	1.11	1.21	1.27	1.20
53	17	IIR-M	2.05	1.71	1.72	1.62	1.92	1.31	1.77	1.77	1.49	1.68	1.65	1.97	1.72
55	15	IIR-M	0.91	0.93	0.94	0.93	0.91	0.91	0.92	0.89	0.99	0.92	0.90	1.02	0.94
56	16	IIR	0.94	0.96	1.02	0.94	0.94	0.94	0.95	0.93	0.92	0.95	0.93	0.92	0.94
57	29	IIR-M	1.21	1.54	1.14	1.38	1.41	1.38	1.56	1.32	1.31	1.64	1.16	1.47	1.36
58	12	IIR-M	0.95	0.93	0.92	0.94	0.93	0.95	0.99	0.92	0.95	0.90	0.93	0.93	0.94
59	19	IIR	0.95	0.95	1.01	0.95	0.94	1.01	0.93	0.95	0.96	0.94	0.90	0.93	0.95
60	23	IIR	0.96	1.01	0.97	0.93	1.01	0.94	0.98	0.92	0.95	1.00	0.98	0.96	0.97
61	2	IIR	1.10	1.05	1.07	1.03	1.06	1.02	1.07	0.98	0.98	0.98	0.97	1.01	1.03
62	25	IIF	1.08	1.00	1.01	1.02	1.09	1.23	1.16	0.99	1.01	1.08	1.03	1.11	1.07
63	1	IIF	1.07	1.00	0.95	0.94	1.06	1.05	1.06	1.06	1.10	1.14	1.15	1.18	1.09
64	30	IIF	1.06	0.91	0.94	1.01	1.04	1.10	0.99	0.92	1.02	1.00	0.98	1.02	1.00
65	24	IIF	2.59	2.26	2.51	2.49	2.75	2.54	2.68	2.43	2.61	2.74	2.61	2.61	2.58
66	27	IIF	0.96	0.95	0.96	0.99	1.03	1.00	1.03	1.01	1.07	0.98	1.02	1.00	1.00
67	6	IIF	0.97	0.96	1.05	0.94	1.05	1.05	1.12	0.98	1.08	1.03	1.14	1.26	1.07
68	9	IIF	0.99	0.92	1.09	1.05	0.94	0.92	1.05	0.91	1.01	0.93	0.92	0.93	0.97
69	3	IIF	1.10	1.22	1.25	1.27	0.95	1.12	1.18	1.25	1.24	1.09	1.03	1.11	1.16
70	32	IIF	0.92	0.97	1.02	0.97	0.89	0.88	0.93	0.93	0.99	1.02	0.99	0.93	0.96
71	26	IIF	1.10	1.09	1.01	1.02	1.05	1.11	1.19	1.25	0.98	0.92	1.02	1.04	1.08
72	8	IIF	2.07	1.92	2.32	2.45	2.06	2.23	2.28	2.35	2.36	2.29	2.35	2.06	2.26
73	10	IIF	0.99	1.04	0.96	0.92	0.91	0.95	1.04	1.09	1.00	0.91	0.97	0.99	0.98
Block IIA			1.64	1.96	2.24	2.05	1.68	1.75	1.49	1.92	1.87	2.06	–	–	1.89
Block IIR			1.22	1.28	1.18	1.14	1.17	1.16	1.21	1.16	1.11	1.16	1.16	1.19	1.18
Block IIF			1.50	1.31	1.40	1.38	1.44	1.44	1.52	1.53	1.45	1.33	1.42	1.40	1.43
All SVs			1.35	1.32	1.35	1.27	1.29	1.29	1.34	1.34	1.26	1.24	1.24	1.27	1.30

Notes: Values not present indicate that the satellite was unavailable during this period. Months during which an SV was available for less than 25 days are shown shaded. Months with the highest SIS RMS URE for a given SV are colored red. The column labeled "2019" is the 95th percentile over all the days in the year. The four rows at the bottom are the monthly 95th percentile values over various sets of SVs.

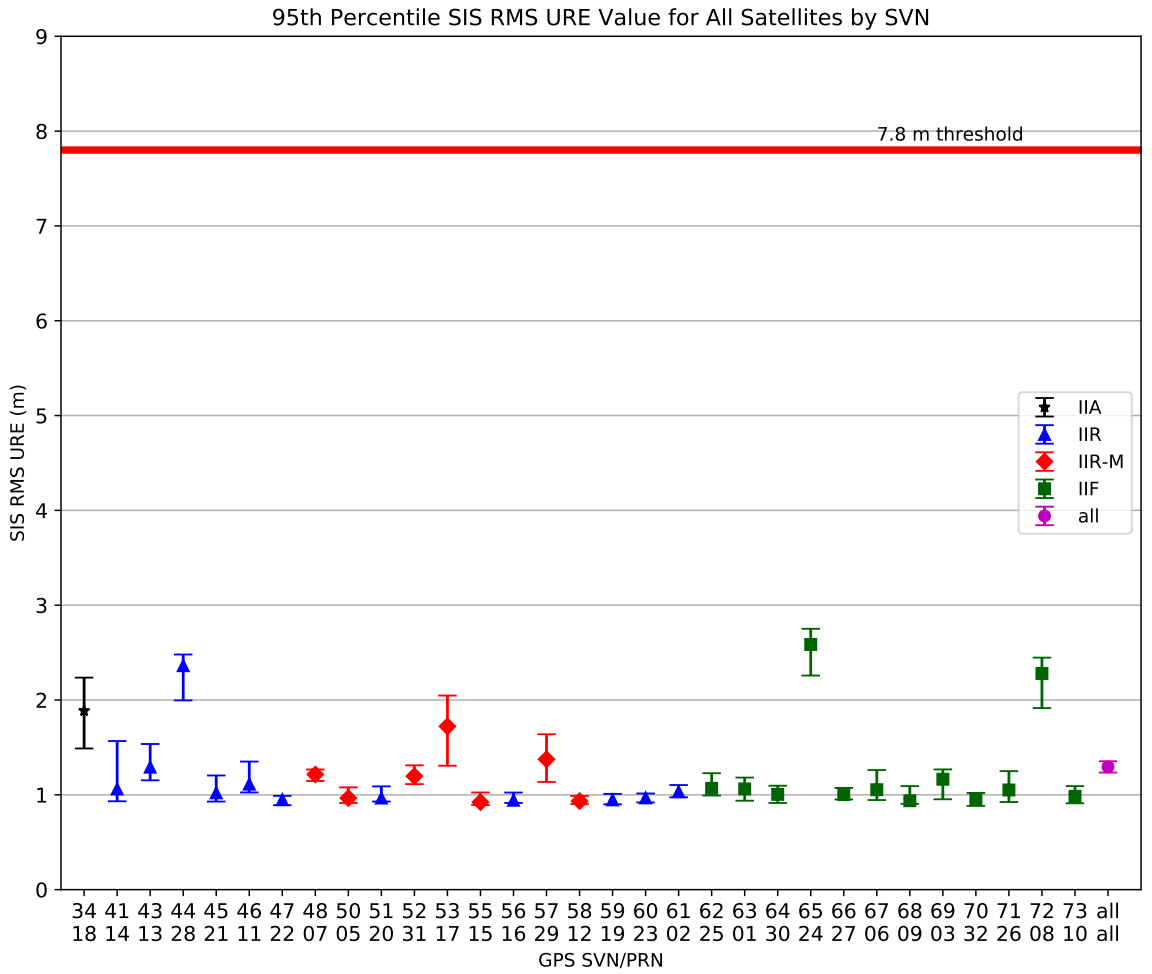

Figure 3.1: Range of the Monthly 95$^{\text{th}}$ Percentile Values for All SVs

Notes: Each SVN with valid data is shown sequentially along the horizontal axis. The median value of the monthly 95th percentile SIS URE is displayed as a point along the vertical axis. The minimum and maximum of the monthly 95th percentile SIS URE for 2019 are shown by whiskers on the vertical bars. Color distinguishes between the Block IIA, Block IIR, Block IIR-M, and Block IIF SVs. The red horizontal line at 7.8 m indicates the upper bound given by the SPSPS08 Section 3.4 performance metric. The marker for "all" represents the monthly 95th percentile values across all satellites.

3.2.1.1 An Alternate Method

It is practical to compute a set of 95th percentile URE values in which the Instantaneous SIS URE values are computed over a sufficiently dense grid and at fixed time intervals separated by uniform time steps throughout the period of interest. The 95th percentile value is then selected from the entire set of Instantaneous SIS URE values. This was done in parallel to the process that produced the results shown in Section 3.2.1. The evaluation was performed at a 5 minute cadence. For each SV at each evaluation time, the point on the Earth immediately below the SV (nadir direction) was used as the center of the uniformly spaced 577 point grid that extends over the area visible to the satellite above the 5° minimum elevation angle. Further details on the implementation are provided in Appendix B.1.3.

Table 3.3 presents a summary of the results obtained by this alternate method. Figure 3.2 presents the values in Table 3.3 in a graphical manner. Table 3.3 and Figure 3.2 have the same format as Table 3.2 and Figure 3.1. The values in Table 3.3 are larger than the values in Table 3.2 by an average of 0.03 m. The maximum difference [alternate - original] for a given SV-month is +0.12 m; the minimum difference is -0.03 m.

Figure 3.3 is an illustration of the differences between the monthly 95th percentile SIS URE values calculated by the two different methods. Each pair of monthly values for a given SV found in Table 3.2 and Table 3.3 were taken and the difference computed as the quantity [alternate - original]. The median, maximum, and minimum differences were then selected from each set and plotted in Figure 3.3. Figure 3.3 illustrates that the two methods agree to within 20 cm and generally a good deal less with the alternate method typically being a few cm larger.

None of the values in Table 3.3 exceed the threshold of 7.8 m. Therefore, the threshold is met for 2019 even under this alternate interpretation of the metric.

Table 3.3: Monthly 95th Percentile Values of SIS Instantaneous URE for All SVs in Meters (via Alternate Method)

SVN	PRN	Block	Jan	Feb	Mar	Apr	May	Jun	Jul	Aug	Sep	Oct	Nov	Dec	2019
34	18	IIA	1.70	2.00	2.28	2.10	1.70	1.80	1.52	1.96	1.88	2.12	–	–	1.91
41	14	IIR	1.07	1.58	1.25	1.11	1.02	1.07	1.06	1.08	1.01	1.07	1.12	0.95	1.10
43	13	IIR	1.52	1.40	1.25	1.31	1.41	1.39	1.17	1.17	1.19	1.36	1.30	1.23	1.30
44	28	IIR	2.41	2.40	2.49	2.23	2.40	2.38	2.30	2.36	2.02	2.09	2.43	2.24	2.33
45	21	IIR	1.11	1.08	1.03	1.02	1.04	1.13	1.25	1.02	0.96	1.06	1.02	1.08	1.06
46	11	IIR	1.19	1.47	1.28	1.14	1.09	1.31	1.40	1.11	1.06	1.11	1.14	1.22	1.22
47	22	IIR	0.98	1.05	0.95	0.99	0.91	1.02	1.00	1.03	0.96	0.96	0.95	0.96	0.98
48	7	IIR-M	1.22	1.24	1.23	1.16	1.24	1.28	1.30	1.27	1.25	1.26	1.22	1.22	1.24
50	5	IIR-M	0.96	0.99	0.96	0.95	0.98	1.02	1.05	1.01	1.11	0.98	0.93	0.93	0.99
51	20	IIR	1.00	1.08	0.95	1.00	1.02	0.97	1.02	1.00	0.95	0.96	1.01	0.97	0.99
52	31	IIR-M	1.21	1.35	1.23	1.23	1.16	1.17	1.27	1.31	1.17	1.14	1.24	1.27	1.22
53	17	IIR-M	2.14	1.72	1.74	1.66	1.93	1.36	1.85	1.80	1.51	1.72	1.66	2.02	1.75
55	15	IIR-M	0.93	0.95	0.97	0.96	0.92	0.93	0.94	0.91	1.04	0.96	0.93	1.04	0.96
56	16	IIR	0.97	0.97	1.02	0.96	0.95	0.97	0.96	0.94	0.93	0.96	0.94	0.95	0.96
57	29	IIR-M	1.21	1.61	1.17	1.42	1.45	1.42	1.58	1.45	1.38	1.63	1.21	1.49	1.41
58	12	IIR-M	0.98	0.96	0.95	0.96	0.96	0.97	1.02	0.96	0.97	0.94	0.95	0.96	0.96
59	19	IIR	0.97	0.97	1.04	0.97	0.97	1.03	0.96	0.97	0.99	0.98	0.92	0.96	0.98
60	23	IIR	1.01	1.05	1.00	0.95	1.05	0.97	1.01	0.94	0.98	1.05	1.03	1.02	1.00
61	2	IIR	1.15	1.09	1.10	1.07	1.12	1.07	1.10	1.00	1.01	1.03	1.03	1.05	1.07
62	25	IIF	1.07	1.02	1.03	1.04	1.11	1.24	1.19	1.01	1.04	1.10	1.08	1.17	1.09
63	1	IIF	1.16	1.03	0.97	0.98	1.08	1.08	1.08	1.09	1.16	1.18	1.21	1.25	1.12
64	30	IIF	1.07	0.94	0.96	1.02	1.07	1.11	1.01	0.93	1.02	1.02	1.01	1.08	1.03
65	24	IIF	2.59	2.27	2.50	2.50	2.77	2.57	2.71	2.44	2.60	2.76	2.62	2.61	2.59
66	27	IIF	0.99	0.97	0.98	1.01	1.06	1.02	1.10	1.02	1.08	1.01	1.05	1.02	1.03
67	6	IIF	0.99	0.98	1.08	0.96	1.09	1.08	1.14	1.01	1.10	1.10	1.17	1.29	1.10
68	9	IIF	1.01	0.94	1.10	1.07	0.95	0.94	1.05	0.92	1.01	0.94	0.94	0.96	0.99
69	3	IIF	1.12	1.26	1.27	1.29	0.98	1.13	1.20	1.27	1.25	1.15	1.08	1.14	1.19
70	32	IIF	0.96	0.99	1.04	1.00	0.90	0.90	0.95	0.96	1.00	1.05	1.02	0.96	0.98
71	26	IIF	1.12	1.14	1.04	1.03	1.08	1.13	1.23	1.27	1.00	0.94	1.04	1.05	1.10
72	8	IIF	2.14	1.95	2.33	2.45	2.12	2.24	2.31	2.38	2.37	2.28	2.41	2.11	2.28
73	10	IIF	1.00	1.07	1.00	0.94	0.94	0.97	1.04	1.12	1.05	0.93	1.01	1.02	1.01
Block IIA			1.70	2.00	2.28	2.10	1.70	1.80	1.52	1.96	1.88	2.12	–	–	1.91
Block IIR			1.25	1.31	1.22	1.17	1.20	1.20	1.23	1.19	1.14	1.18	1.18	1.21	1.20
Block IIF			1.51	1.33	1.42	1.40	1.45	1.46	1.52	1.53	1.47	1.36	1.44	1.42	1.44
All SVs			1.37	1.35	1.37	1.29	1.31	1.32	1.35	1.35	1.28	1.26	1.27	1.29	1.32

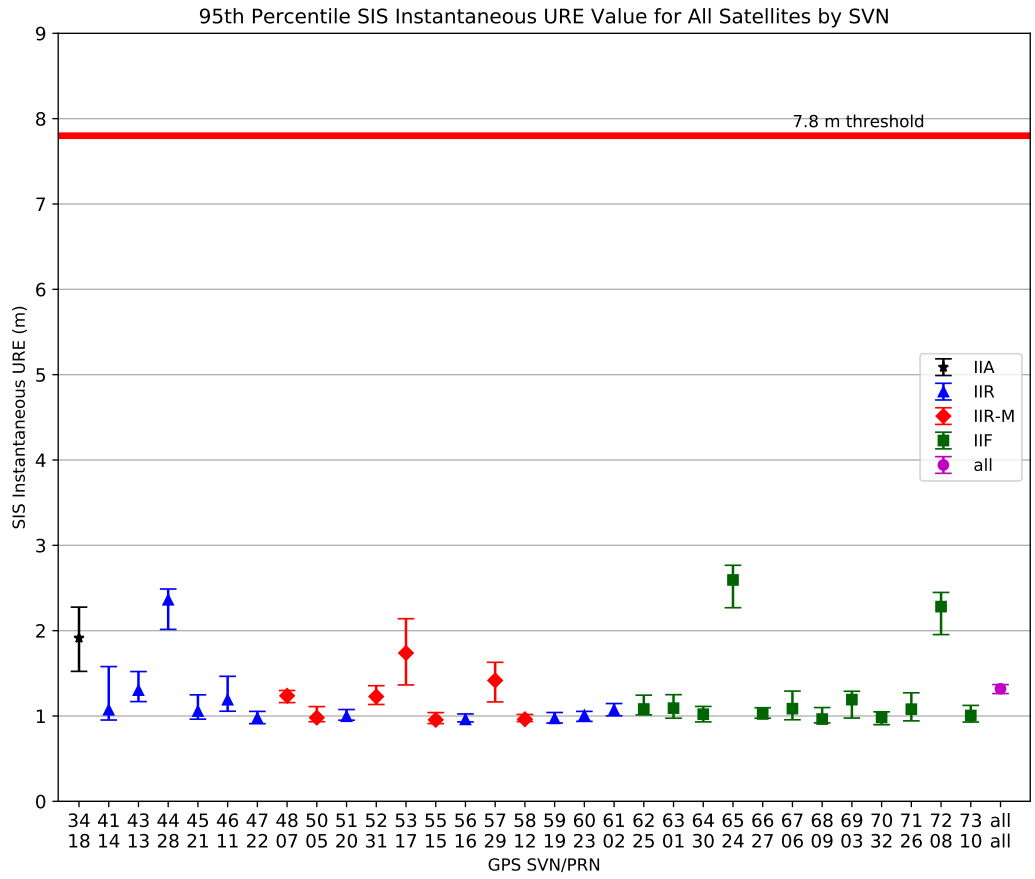

Figure 3.2: Range of the Monthly 95th Percentile Values for All SVs (via Alternate Method)

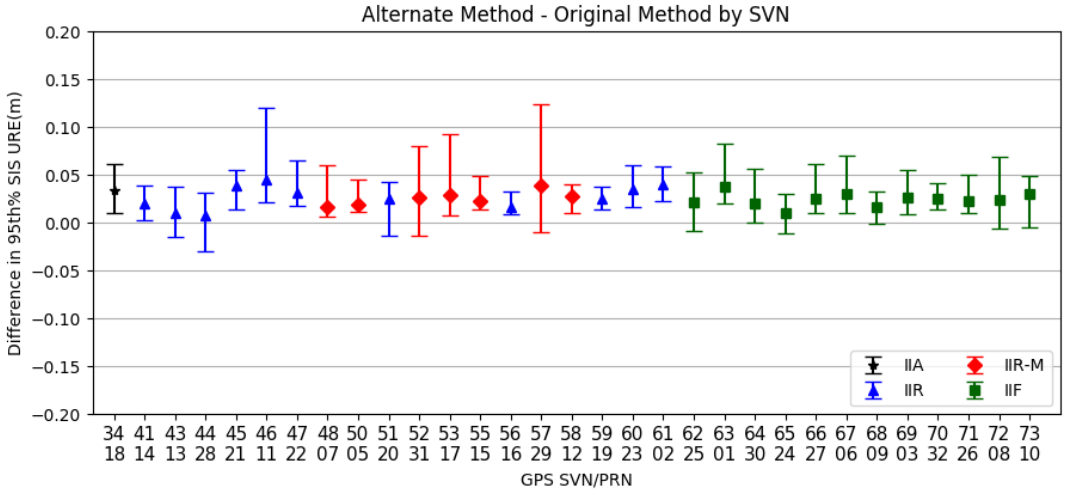

Figure 3.3: Range of Differences in Monthly Values between Methods for All SVs

3.2.2 URE at Any AOD

The next URE metric considered is the calculation of URE at any AOD. This is associated with the following SPSPS08 Section 3.4 metric:

- *"≤ 12.8 m 95% Global Average URE during Normal Operations at Any AOD"*

This metric may be decomposed in a manner similar to the previous metric. The key differences are the term "at any AOD" and the change in the threshold value. The phrase "at any AOD" is interpreted to mean that at any AOD where sufficient data can be collected to constitute a reasonable statistical set the value of the required statistic should be $\leq$ 12.8 m. See Section 4.2 for a discussion of how the AOD is computed.

To examine this requirement, the set of 30 s Instantaneous RMS SIS URE values used in Section 3.2.1 was analyzed as described in Appendix A. In summary, the RMS SIS URE values for each satellite for the entire year were divided into bins based on 15 minute intervals of AOD. The 95$^{\text{th}}$ percentile values for each bin were selected and the results were plotted as a function of the AOD.

Figures 3.4 through 3.7 show two curves: shown in blue is the 95$^{\text{th}}$ percentile URE vs. AOD (in hours), and shown in green is the count of points in each bin as a function of AOD. For satellites that are operating on the normal pattern (roughly one upload per day), the count of points in each bin is roughly equal from the time the upload becomes available until about 24 hours AOD. In fact, the nominal number of points can be calculated by multiplying the number of expected 30 s estimates in a 15 minute bin (30 estimates per bin) by the number of days in the year. There are just under 11,000 points in each bin. This corresponds well to the plateau area of the green curve for the well-performing satellites (e.g. Figures 3.4 and 3.5). For satellites that are uploaded more frequently, the green curve will show a left-hand peak higher than the nominal count decreasing to the right. This is a result of the fact that there will be fewer points at higher AOD due to the more frequent uploads. The vertical scales on Figures 3.4 through 3.7 and the figures in Appendix A have been constrained to a constant value to aid in comparisons between the charts. In 2019, the only SV with lower than nominal counts was SVN 34/PRN 18 (removed from the constellation in October).

The representative best performers for Block IIR/IIR-M and Block IIF are shown in Figures 3.4 and 3.5. These are SVN 58/PRN 12 and SVN 66/PRN 27, respectively. For both blocks, several SVs have similar good results. Best performers exhibit a low and very flat distribution of AODs, and the UREs appear to degrade roughly linearly with time, at least to the point that the distribution (represented by the green curve) shows a marked reduction in the number of points.

Figures 3.6 and 3.7 show the worst performing (i.e. highest URE values) Block IIR/IIR-M and Block IIF SVs. These are SVN 44/PRN 28 and SVN 65/PRN 24, respectively. Note that the distribution of AOD samples for SVN 65/PRN 24 is biased toward shorter values of AOD, which indicates that uploads are occurring more frequently than once-per-day on occasion.

The plots for all satellites are contained in Appendix A. A review of the full set of plots leads to the conclusion that the rate of URE growth for the two Block IIF SVs using Cesium frequency standards is noticeably higher. While there are differences between individual satellites, all the results are well within the assertion for this metric.

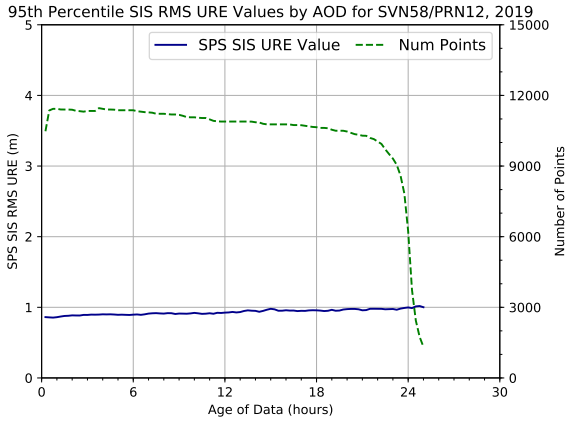

Figure 3.4: Best Performing Block IIR/IIR-M SV in Terms of URE over Any AOD

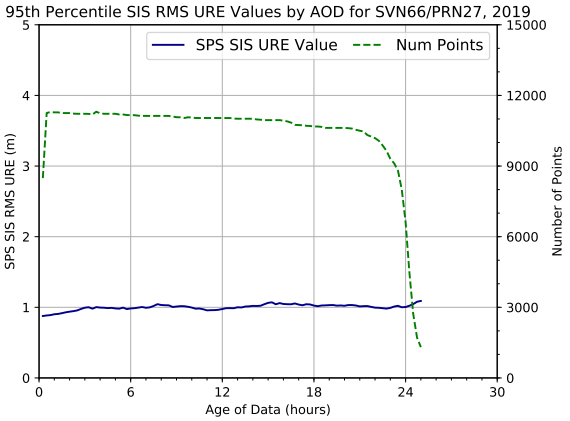

Figure 3.5: Best Performing Block IIF SV in Terms of URE over Any AOD

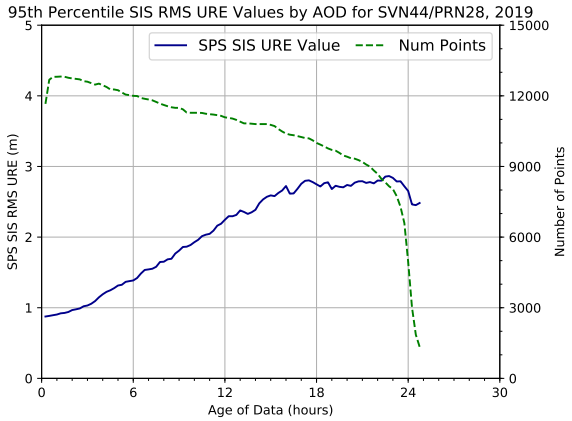

Figure 3.6: Worst Performing Block IIR/IIR-M SV in Terms of URE over Any AOD

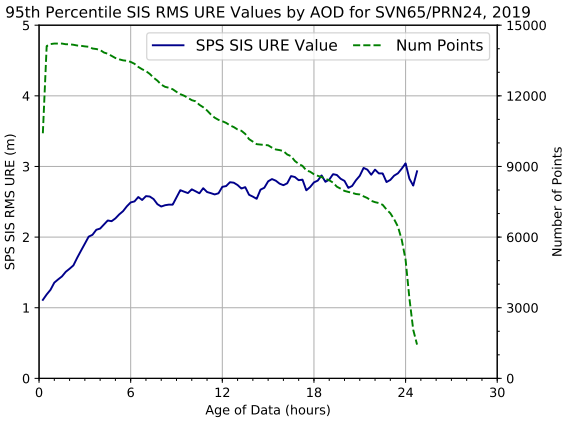

Figure 3.7: Worst Performing Block IIF SV in Terms of URE over Any AOD

3.2.3 URE at Zero AOD

Another URE metric considered is the calculation of URE at Zero Age of Data (ZAOD). This is associated with the SPSPS08 Section 3.4 metric:

- *"≤ 6.0 m 95% Global Average URE during Normal Operations at Zero AOD"*

This metric may be decomposed in a manner similar to the previous two metrics. The key differences are the term "at Zero AOD" and the change in the threshold value.

The broadcast ephemeris is never available to user equipment at ZAOD due to the delays inherent in preparing the broadcast ephemeris and uploading it to the SV. However, we can still make a case that this assertion is met by examining the 95^{th} percentile SIS RMS URE value at 15 minutes AOD. These values are represented by the left-most data point on the blue lines shown in Figure 3.4 through Figure 3.7. The ZAOD values should be slightly better than the 15 minute AOD values, or at worst roughly comparable. Inspection of the 15 minute AOD values shows that the values for all SVs are well within the 6.0 m value associated with the assertion. Therefore the assertion is considered fulfilled.

3.2.4 URE Bounding

The SPSPS08 asserts the following requirements for single-frequency C/A-code:

- *"≤ 30 m 99.94% Global Average URE during Normal Operations"*
- *"≤ 30 m 99.79% Worst Case Single Point Average URE during Normal Operations"*

Note that the first assertion states "Global Average URE", which is interpreted to mean the Instantaneous SIS RMS URE values, while the second assertion states "Worst Case Single Point Average URE", which is interpreted to mean the Instantaneous SIS URE. Therefore, to evaluate the first assertion, the 30 s Instantaneous SIS RMS URE values computed as part of the evaluation described in Section 3.2.1 were checked to determine whether any exceeded the 30 m threshold.

To evaluate the second assertion, the Instantaneous SIS URE values computed as part of the evaluation described in Section 3.2.1.1 were checked to determine whether any exceeded the 30 m threshold. This provides a set of 577 Instantaneous SIS URE values distributed across the area visible to a given SV at each 5 min epoch, which yields a set of over 60 million Instantaneous SIS URE values per SV per year. The distribution of the points is described in Appendix B.1.3.

However, there are limitations to our technique of estimating UREs that are worth noting such as fits across orbit/clock discontinuities, thrust events, and clock run-offs. These are discussed in Appendix B.1.4. As a result of these limitations, a set of observed range deviations (ORDs) was also examined as a cross-check.

The ORDs were formed using the NGA observation data collected to support the position accuracy analysis described in Section 3.6.3. In the case of ORDs, the observed range is differenced from the range predicted by the geometric distance from the known station position to the SV location derived from the broadcast ephemeris. The ORDs are similar to the Instantaneous SIS URE in that both represent the error along a specific line-of-sight. However, the ORDs are not true SIS measurements due to the presence of residual atmospheric effects and receiver noise. The selected stations are geographically distributed such that at least two sets of observations are available for each SV at all times. As a result, any actual SV problems that would lead to a violation of this assertion will produce large ORDs from multiple stations.

None of these three checks found any values that exceeded the 30m threshold. Based on these results, these assertions are considered satisfied.

3.2.5 URE After 14 Days Without Upload

The SPS PS provides the following assertion regarding URE after 14 days without an upload:

- *"≤ 388 m 95% Global Average URE after 14 days without upload"*

This standard is not evaluated as there were no periods in 2019 during which SVs were transmitting a healthy signal while operating after 14 days without an upload.

3.2.6 URRE Over All AOD

The performance standard provides the following assertion for the user range rate error (URRE).

- *"≤0.006 m/sec 95% Global Average URRE over any 3-second interval during Normal Operations at Any AOD"*

This is subject to the same general constraints from SPSPS08 Section 3.4 as the URE assertions.

The URRE cannot be evaluated by comparison of the BCP to the TCP. This is due to two factors:

1. as described in Note 1 to SPS PS Table 3.4-2, the primary contributing factor to the URRE is the noise from the SV frequency standards (clocks), and
2. the assertion states *"over any 3-second interval"*.

In the precise orbits used for the TCP, the noise due to the SV clocks is smoothed over long periods. As a result, the comparison of BCP and TCP derivatives will not reveal short term (i.e. 3 s) changes in SV clock behavior.

To address this, a different evaluation process is used. This process uses the TCP along with the measured carrier phase observations and the known station positions to form the URRE values by differencing the range errors. The carrier phase observations have much lower noise than the pseudorange values, and because both phase and range are based on the same SV clock and the same receiver clock, the result will be a more precise measurement of the range rate error.

The observation data from the NGA MSN is collected at a 1.5 s rate. This rate allows examination of the URRE at the desired cadence. Dual-frequency observations are used in order to reduce ionospheric errors and come as close as practical to the constraint that the results are to be based on SIS. In a similar manner, a tropospheric model based on weather observed at the stations is used to reduce tropospheric errors.

These steps are all helpful, but the individual observations retain enough noise to be unable to verify the assertion based on data from single receivers. However, there are additional conditions that provide a way to further reduce the effects of the noise in the data.

- Note 2 to SPS PS Table 3.4-2 notes that the User-Equivalent Range Rate Error (UERRE) is the root-sum-square of the SIS-caused URRE and the receiver-caused pseudorange rate error after neglecting any correlated components. The SIS-caused URRE is what we are attempting to evaluate, however, the UERRE is observable quantity derived in the preceding process, as receiver data is directly used. Therefore we remove the correlated errors, which are present as constant biases for a given SV-receiver pass, in order to better approximate the SIS-caused URRE.

- The assertion states that the URRE is to be considered as a global average. SV clock errors will have constant effect across the area that can view the SV. Therefore, URRE errors for a specific SV-epoch will be constant across the field of view. This is not true for orbit errors where the effect on URE will vary from station-to-station due to geometry. However, the URRE effect on orbit errors over a 3 s interval will be negligible (assuming no thrust events). This allows us to average all the URRE values for a given SV-epoch in order to reduce the noise in the URRE samples.

Table 3.4 contains the monthly 95^{th} percentile values of the URRE based on the assumptions and constraints described above. For each SV, the worst value across the year is marked in red. Figure 3.8 provides a summary of these results for the entire constellation. For each SV, shown along the horizontal axis, the monthly values from Table 3.4 are plotted. These results are conservative in the sense that there has been no attempt to account for receiver noise in the observation data.

No values in Table 3.4 exceed 0.006 m/sec (6 mm/sec) and so this requirement is considered met for 2019.

Table 3.4: Monthly 95th Percentile Values of PPS Dual-Frequency SIS RMS URRE for All SVs in mm/s

SVN	PRN	Block	Jan	Feb	Mar	Apr	May	Jun	Jul	Aug	Sep	Oct	Nov	Dec
34	18	IIA	3.41	3.44	3.44	3.41	3.42	3.42	3.48	3.46	3.47	3.45	–	–
41	14	IIR	2.63	2.54	2.57	2.57	2.57	2.57	2.61	2.59	2.54	2.53	2.48	2.51
43	13	IIR	2.55	2.71	2.76	2.72	2.72	2.58	2.63	2.64	2.85	2.81	2.92	2.63
44	28	IIR	2.71	2.54	2.55	2.55	2.59	2.57	2.58	2.59	2.53	2.49	2.49	2.52
45	21	IIR	3.08	2.80	2.76	2.74	2.89	2.91	2.80	2.73	2.60	2.62	2.75	2.92
46	11	IIR	2.93	2.85	2.83	2.87	2.89	2.90	2.95	2.94	2.89	2.91	2.91	2.91
47	22	IIR	2.54	2.47	2.42	2.34	2.35	2.41	2.46	2.46	2.38	2.33	2.31	2.41
48	7	IIR-M	2.61	2.51	2.50	2.54	2.66	2.60	2.55	2.52	2.55	2.57	2.60	2.60
50	5	IIR-M	3.15	3.24	3.10	2.88	2.73	2.90	3.08	3.18	3.06	2.87	2.80	3.09
51	20	IIR	2.63	2.59	2.57	2.55	2.56	2.55	2.59	2.55	2.54	2.52	2.53	2.59
52	31	IIR-M	2.50	2.40	2.40	2.37	2.43	2.40	2.37	2.34	2.34	2.41	2.47	2.44
53	17	IIR-M	3.02	2.92	2.96	3.00	2.93	2.88	2.83	2.87	3.02	3.09	2.99	3.02
55	15	IIR-M	2.64	2.64	2.73	2.70	2.68	2.63	2.62	2.69	2.75	2.71	2.67	2.62
56	16	IIR	3.06	2.94	2.89	2.76	2.73	2.68	2.89	2.87	2.81	2.82	2.94	3.11
57	29	IIR-M	2.54	2.48	2.52	2.53	2.50	2.45	2.48	2.48	2.56	2.55	2.48	2.48
58	12	IIR-M	3.10	3.02	2.96	2.88	2.91	2.95	3.12	2.94	2.90	2.84	2.84	2.96
59	19	IIR	2.74	2.67	2.71	2.74	2.71	2.72	2.74	2.73	2.79	2.80	2.79	2.82
60	23	IIR	2.50	2.47	2.51	2.48	2.47	2.44	2.44	2.45	2.44	2.39	2.38	2.40
61	2	IIR	2.76	2.62	2.64	2.62	2.66	2.66	2.72	2.70	2.67	2.68	2.69	2.71
62	25	IIF	2.33	2.30	2.35	2.33	2.38	2.36	2.37	2.30	2.32	2.31	2.31	2.30
63	1	IIF	2.39	2.37	2.41	2.42	2.42	2.40	2.44	2.38	2.39	2.36	2.37	2.34
64	30	IIF	1.90	1.85	1.87	1.88	1.90	1.85	1.84	1.83	1.79	1.73	1.67	1.70
65	24	IIF	4.96	4.98	5.05	5.00	4.99	4.98	5.08	5.02	5.04	5.01	5.04	5.05
66	27	IIF	2.18	2.15	2.18	2.18	2.18	2.19	2.28	2.26	2.27	2.23	2.22	2.22
67	6	IIF	1.96	1.93	2.06	1.94	1.89	1.85	1.85	1.85	1.82	1.85	1.94	1.94
68	9	IIF	1.90	1.87	1.90	1.86	1.88	1.86	1.89	1.84	1.82	1.81	1.84	1.89
69	3	IIF	2.02	1.98	2.05	1.98	2.04	2.03	2.00	1.97	1.94	1.96	1.98	1.98
70	32	IIF	2.11	2.03	2.04	2.02	2.02	2.03	2.07	2.05	2.00	2.03	2.00	2.02
71	26	IIF	1.96	1.84	1.92	1.91	1.94	1.93	1.95	1.92	1.87	1.89	1.93	1.96
72	8	IIF	3.53	3.50	3.55	3.53	3.56	3.56	3.59	3.65	3.64	3.65	3.68	3.74
73	10	IIF	1.87	1.82	1.84	1.83	1.86	1.84	1.87	1.85	1.84	1.84	1.81	1.81
All SVs			2.69	2.63	2.65	2.62	2.63	2.62	2.66	2.64	2.63	2.61	2.60	2.63

Notes: Values not present indicate that the satellite was unavailable during this period. Months during which an SV was available for less than 25 days are shown shaded. Months with the highest URRE for a given SV are colored red. The row at the bottom is the monthly 95th percentile values over all SVs.

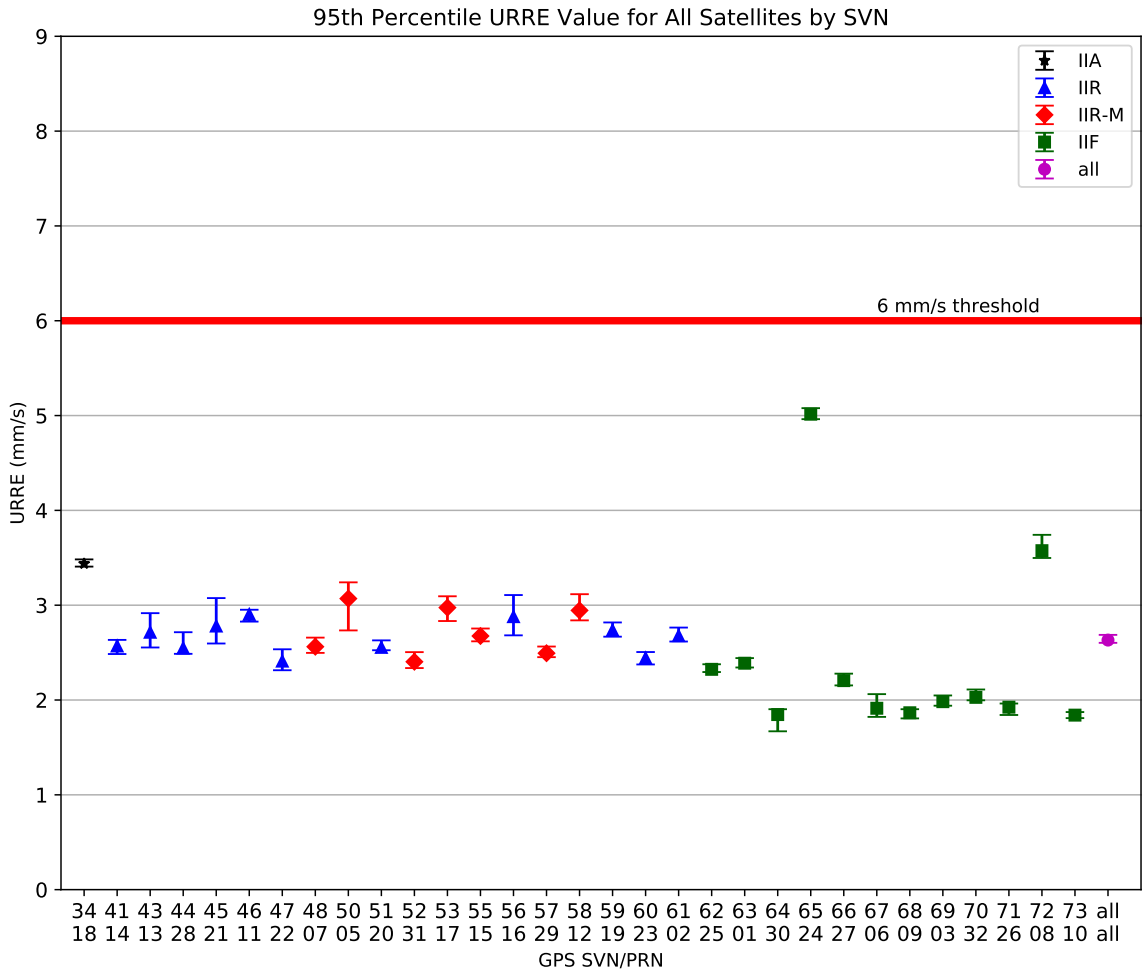

Figure 3.8: Range of the Monthly URRE 95th Percentile Values for All SVs

Notes: Each SVN with valid data is shown sequentially along the horizontal axis. The median value of the monthly 95th percentile URRE is displayed as a point along the vertical axis. The minimum and maximum of the monthly 95th percentile URRE for 2019 are shown by whiskers on the vertical bars. Color distinguishes between the Block IIA, Block IIR, Block IIR-M, and Block IIF SVs. The red horizontal line at 6.0 mm/s indicates the upper bound given by the SPSPS08 Section 3.4 performance metric. The marker for "all" represents the monthly 95th percentile values across all satellites.

3.2.7 URAE Over All AOD

The performance standard provides the following assertion for the user range acceleration error (URAE).

- *"≤0.002 m/sec/sec 95% Global Average URAE over any 3-second interval during Normal Operations at Any AOD"*

This is subject to the same general constraints from and SPSPS08 Section 3.4 as the URE assertions.

The URAE values were obtained by differencing the URRE values derived in support of the previous section. Table 3.5 contains the monthly 95$^{\text{th}}$ percentile values of the URRE based on the assumptions and constraints described above. For each SV, the worst value across the year is marked in red. Figure 3.9 provides a summary of these results for the entire constellation. No values exceed 0.002 m/sec/sec (2 mm/sec^2) and so this requirement is considered met for 2019.

Table 3.5: Monthly 95th Percentile Values of PPS Dual-Frequency SIS RMS URAE for All SVs in mm/s^2

SVN	PRN	Block	Jan	Feb	Mar	Apr	May	Jun	Jul	Aug	Sep	Oct	Nov	Dec
34	18	IIA	1.25	1.25	1.25	1.24	1.25	1.23	1.24	1.23	1.21	1.21	–	–
41	14	IIR	0.75	0.74	0.75	0.75	0.75	0.75	0.76	0.74	0.73	0.74	0.72	0.72
43	13	IIR	0.78	0.78	0.79	0.78	0.79	0.79	0.81	0.80	0.80	0.81	0.81	0.79
44	28	IIR	0.78	0.77	0.78	0.77	0.79	0.79	0.79	0.77	0.76	0.76	0.74	0.75
45	21	IIR	0.77	0.75	0.74	0.74	0.76	0.76	0.74	0.72	0.70	0.72	0.72	0.74
46	11	IIR	0.80	0.80	0.81	0.80	0.81	0.81	0.82	0.82	0.79	0.80	0.79	0.79
47	22	IIR	0.71	0.71	0.70	0.69	0.70	0.70	0.70	0.69	0.67	0.66	0.66	0.67
48	7	IIR-M	0.74	0.73	0.74	0.75	0.76	0.76	0.75	0.73	0.72	0.74	0.73	0.73
50	5	IIR-M	0.85	0.85	0.85	0.79	0.79	0.81	0.83	0.83	0.81	0.79	0.79	0.85
51	20	IIR	0.73	0.72	0.73	0.72	0.73	0.73	0.73	0.72	0.70	0.71	0.69	0.70
52	31	IIR-M	0.72	0.71	0.73	0.71	0.72	0.72	0.73	0.70	0.69	0.71	0.70	0.70
53	17	IIR-M	0.74	0.73	0.75	0.75	0.75	0.75	0.75	0.73	0.74	0.76	0.75	0.75
55	15	IIR-M	0.74	0.74	0.76	0.75	0.76	0.74	0.74	0.74	0.73	0.74	0.72	0.72
56	16	IIR	0.77	0.76	0.76	0.74	0.75	0.75	0.80	0.78	0.75	0.75	0.74	0.76
57	29	IIR-M	0.72	0.71	0.72	0.72	0.71	0.70	0.69	0.67	0.67	0.68	0.66	0.67
58	12	IIR-M	0.76	0.74	0.74	0.72	0.74	0.74	0.76	0.71	0.70	0.70	0.69	0.70
59	19	IIR	0.77	0.76	0.77	0.76	0.76	0.76	0.76	0.73	0.73	0.75	0.75	0.76
60	23	IIR	0.74	0.73	0.74	0.73	0.74	0.73	0.72	0.71	0.70	0.70	0.69	0.71
61	2	IIR	0.69	0.69	0.70	0.69	0.71	0.70	0.71	0.68	0.68	0.69	0.68	0.68
62	25	IIF	0.68	0.67	0.69	0.68	0.68	0.68	0.69	0.66	0.65	0.66	0.64	0.64
63	1	IIF	0.73	0.72	0.74	0.74	0.75	0.75	0.76	0.74	0.73	0.72	0.71	0.70
64	30	IIF	0.67	0.66	0.67	0.66	0.67	0.66	0.65	0.64	0.63	0.63	0.62	0.63
65	24	IIF	1.67	1.67	1.70	1.67	1.68	1.68	1.69	1.69	1.68	1.68	1.68	1.69
66	27	IIF	0.70	0.69	0.70	0.70	0.70	0.71	0.72	0.72	0.70	0.71	0.68	0.68
67	6	IIF	0.67	0.66	0.71	0.67	0.67	0.67	0.68	0.66	0.65	0.66	0.67	0.67
68	9	IIF	0.68	0.68	0.69	0.67	0.67	0.67	0.67	0.64	0.63	0.64	0.63	0.65
69	3	IIF	0.66	0.65	0.67	0.65	0.67	0.67	0.66	0.64	0.63	0.62	0.62	0.62
70	32	IIF	0.67	0.66	0.67	0.66	0.66	0.67	0.68	0.65	0.65	0.66	0.64	0.64
71	26	IIF	0.69	0.68	0.70	0.69	0.69	0.69	0.70	0.68	0.67	0.67	0.66	0.66
72	8	IIF	1.21	1.21	1.22	1.22	1.23	1.23	1.25	1.25	1.25	1.26	1.26	1.28
73	10	IIF	0.66	0.66	0.66	0.66	0.67	0.66	0.66	0.65	0.64	0.65	0.63	0.63
All SVs			0.80	0.79	0.80	0.79	0.80	0.80	0.80	0.79	0.78	0.78	0.76	0.77

Notes: Values not present indicate that the satellite was unavailable during this period. Months during which an SV was available for less than 25 days are shown shaded. Months with the highest URAE for a given SV are colored red. The row at the bottom is the monthly 95th percentile values over all SVs.

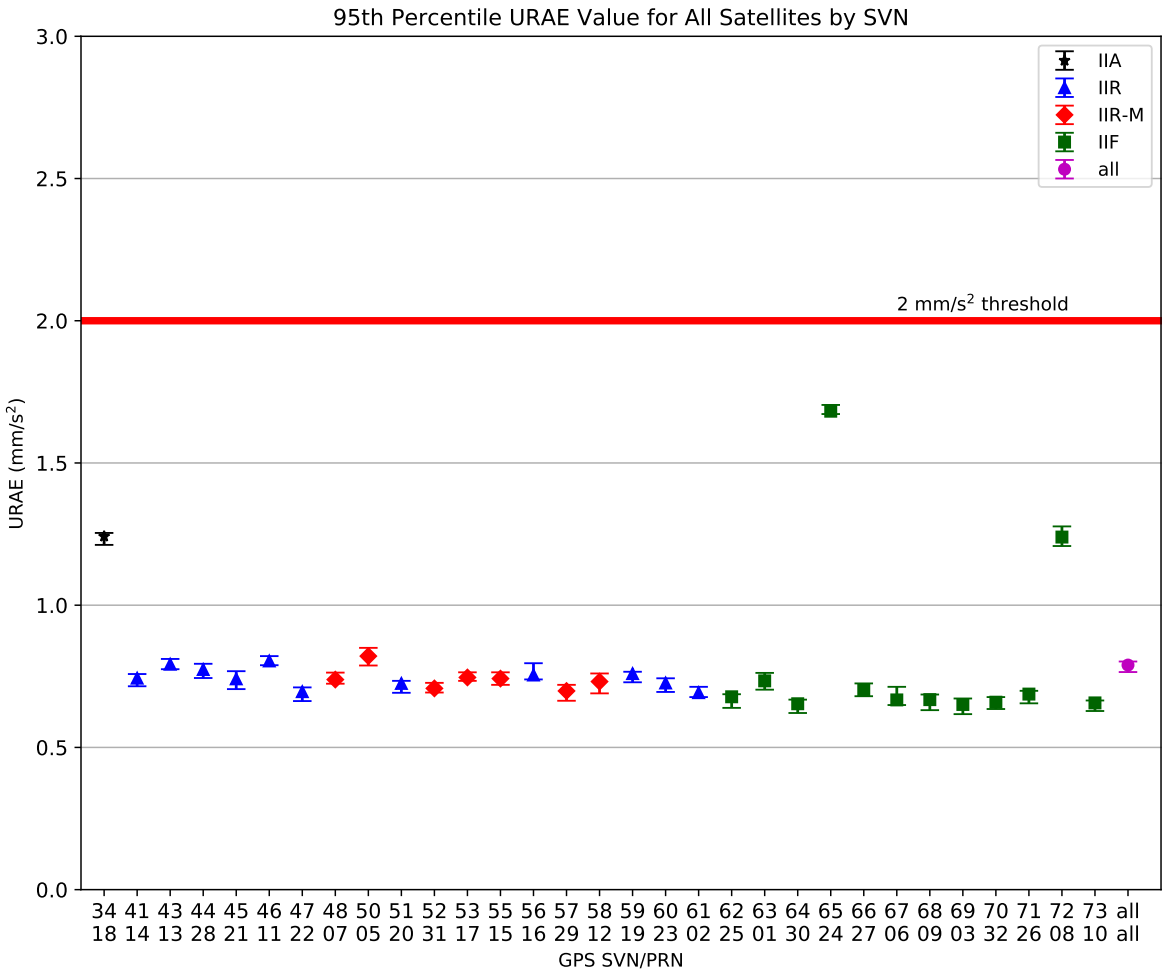

Figure 3.9: Range of the Monthly URAE 95$^{\text{th}}$ Percentile Values for All SVs

Notes: Each SVN with valid data is shown sequentially along the horizontal axis. The median value of the monthly 95th percentile URAE is displayed as a point along the vertical axis. The minimum and maximum of the monthly 95th percentile URAE for 2019 are shown by whiskers on the vertical bars. Color distinguishes between the Block IIA, Block IIR, Block IIR-M, and Block IIF SVs. The red horizontal line at 2.0 mm/s^2 indicates the upper bound given by the SPSPS08 Section 3.4 performance metric. The marker for "all" represents the monthly 95th percentile values across all satellites.

3.2.8 UTC Offset Error Accuracy

The SPS PS provides the following assertion regarding the UTC offset error (UTCOE) Accuracy:

- *"≤ 40 nsec 95% Global Average UTCOE during Normal Operations at Any AOD"*

The conditions and constraints state that this assertion should be true for any healthy SPS SIS.

This assertion was evaluated by calculating the global average UTCOE at each 15 minute interval in the year. The GPS-UTC offset available to the user was calculated based on the GPS broadcast navigation message data available from the SV at that time. The GPS-UTC offset truth information was provided by the USNO daily GPS-UTC offset values. The USNO value for GPS-UTC at each evaluation epoch was derived from a multi-day spline fit to the daily truth values.

The selection and averaging algorithms are a key part of this process. The global average at each 15 minute epoch is determined by evaluating the UTCOE across the surface of the earth at each point on a 111 km × 111 km grid. (This grid spacing corresponds to roughly 1° at the Equator.) At each grid point, the algorithm determines the set of SVs visible at or above the 5° minimum elevation angle that broadcast a healthy indication in the navigation message. For each of these SVs, the UTC offset information in subframe 4 page 18 of the navigation message was compared to determine the data set that has an epoch time (t_{ot}) that is the latest of those that fall in the range *current time* $\leq t_{ot} \leq$ *current time + 72 hours*. These data are used to form the UTC offset and UTCOE for that time-grid point. (The 72 hour value is derived from the 144 hour fit interval shown in IS-GPS-200 Table 20-XIII [2].)

The global averages at each evaluation epoch are assembled into monthly data sets. The 95$^{\text{th}}$ percentile values are then selected from these sets.

Figure 3.10 provides additional supporting information in the form of a time-history of global average UTCOE values at each 15 minute epoch for the year. Table 3.6 provides the results for each month of 2019. None of these values exceed the assertion of 40 nsec. Therefore the assertion is verified for 2019.

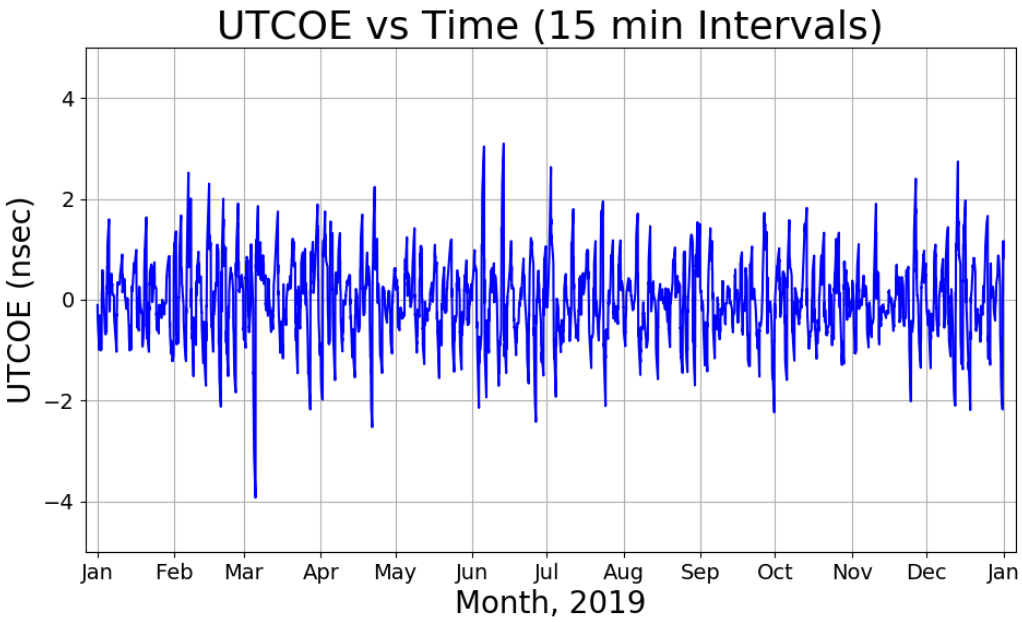

Figure 3.10: UTCOE Time Series for 2019

Table 3.6: 95th Percentile Global Average UTCOE for 2019

Month	**95th Percentile Global Avg. UTCOE (nsec)**
Jan.	1.149
Feb.	1.871
Mar.	1.739
Apr.	1.671
May	1.184
Jun.	2.198
Jul.	1.630
Aug.	1.402
Sep.	1.344
Oct.	1.323
Nov.	1.399
Dec.	1.900

3.3 SIS Integrity

3.3.1 URE Integrity

Under the heading of SIS Integrity, the SPSPS08 makes the following assertion in Section 3.5.1, Table 3.5-1:

- *"$\leq 1 \times 10^{-5}$ Probability Over Any Hour of the SPS SIS Instantaneous URE Exceeding the NTE Tolerance Without a Timely Alert During Normal Operations"*

The associated conditions and constraints include a limitation to healthy SIS, a Not to Exceed (NTE) tolerance ±4.42 times the upper bound on the user range accuracy (URA) currently broadcast, and a worst case for a delayed alert of 6 hours.

The reference to "a Timely Alert" in the assertion refers to any of a number of ways to issue an alert to the user through the GPS signal or navigation message. See SPSPS08 Section A.5.5 for a complete description.

This assertion was verified using two methods:

- The Instantaneous SIS URE values at the worst case location in view of each SV at each 30 s interval were examined to determine the number of values that exceed ±4.42 times the URA. (The worst location was selected from the set of Instantaneous SIS URE values computed for each SV as described in Section 3.2.1.1.)
- ORDs from the NGA MSN tracking stations were examined to determine the number of values that exceed ±4.42 times the URA.

Two methods were used due to the fact that each method may result in false positives in rare cases. For example, the URE values may be incorrect near discontinuities in the URE (as described in Appendix B.1.4). Similarly, the ORD values may be incorrect due to receiver or reception issues. Therefore, all reported violations are examined manually to determine whether a violation actually occurred, and if so, the extent of the violation.

Screening the 30 s Instantaneous SIS URE values and the ORD data did not reveal any events for which this threshold was exceeded. Therefore the assertion is verified for 2019.

3.3.2 UTCOE Integrity

The SPS PS provides the following assertion regarding UTCOE Integrity in Section 3.5.4:

- *"$\leq$ 1 $\times$ 10^{-5} Probability Over Any Hour of the SPS SIS Instantaneous UTCOE Exceeding the NTE Tolerance Without A Timely Alert during Normal Operations"*

The associated conditions and constraints include a limitation to healthy SIS, a NTE tolerance of $\pm$120 nsec, and the note that this holds true for any healthy SPS SIS. The reference to "a Timely Alert" in the assertion refers to any of a number of ways to issue an alert. See SPSPS08 Section A.5.5 for a complete description.

This assertion was evaluated by calculating the UTC offset for the navigation message subframe 4 page 18 data broadcast by each SV transmitting a healthy indication in the navigation message at each 15 minute interval. As in Section 3.2.8, only UTC offset information with an epoch time (t_{ot}) that is in the range *current time* $\leq t_{ot} \leq$ *current time + 72 hours* were considered valid. That offset was used to compute the corresponding UTCOE from truth data obtained from USNO [7]. If any UTCOE values exceed the NTE threshold of $\pm$120 nsec they would be investigated to determine if they represented actual violations of the NTE threshold or were artifacts of data processing.

No values exceeding the NTE threshold were found in 2019. The value farthest from zero for the year was -3.923 nsec during March (see Figure 3.10). Therefore the assertion is verified for 2019.

3.4 SIS Continuity

3.4.1 Unscheduled Failure Interruptions

The SIS Continuity metric is stated in SPSPS08 Table 3.6-1 as follows:

- *"≥ 0.9998 Probability Over Any Hour of Not Losing the SPS SIS Availability from a Slot Due to Unscheduled Interruption"*

The conditions and constraints note the following:

- The empirical estimate of the probability is calculated as an average over all slots in the 24-slot constellation, normalized annually.
- The SPS SIS is available from the slot at the start of the hour.

The notion of SIS continuity is slightly more complex for an expandable slot, because multiple SVs are involved. Following SPSPS08 Section A.6.5, a loss of continuity is considered to occur when,

> *"The expandable slot is in the expanded configuration, and either one of the pair of satellites occupying the orbital locations defined in Table 3.2-2 for the slot loses continuity."*

Hence, the continuity of signal of the expanded slot will be determined by whether either SV loses continuity.

Another point is that there is some ambiguity in this metric, which is stated in terms of "a slot" while the associated conditions and constraints note that the assertion is an average over all slots. Therefore both the per-slot and 24-slot constellation averages have been computed. As discussed below, while the per-slot values are interesting, the constellation average is the correct value to compare to the performance standard metric.

Three factors must be considered in looking at this metric:

1. We must establish which SVs were assigned to which slots during the period of the evaluation.
2. We must determine when SVs were not transmitting (or not transmitting a PRN available to users).
3. We must determine which interruptions were scheduled vs. unscheduled.

The derivation of the SV/slot assignments is described in Appendix E.

For purposes of this report, interruptions were considered to have occurred if one or more of the SVs assigned to the given slot are unhealthy in the sense of SPSPS08 Section 2.3.2.

The following specific indications were considered:

- If the health bits in navigation message subframe 1 are set to anything other than all zeros.
- If an appropriately distributed worldwide network of stations failed to collect any pseudorange data sets for a given measurement interval.

The latter case (failure to collect any data) indicates that the satellite signal was removed from service (e.g. non-standard code or some other means). The NGA MSN provides at least two-station visibility (and at least 90% three-station visibility) with redundant receivers at each station, both continuously monitoring up to 12 SVs in view. Therefore, if no data for a satellite are received for a specific time, it is highly likely that the satellite was not transmitting on the assigned PRN at that time. The 30 s Receiver Independent Exchange format (RINEX) [8] observation files from this network were examined for each measurement interval (i.e. every 30 s) for each SV. If at least one receiver collected a pseudorange data set on L1 C/A, L1 P(Y), and L2 P(Y) with a signal-to-noise level of at least 25 dB-Hz on all frequencies and no loss-of-lock flags, the SV is considered trackable at that moment. In addition, the 30 s IGS data collected to support the position accuracy estimates (Section 3.6.3) were examined in a similar fashion to guard against any MSN control center outages that could have led to missing data across multiple stations simultaneously. This allows us to define an epoch-by-epoch availability for each satellite. Then, for each slot, each hour in the year was examined, and if an SV occupying the slot was not available at the start of the hour, the hour was not considered as part of the evaluation of the metric. If the slot was determined to be available, then the remaining data was examined to determine if an outage occurred during the hour.

The preceding criteria were applied to determine times and durations of interruptions. After this, the Notice Advisories to Navstar Users (NANUs) effective in 2019 were reviewed to determine which of these interruptions could be considered scheduled interruptions as defined in SPSPS08 Section 3.6. The scheduled interruptions were removed from consideration for purposes of assessing continuity of service. When a slot was available at the start of an hour but a scheduled interruption occurred during the hour, the hour was assessed based on whether data were available prior to the scheduled outage.

Scheduled interruptions as defined in the ICD-GPS-240 [9] have a nominal notification time of 96 hours prior to the outage. Following the SPSPS08 Section 2.3.5, scheduled interruptions announced 48 hours in advance are not to be considered as contributing to the loss of continuity. So to contribute to a loss of continuity, the notification time for a scheduled interruption must occur less than 48 hours in advance of the interruption. In the case of an interruption not announced in a timely manner, the time from the start of the interruption to the moment 48 hours after notification time can be considered as a potential unscheduled interruption (for continuity purposes).

The following NANU types are considered to represent (or modify) scheduled interruptions (assuming the 48-hour advance notice is met):

- FCSTDV - Forecast Delta-V
- FCSTMX - Forecast Maintenance
- FCSTEXTD - Forecast Extension
- FCSTRESCD - Forecast Rescheduled
- FCSTUUFN - Forecast Unusable Until Further Notice

The FCSTSUMM (Forecast Summary) NANU that occurs after the outage is referenced to confirm the actual beginning and ending time of the outage.

For scheduled interruptions that extend beyond the period covered by a FCSTDV or FCSTMX NANU, the uncovered portion will be considered an unscheduled interruption. If a FCSTEXTD NANU extending the length of a scheduled interruption is published 48 hours in advance of the effective time of extension, we categorize the interruption as scheduled. It is worth reiterating that, for the computation of the metric, only those hours for which a valid SIS is available from the slot at the start of the hour are actually considered in the computation of the values.

The results of the assessment of SIS continuity are summarized in Table 3.7. The metric is averaged over the constellation, therefore the value in the bottom row (labeled "All Slots") must be greater than 0.9998 in order to meet the assertion.

To put this in perspective, there are 8760 hours in a year (8784 for a leap year). The required probability of not losing SPS SIS availability is calculated as an average over all slots in the 24-slot constellation, which implies that the maximum number of unscheduled interruptions over the year is given by $8760 \times (1 - 0.9998) \times 24 = 42$ unscheduled hours that experience interruptions. This is less than two unscheduled interruptions per SV per year but allows for the possibility that some SVs may have no unscheduled interruptions while others may have more than one.

Returning to Table 3.7, across the slots in the Expanded 24 constellation the total number of hours lost was 3. This is smaller than the maximum number of hours of unscheduled interruptions (42) available to meet the metric and leads to empirical value for the fraction of hours in which SPS SIS continuity was maintained of 0.999986. Therefore, this assertion is considered fulfilled in 2019.

Table 3.7: Probability Over Any Hour of Not Losing Availability Due to Unscheduled Interruption for 2019

Plane-Slot	**# of Hours with the SPS SIS available at the start of the hour**[b]	**# of Hours with Unscheduled Interruption**[c]	**Fraction of Hours in Which Availability was Maintained**
A1	8751	0	1.000000
A2	8756	0	1.000000
A3	8747	0	1.000000
A4	8753	0	1.000000
B1[a]	8745	0	1.000000
B2	8755	0	1.000000
B3	8760	0	1.000000
B4	8755	0	1.000000
C1	8732	1	0.999885
C2	8749	0	1.000000
C3	8751	0	1.000000
C4	8754	0	1.000000
D1	8749	1	0.999886
D2[a]	8726	1	0.999885
D3	8755	0	1.000000
D4	8750	0	1.000000
E1	8751	0	1.000000
E2	8756	0	1.000000
E3	8755	0	1.000000
E4	8754	0	1.000000
F1	8750	0	1.000000
F2[a]	8755	0	1.000000
F3	8756	0	1.000000
F4	8755	0	1.000000
All Slots	210020	3	0.999986

[a] *When B1, D2, and F2 are configured as expandable slots, both slot locations must be occupied by an available satellite for the slot to be counted as available.*

[b] *There were 8760 hours in the evaluation period.*

[c] *Number of hours in which SPS SIS was available at the start of the hour and during the hour either (1.) an SV transmitted navigation message with subframe 1 health bits set to other than all zeroes without a scheduled outage, (2.) signal lost without a scheduled outage, or (3.) the URE NTE tolerance was violated.*

3.4.2 Status and Problem Reporting Standards

3.4.2.1 Scheduled Events

The SPSPS08 makes the following assertion in Section 3.6.3 regarding notification of scheduled events affecting service:

- *"Appropriate NANU issued to the Coast Guard and the FAA at least 48 hours prior to the event"*

While beyond the assertion in the performance standards, ICD-GPS-240 [9] states a threshold of no less than 48 hours and a nominal notification time of 96 hours prior to outage start.

This metric was evaluated by comparing the NANU periods to outages observed in the data. In general, scheduled events are described in a pair of NANUs. The first NANU is a forecast of when the outage will occur. The second NANU is provided after the outage and summarizes the actual start and end times of the outage. (This is described in ICD-GPS-240 Section 10.1.1.)

Table 3.8 summarizes the pairs found for 2019. The two leftmost columns provide the SVN/PRN of the subject SV. The next three columns specify the NANU #, type, and date/time of the NANU for the forecast NANU. These are followed by three columns that specify the NANU #, the date/time of the NANU for the FCSTSUMM NANU provided after the outage, and the date/time of the beginning of the outage. The final column is the time difference between the time the forecast NANU was released and the beginning of the actual outage (in hours). This represents the length of time between the release of the forecast and the actual start of the outage. In previous years, notice times less than 48 hours were shown in red. The average notice in 2019 was over 141 hours.

To meet the assertion in the performance standard, the number of hours in the rightmost column of Table 3.8 should always be greater than 48.0. There were no cases in which the forecast was less than the 48 hour assertion. Therefore, the assertion has been met.

One satellite was decommissioned in 2019. Table 3.9 provides the details on how this was represented in the NANUs.

Table 3.8: Scheduled Events Covered in NANUs for 2019

SVN	PRN	Prediction NANU			Summary NANU (FCSTSUMM)			Notice (hrs)
		NANU #	TYPE	Release Time	NANU #	Release Time	Start Of Outage	
66	27	2019005	FCSTDV	07 Jan 1601Z	2019007	10 Jan 2029Z	10 Jan 1446Z	70.75
52	31	2019006	FCSTRESCD	08 Jan 2221Z	2019008	12 Jan 0158Z	11 Jan 2045Z	70.40
34	18	2019010	FCSTDV	17 Jan 2149Z	2019016	24 Jan 2256Z	24 Jan 1445Z	160.93
45	21	2019015	FCSTDV	24 Jan 1807Z	2019019	31 Jan 1246Z	31 Jan 0715Z	157.13
71	26	2019022	FCSTDV	08 Feb 1514Z	2019023	14 Feb 2329Z	14 Feb 1745Z	146.52
67	06	2019027	FCSTDV	25 Feb 1519Z	2019029	01 Mar 0717Z	01 Mar 0236Z	83.28
56	16	2019032	FCSTDV	07 Mar 2237Z	2019038	15 Mar 1435Z	15 Mar 0821Z	177.73
57	29	2019037	FCSTDV	15 Mar 1355Z	2019041	22 Mar 1147Z	22 Mar 0522Z	159.45
70	32	2019043	FCSTDV	28 Mar 1534Z	2019047	04 Apr 1147Z	04 Apr 1016Z	162.70
70	32	2019049	FCSTDV	05 Apr 1543Z	2019054	09 Apr 1405Z	09 Apr 0941Z	89.97
47	22	2019050	FCSTDV	05 Apr 1547Z	2019059	12 Apr 1436Z	12 Apr 0829Z	160.70
69	03	2019057	FCSTDV	10 Apr 1813Z	2019061	19 Apr 1438Z	19 Apr 0912Z	206.98
63	01	2019062	FCSTMX	19 Apr 1618Z	2019064	25 Apr 1731Z	24 Apr 1856Z	122.63
48	07	2019066	FCSTDV	29 Apr 1603Z	2019067	02 May 2307Z	02 May 1604Z	72.02
64	30	2019080	FCSTDV	31 May 1718Z	2019083	06 Jun 1729Z	06 Jun 1222Z	139.07
62	25	2019100	FCSTMX	11 Jul 2121Z	2019105	15 Jul 2229Z	15 Jul 1722Z	92.02
64	30	2019101	FCSTMX	11 Jul 2129Z	2019107	18 Jul 0102Z	17 Jul 1649Z	139.33
60	23	2019099	FCSTDV	11 Jul 1412Z	2019109	19 Jul 0955Z	19 Jul 0447Z	182.58
67	06	2019102	FCSTMX	11 Jul 2138Z	2019110	19 Jul 1926Z	19 Jul 1456Z	185.30
66	27	2019106	FCSTMX	17 Jul 2310Z	2019112	22 Jul 1917Z	22 Jul 1442Z	111.53
51	20	2019108	FCSTDV	18 Jul 2203Z	2019114	24 Jul 0519Z	23 Jul 2325Z	121.37
72	08	2019111	FCSTMX	22 Jul 1424Z	2019115	24 Jul 1859Z	24 Jul 1526Z	49.03
71	26	2019113	FCSTMX	23 Jul 2248Z	2019121	26 Jul 1652Z	26 Jul 1252Z	62.07
70	32	2019117	FCSTMX	25 Jul 1917Z	2019123	29 Jul 2030Z	29 Jul 1651Z	93.57
65	24	2019118	FCSTMX	25 Jul 1930Z	2019127	31 Jul 1515Z	31 Jul 1148Z	136.30
73	10	2019119	FCSTMX	25 Jul 1932Z	2019129	02 Aug 1835Z	02 Aug 1452Z	187.33
69	03	2019125	FCSTMX	30 Jul 2026Z	2019130	05 Aug 2105Z	05 Aug 1745Z	141.32
68	09	2019126	FCSTMX	30 Jul 2034Z	2019131	07 Aug 1703Z	07 Aug 1341Z	185.12
53	17	2019128	FCSTDV	01 Aug 1441Z	2019132	08 Aug 2037Z	08 Aug 1431Z	167.83
72	08	2019133	FCSTDV	08 Aug 2136Z	2019135	16 Aug 1414Z	16 Aug 0825Z	178.82
61	02	2019136	FCSTDV	22 Aug 1632Z	2019143	29 Aug 2136Z	29 Aug 1523Z	166.85
55	15	2019142	FCSTDV	28 Aug 1428Z	2019145	06 Sep 0135Z	05 Sep 2023Z	197.92
65	24	2019153	FCSTDV	02 Oct 1653Z	2019160	10 Oct 1155Z	10 Oct 0700Z	182.12
50	05	2019162	FCSTRESCD	25 Oct 2127Z	2019165	31 Oct 1850Z	31 Oct 1329Z	136.03
58	12	2019168	FCSTDV	08 Nov 2224Z	2019170	15 Nov 1027Z	15 Nov 0506Z	150.70
41	14	2019169	FCSTDV	13 Nov 2254Z	2019171	21 Nov 1556Z	21 Nov 0946Z	178.87
46	11	2019172	FCSTDV	10 Dec 2225Z	2019173	20 Dec 0000Z	19 Dec 1549Z	209.40
Average Notice Period								141.50

Table 3.9: Decommissioning Events Covered in NANUs for 2019

SVN	PRN	FCSTUUFN NANU		DECOM NANU			Notice (hrs)
		NANU #	Release Time	NANU #	Release Time	End of Unusable Period	
34	18	2019156	03 Oct 2211Z	2019158	09 Oct 2314Z	07 Oct 2000Z	93.82
Average Notice Period							93.82

3.4.2.2 Unscheduled Outages

The SPS PS provides the following assertion in Section 3.6.3 regarding notification of unscheduled outages or problems affecting service:

- *"Appropriate NANU issued to the Coast Guard and the FAA as soon as possible after the event"*

The ICD-GPS-240 states that the nominal notification time is 15 minutes after the start of an outage with a threshold of less than 1 hour.

This metric was evaluated by examining the NANUs provided throughout the year and comparing the NANU periods to outages observed in the data. Unscheduled events may be covered by either a single NANU or a pair of NANUs. In the case of a brief outage, a NANU with type UNUNOREF (unusable with no reference) is provided to detail the period of the outage. In the case of longer outages, a UNUSUFN (unusable until further notice) is provided to inform users of an ongoing outage or problem. This is followed by a NANU with type UNUSABLE after the outage is resolved. (This is described in detail in ICD-GPS-240 Section 10.1.2.)

Table 3.10 provides a list of the unscheduled outages found in the NANU information for 2019. The two leftmost columns provide the SVN/PRN of the subject SV. The third column provides the plane-slot of the SV to assist in relating these events to the information in Table 3.7. The next two columns provide the NANU # and date/time of the UNUSUFN NANU. These are followed by three columns that specify the NANU #, the date/time of the NANU for the UNUSABLE NANU provided after the outage, and the date/time of the beginning of the outage. The final column is the time difference between the outage start time and the UNUSUFN NANU release time (in minutes). Values in the final column are shown in red if they have a lag time of greater than 60 minutes.

There were far more UNUNOREF NANUs in 2019 than in previous years. The majority of these were related to SVN 34/PRN 18. Therefore Table 3.10 contains all unscheduled events for SVs other than SVN 34/PRN 18 while Table 3.11 contains the unscheduled events for SVN 34/PRN 18. The NANUs for SVN 34/PRN 18 cease when the SV was removed from the constellation in early October. Table 3.10 contains 11 entries. Setting aside SVN 34/PRN 18, the rate of unscheduled outages was comparable to that of previous years.

Because the performance standard states only "as soon as possible after the event", there is no threshold check to be performed. However, the data are provided for information. With respect to the notification times provided in ICD-GPS-240, for events listed in Table 3.10 the threshold time was met for all events and the nominal times was met for 9 of the 11 events. For events listed in Table 3.11 the threshold was met for all events and the nominal for all but two events in 2019.

Table 3.10: Unscheduled Events Covered in NANUs for 2019 (Excl. SVN 34/PRN 18)

SVN	PRN	Plane-Slot[a]	UNUSUFN NANU		UNUSABLE/UNUNOREF NANU			Lag Time (minutes)
			NANU #	Release Time	NANU #	Release Time	Start Of Event	
69	03	E1	–	–	2019020	01 Feb 0012Z	01 Feb 0000Z	12.00
46	11	D2F	–	–	2019026	23 Feb 2040Z	23 Feb 2001Z	39.00
69	03	E1	–	–	2019085	07 Jun 1608Z	07 Jun 1600Z	8.00
69	03	E1	–	–	2019086	08 Jun 1549Z	08 Jun 1600Z	-11.00[b]
61	02	D1	2019090	23 Jun 1356Z	2019091	23 Jun 1504Z	23 Jun 1350Z	6.00
57	29	C1	–	–	2019093	24 Jun 1633Z	24 Jun 1628Z	5.00
43	13	F2F	2019094	24 Jun 1824Z	2019095	24 Jun 1839Z	24 Jun 1818Z	6.00
63	01	D2A	2019147	09 Sep 2123Z	2019148	10 Sep 0034Z	09 Sep 2112Z	11.00
61	02	D1	2019154	03 Oct 1550Z	2019155	03 Oct 2100Z	03 Oct 1546Z	4.00
69	03	E1	2019163	28 Oct 0613Z	2019164	28 Oct 0645Z	28 Oct 0559Z	14.00
57	29	C1	2019166	04 Nov 2213Z	2019167	05 Nov 1915Z	04 Nov 2128Z	45.00
Average Lag Time								15.00

[a] *If an SV is not in a defined slot, only the plane is specified.*
[b] *NANU release time is prior to event start time. Event not included in average lag time.*

3.4.2.3 Notable NANUs

The following NANUs were notable in 2019.

- NANU 2018076 is an UNUNOREF NANU numbered for 2018, but released in 2019 and issued for dates entirely within 2019.
- NANU 2019086 is an UNUNOREF NANU that was issued for SVN 69/PRN 03. However, we see no evidence of an outage for this SV during the stated window.
- NANU 2019159 is a LAUNCH NANU for SVN 74/PRN 04 issued on 10 October 2019. It follows the format specified in ICD-GPS-240. However, that format does not allow for the launch date and LAUNCH NANU to occur in different years. As a result, the year of the launch is not contained in the NANU and the statement that the SV was launched on Day 357 (23 December) confused some readers. The USCG NAVCEN sent an email to their mail list to clarify that the launch had actually occurred nearly 10 months previous to the release of the NANU.
- NANU 2019164 is an UNUSABLE NANU that was issued for SVN 69/PRN 03 on 28 October 2019. This SV was set healthy at the indicated time and range errors were nominal.

Table 3.11: Unscheduled Events Covered in NANUs for 2019 for SVN 34/PRN 18

UNUNOREF NANU			Lag Time
NANU #	Release Time	Start Of Event	(minutes)
2018076	01 Jan 0203Z	01 Jan 0200Z	3.00
2019002	03 Jan 0220Z	03 Jan 0215Z	5.00
2019009	15 Jan 2251Z	15 Jan 2255Z	-4.00[a]
2019011	17 Jan 2326Z	17 Jan 2321Z	5.00
2019012	21 Jan 2250Z	21 Jan 2245Z	5.00
2019013	22 Jan 2242Z	22 Jan 2237Z	5.00
2019014	23 Jan 2343Z	23 Jan 2341Z	2.00
2019018	31 Jan 0010Z	31 Jan 0004Z	6.00
2019021	02 Feb 2257Z	02 Feb 2252Z	5.00
2019024	18 Feb 0704Z	18 Feb 0659Z	5.00
2019025	19 Feb 0707Z	19 Feb 0638Z	29.00
2019028	26 Feb 0808Z	26 Feb 0753Z	15.00
2019030	03 Mar 1900Z	03 Mar 1857Z	3.00
2019031	04 Mar 1853Z	04 Mar 1857Z	-4.00[a]
2019033	09 Mar 1438Z	09 Mar 1423Z	15.00
2019034	11 Mar 1338Z	11 Mar 1335Z	3.00
2019035	12 Mar 1337Z	12 Mar 1329Z	8.00
2019036	13 Mar 1329Z	13 Mar 1325Z	4.00
2019039	20 Mar 1338Z	20 Mar 1334Z	4.00
2019042	27 Mar 1050Z	27 Mar 1048Z	2.00
2019044	29 Mar 1307Z	29 Mar 1305Z	2.00
2019045	29 Mar 1316Z	29 Mar 1308Z	8.00
2019046	01 Apr 1406Z	01 Apr 1402Z	4.00
2019048	04 Apr 1354Z	04 Apr 1352Z	2.00
2019051	07 Apr 1353Z	07 Apr 1348Z	5.00
2019052	07 Apr 1406Z	07 Apr 1353Z	13.00
2019053	09 Apr 1336Z	09 Apr 1329Z	7.00
2019055	10 Apr 1324Z	10 Apr 1318Z	6.00
2019056	10 Apr 1330Z	10 Apr 1321Z	9.00
2019058	11 Apr 1328Z	11 Apr 1326Z	2.00
2019060	17 Apr 1309Z	17 Apr 1313Z	-4.00[a]
2019063	25 Apr 1639Z	25 Apr 1636Z	3.00
2019065	27 Apr 1529Z	27 Apr 1526Z	3.00
2019068	03 May 1458Z	03 May 1455Z	3.00
2019069	05 May 1506Z	05 May 1503Z	3.00
2019070	07 May 1537Z	07 May 1534Z	3.00
2019071	08 May 1526Z	08 May 1519Z	7.00
2019072	08 May 1532Z	08 May 1522Z	10.00
2019073	09 May 1514Z	09 May 1530Z	-16.00[a]
2019074	12 May 1532Z	12 May 1522Z	10.00
2019075	16 May 1754Z	16 May 1750Z	4.00
2019076	17 May 1445Z	17 May 1444Z	1.00
2019077	28 May 1552Z	28 May 1547Z	5.00
2019078	29 May 1459Z	29 May 1456Z	3.00
2019079	31 May 1415Z	31 May 1411Z	4.00
2019081	01 Jun 1414Z	01 Jun 1409Z	5.00
2019082	02 Jun 1350Z	02 Jun 1404Z	-14.00[a]
2019084	07 Jun 1555Z	07 Jun 1531Z	24.00
2019087	11 Jun 1505Z	11 Jun 1523Z	-18.00[a]
2019088	13 Jun 1456Z	13 Jun 1508Z	-12.00[a]
2019089	15 Jun 1439Z	15 Jun 1433Z	6.00
2019092	23 Jun 1940Z	23 Jun 1948Z	-8.00[a]
2019096	25 Jun 2010Z	25 Jun 2009Z	1.00
2019097	25 Jun 2012Z	25 Jun 2012Z	0.00[a]
2019098	27 Jun 1944Z	27 Jun 1941Z	3.00
2019103	12 Jul 1837Z	12 Jul 1833Z	4.00
2019116	25 Jul 1545Z	25 Jul 1540Z	5.00
2019120	26 Jul 1541Z	26 Jul 1532Z	9.00
2019122	27 Jul 1518Z	27 Jul 1521Z	-3.00[a]
2019124	30 Jul 1639Z	30 Jul 1653Z	-14.00[a]
2019134	13 Aug 1425Z	13 Aug 1422Z	3.00
2019137	23 Aug 1533Z	23 Aug 1524Z	9.00
2019138	25 Aug 1500Z	25 Aug 1516Z	-16.00[a]
2019139	26 Aug 1456Z	26 Aug 1510Z	-14.00[a]
2019140	28 Aug 1144Z	28 Aug 1137Z	7.00
2019141	28 Aug 1147Z	28 Aug 1140Z	7.00
2019144	04 Sep 1510Z	04 Sep 1508Z	2.00
2019146	08 Sep 1556Z	08 Sep 1554Z	2.00
2019149	13 Sep 1532Z	13 Sep 1522Z	10.00
2019150	13 Sep 1534Z	13 Sep 1527Z	7.00
2019151	17 Sep 1145Z	17 Sep 1138Z	7.00
2019152	02 Oct 1452Z	02 Oct 1446Z	6.00
2019157	04 Oct 1415Z	04 Oct 1412Z	3.00
Average Lag Time			6.02

[a] *NANU release time is prior to event start time. Event not included in average lag time.*

3.5 SIS Availability

3.5.1 Per-Slot Availability

The SPS PS makes the following assertions in Section 3.7.1:

- *"≥ 0.957 Probability that a Slot in the Baseline 24-Slot Configuration will be Occupied by a Satellite Broadcasting a Healthy SPS SIS"*
- *"≥ 0.957 Probability that a Slot in the Expanded Configuration will be Occupied by a Pair of Satellites Each Broadcasting a Healthy SPS SIS"*

The constraints include the note that this is to be calculated as an average over all slots in the 24-slot constellation, normalized annually.

The derivation of the SV/slot assignments is described in Appendix E.

This metric was verified by examining the status of each SV in the Baseline 24-Slot configuration (or pair of SVs in an expandable slot) at every 30 s interval throughout the year. The health status was determined from the subframe 1 health bits of the ephemeris being broadcast at the time of interest. In addition, data from both the MSN and the IGS networks were examined to verify that the SV was broadcasting a trackable signal at the time. The results are summarized in Table 3.12. The metric is averaged over the constellation, therefore the value in the bottom row (labeled "All Slots") must be greater than 0.957 in order for the assertion to be met.

Regardless of the individual slot availabilities, the average availability for the constellation was 0.999 , which is above the threshold of 0.957. Therefore the assertion being evaluated in this section was met.

Table 3.12: Per-Slot Availability for 2019

Plane-Slot	**# Missing Epochs**[b]	**Availability**
A1	997	0.999052
A2	493	0.999531
A3	1561	0.998515
A4	840	0.999201
B1[a]	1859	0.998232
B2	610	0.999420
B3	0	1.000000
B4	630	0.999401
C1	3334	0.996828
C2	1210	0.998849
C3	1117	0.998937
C4	728	0.999307
D1	1354	0.998712
D2[a]	4070	0.996128
D3	630	0.999401
D4	1082	0.998971
E1	1031	0.999019
E2	453	0.999569
E3	650	0.999382
E4	696	0.999338
F1	1120	0.998935
F2[a]	621	0.999409
F3	399	0.999620
F4	612	0.999418
All Slots	26097	0.998966

[a] *When B1, D2, and F2 are configured as expandable slots, both slot locations must be occupied by an available satellite for the slot to be counted as available.*

[b] *For each slot there were 1051200 total 30 s epochs in the evaluation period.*

3.5.2 Constellation Availability

The SPSPS08 makes the following assertions in Section 3.7.2:

- *"≥ 0.98 Probability that at least 21 Slots out of the 24 Slots will be Occupied Either by a Satellite Broadcasting a Healthy SPS SIS in the Baseline 24-Slot Configuration or by a Pair of Satellites Each Broadcasting a Healthy SPS SIS in the Expanded Slot Configuration"*
- *"≥ 0.99999 Probability that at least 20 Slots out of the 24 Slots will be Occupied Either by a Satellite Broadcasting a Healthy SPS SIS in the Baseline 24-Slot Configuration or by a Pair of Satellites Each Broadcasting a Healthy SPS SIS in the Expanded Slot Configuration"*

To evaluate this metric the subframe 1 health condition and the availability of signal were evaluated for each SV every 30 s for all of 2019. Following a literal reading of the requirement, the number of SVs broadcasting a healthy SIS was examined for each measurement interval and assigned to the correct slot. For non-expanded baseline slots, if an SV qualified as being in the slot and was transmitting a healthy signal, the slot was counted as occupied. For expanded slots, the slot was counted as occupied if two healthy SVs were found: one in each of the two portions of the expanded slot. If the count of occupied slots was greater than 20, the measurement interval was counted as a 1; otherwise the measurement interval was assigned a zero. The sum of the 1 values was then divided by the total number of measurement intervals. The value for 2019 is 1.00. Thus, both requirements are satisfied.

While this satisfies the metric, it does not provide much information on exactly how many SVs are typically healthy. To address this, at each 30 s interval the number of SVs broadcasting a healthy SIS was counted. This was done for both the count of occupied slots and for the number of SVs. The daily averages as a function of time are shown in Figure 3.11. As is clear, the number of occupied slots always exceeded 21.

3.5.3 Operational Satellite Counts

Table 3.7-3 of the SPSPS08 states:

- *"≥ 0.95 Probability that the Constellation will Have at least 24 Operational Satellites Regardless of Whether Those Operational Satellites are Located in Slots or Not"*

Under "Conditions and Constraints" the term Operational is defined as

> *"any satellite which appears in the transmitted navigation message almanac... regardless of whether that satellite is currently broadcasting a healthy SPS SIS or not or whether the broadcast SPS SIS also satisfies the other performance standards in this SPS PS or not."*

Given the information presented in Sections 3.5.1 and 3.5.2, we conclude that at least 24 SVs were operational 100% of the time for 2019, thus meeting the assertion. However, to evaluate this more explicity, the almanac status was examined directly. The process consisted of selecting an almanac for each day in 2019. IS-GPS-200 Section 20.3.3.5.1.3 [2] assigns a special meaning to the SV health bits in the almanac's subframe 4 page 25 and subframe 5 page 25 (Data ID 51 and 63). When these bits are set to all ones it indicates "the SV which has that ID is not available, and there might be no data regarding that SV in that page of subframes 4 and 5..." Given this definition, the process examines the subframe 4 and 5 health bits for the individual SVs and counts the number of SVs for which the health bits are other than all ones. The results are shown in Figure 3.12. This plot is very similar to the full constellation healthy satellite count shown in Figure 3.11. The almanac health data are not updated as frequently as those in subframe 1. As a result, the plot in Figure 3.12 contains only integer values. Therefore, on days when it appears the operational SV count is lower than the number of healthy SVs in the constellation, these reflect cases where an SV was set unhealthy for a small portion of the day. In Figure 3.11, such effects are averaged over the day, yielding a higher availability.

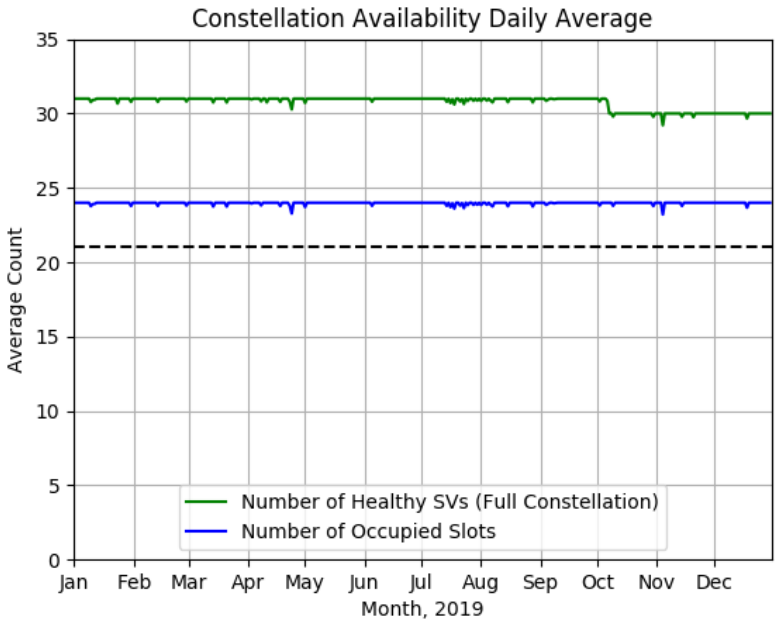

Figure 3.11: Daily Average Number of Occupied Slots

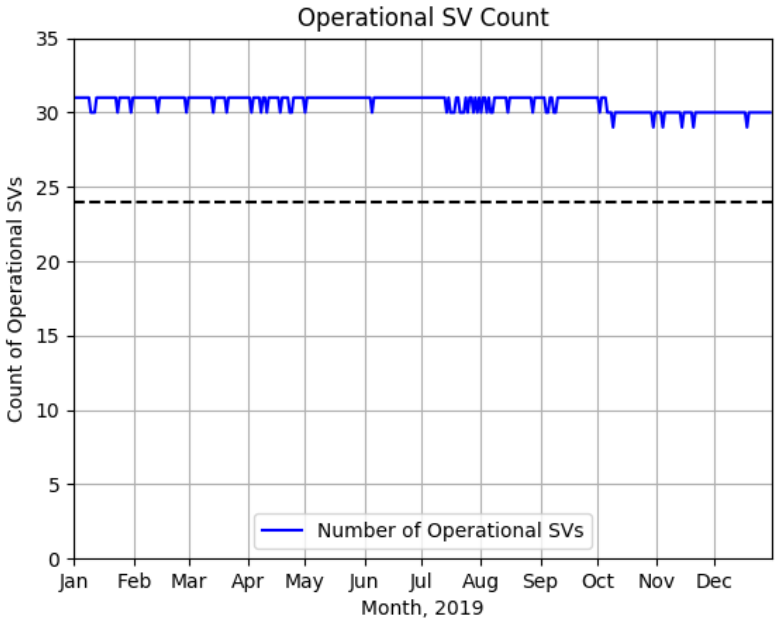

Figure 3.12: Count of Operational SVs by Day for 2019

3.6 Position/Time Domain Standards

3.6.1 Evaluation of DOP Assertions

Dilution of precision (DOP) measures the geometric diversity of a set of observations. That is to say, the diversity of the lines of sight from a user to the SVs that are observed. There are a variety of types of DOP including

- position dilution of precision (PDOP),
- geometric dilution of precision (GDOP),
- horizontal dilution of precision (HDOP),
- vertical dilution of precision (VDOP), and
- time dilution of precision (TDOP).

Accurate position and time solutions require a sufficient number of accurate signals with acceptable geometric diversity. The former requirement is addressed by the URE assertions in Section 3.4 of the performance standards. The requirement for geometric diversity is addressed by the PDOP assertions in Section 3.8.1 of the SPSPS08.

Section 3.6.1.1 provides the evaluation of the PDOP assertions stated in SPSPS08. Section 3.6.1.2 provides additional supporting information beyond the stated assertion and includes results specific to the various types of DOP.

3.6.1.1 PDOP Availability

Given representative user conditions and considering any 24 hour interval the SPSPS08 calls for:

- *"≥ 98% global PDOP of 6 or less"*
- *"≥ 88% worst site PDOP of 6 or less"*

Based on the definition of a representative receiver contained in SPS PS Section 3.8, a 5° minimum elevation angle is used for this evaluation.

These assertions were verified empirically throughout 2019 using a uniformly-spaced grid, containing N_{grid} points, to represent the terrestrial service volume at zero altitude, and an archive of the broadcast ephemerides transmitted by the SVs throughout the year. All healthy, transmitting SVs were considered. The grid was 111 km × 111 km (roughly 1° × 1° at the Equator). The time started at 0000Z each day and stepped through the entire day at one minute intervals (1440 points/day, defined as $1 \leq N_t \leq 1440$). The overall process followed is similar to that defined in Section 5.4.6 of the GPS Civil Monitoring Performance Specification (CMPS) [10].

The PDOP values were formed using the traditional PDOP algorithm [11], without regard for the impact of terrain. The coordinates of the grid locations provided the ground positions at which the PDOP was computed. The position of each SV was computed from the broadcast ephemeris available to a receiver at the time of interest. The only filtering performed was the exclusion of any unhealthy SVs (those with subframe 1 health bits set to other than all zeroes). The results of each calculation were tested with respect to the threshold of PDOP ≤ 6. If the condition was violated, a bad PDOP counter associated with the particular grid point, b_i for $1 \leq i \leq N_{grid}$, was incremented.

At least four SVs must be available to a receiver for a valid PDOP computation. This condition was fulfilled for all grid points at all times in 2019.

Once the PDOPs had been computed across all grid points, for each of the 1440 time increments during the day, the percentage of time PDOP ≤ 6 for the day was computed using the formula:

$$(\%PDOP \leq 6) = 100 \left(1 - \frac{\sum_{i=1}^{N_{grid}} b_i}{N_{grid} N_t} \right)$$

The worst site for a given day was identified from the same set of counters by finding the site with the maximum bad count: $b_{max} = \max_i(b_i)$. The ratio of b_{max} to N_t is an estimate of the fraction of time the worst site PDOP exceeds the threshold. This value was averaged over the year, and the percentage of time PDOP ≤ 6 was computed.

Table 3.13 summarizes the results of this analysis for the configurations of all SVs available. The second column ("Average daily % over 2019") provides the values for the assertions. The additional column is provided to verify that no single-day value actually dropped below the goal. From this table we conclude that the PDOP availability metrics are met for 2019.

Table 3.13: Summary of PDOP Availability

Metric	**Average daily % over 2019**	**Minimum daily % over 2019**
$\geq 98\%$ Global Average PDOP ≤ 6	99.999	99.099
$\geq 88\%$ Worst site PDOP ≤ 6	99.990	97.917

In addition to verifying the assertion, several additional analyses go beyond the direct question and speak to the matter of how well the system is performing on a more granular basis. The remainder of this chapter describes those analyses and results.

3.6.1.2 Additional DOP Analysis

There are several ways to look at DOP values when various averaging techniques are taken into account. Assuming a set of DOP values, each identified by latitude (λ), longitude (θ), and time (t), then each individual value is represented by $DOP_{\lambda,\theta,t}$.

The global average DOP for a day, $\langle DOP \rangle(day)$, is defined to be

$$\langle DOP \rangle(day) = \frac{\sum_t \sum_\theta \sum_\lambda DOP_{\lambda,\theta,t}}{N_{grid} \times N_t}$$

Another measure of performance is the average DOP over the day at the worst site,$\langle DOP \rangle_{worst\,site}$. In this case the average over a day is computed for each unique latitude/longitude combination and the worst average of the day is taken as the result.

$$\langle DOP \rangle_{worst\,site}(day) = \max_{\lambda,\theta} \left(\frac{\sum_t DOP_{\lambda,\theta,t}}{N_t} \right)$$

This statistic is the most closely related to the description of worst site used in Section 3.6.1.1.

The average of worst site DOP, $\langle DOP_{worst\,site} \rangle$, is calculated by obtaining the worst DOP in the latitude/longitude grid at each time, then averaging these values over the day.

$$\langle DOP_{worst\,site} \rangle(day) = \frac{\sum_t \max_{\lambda,\theta} (DOP_{\lambda,\theta,t})}{N_t}$$

This represents a measure of the worst DOP performance. It is not particularly useful from the user's point of view because the location of the worst site varies throughout the day.

Given that the $\langle DOP \rangle_{worst\,site}(day)$ is most closely related to the worse site definition used in Section 3.6.1.1, this is the statistic that will be used for "worst site" in the remainder of this section. For 2019, both $\langle DOP \rangle_{worst\,site}(day)$ and $\langle DOP_{worst\,site} \rangle(day)$ satisfy the SPS PS assertions.

It is worth noting the following mathematical relationship between these quantities:

$$\langle DOP \rangle \leq \langle DOP \rangle_{worst\,site} \leq \langle DOP_{worst\,site} \rangle$$

This serves as a sanity check on the DOP results in general and establishes that these metrics are increasingly sensitive to outliers in $DOP_{\lambda,\theta,t}$.

In calculating the percentage of the time that the $\langle DOP \rangle$ and $\langle DOP \rangle_{worst\,site}$ are within bounds, several other statistics were calculated which provide insight into the availability of the GPS constellation throughout the world. Included in these statistics are the annual means of the daily global average DOP and the $\langle DOP \rangle_{worst\,site}$ values. These values are presented in Table 3.14, with values for 2016 through 2018 provided

for comparison. The average number of satellites and the fewest satellites visible across the grid are calculated as part of the DOP calculations. Also shown in Table 3.14 are the annual means of the global average number of satellites visible to grid cells on a 111 km × 111 km (latitude by longitude) global grid and the annual means of the number of satellites in the worst-site grid cell (defined as seeing the fewest number of satellites). It should be noted that the worst site for each of these values was not only determined independently from day-to-day, it was also determined independently for each metric. That is to say, it is not guaranteed that the worst site with respect to Horizontal DOP (HDOP) is the same as the worst site with respect to PDOP. For all quantities shown in Table 3.14 the values are very similar across all four years.

Table 3.14: Additional DOP Annually-Averaged Visibility Statistics for 2016 – 2019

	$\langle$**DOP**$\rangle$				$\langle$**DOP**$\rangle_{\textbf{worst site}}$			
	2016	**2017**	**2018**	**2019**	**2016**	**2017**	**2018**	**2019**
Horizontal DOP	0.83	0.83	0.84	0.84	0.94	0.94	0.95	0.96
Vertical DOP	1.34	1.35	1.36	1.36	1.68	1.68	1.70	1.70
Time DOP	0.78	0.78	0.79	0.79	0.89	0.89	0.91	0.90
Position DOP	1.58	1.59	1.60	1.60	1.84	1.83	1.86	1.86
Geometry DOP	1.77	1.77	1.79	1.79	2.04	2.04	2.07	2.06
Number of visible SVs	10.39	10.49	10.42	10.42	5.93	5.95	5.32	5.02

There are a few other statistics that can add insight regarding the GPS system availability. The primary availability metric requires that the globally averaged PDOP be in-bounds at least 98% of the time. There are two related values: the number of days for which the PDOP is in bounds and the 98$^{\text{th}}$ percentile of the daily globally averaged PDOP values. Similarly, calculations can be done for $\langle DOP \rangle_{worst\,site}$ criteria of having the PDOP ≤ 6 greater than 88% of the time. Table 3.15 presents these values.

Table 3.15: Additional PDOP Statistics

	2016	**2017**	**2018**	**2019**
% of Days with the $\langle PDOP \rangle \leq 6$	100.00	100.00	100.00	100.00
% of Days with the $\langle PDOP \rangle$ at Worst Site ≤ 6	100.00	100.00	100.00	100.00
98$^{\text{th}}$ Percentile of $\langle PDOP \rangle$	1.63	1.60	1.64	1.62
88$^{\text{th}}$ Percentile of $\langle PDOP \rangle_{worst\,site}$	1.89	1.84	1.87	1.89

Table 3.15 shows that the average DOP values for 2019 are nearly identical to previous years.

Behind the statistics are the day-to-day variations. Figure 3.13 provides a time history of PDOP metrics considering all satellites for 2019. Three metrics are plotted:

- Daily Global Average PDOP: $\langle PDOP \rangle$
- Average Worst Site PDOP: $\langle PDOP \rangle_{worst\ site}$
- Average PDOP at Worst Site: $\langle PDOP_{worst\ site} \rangle$

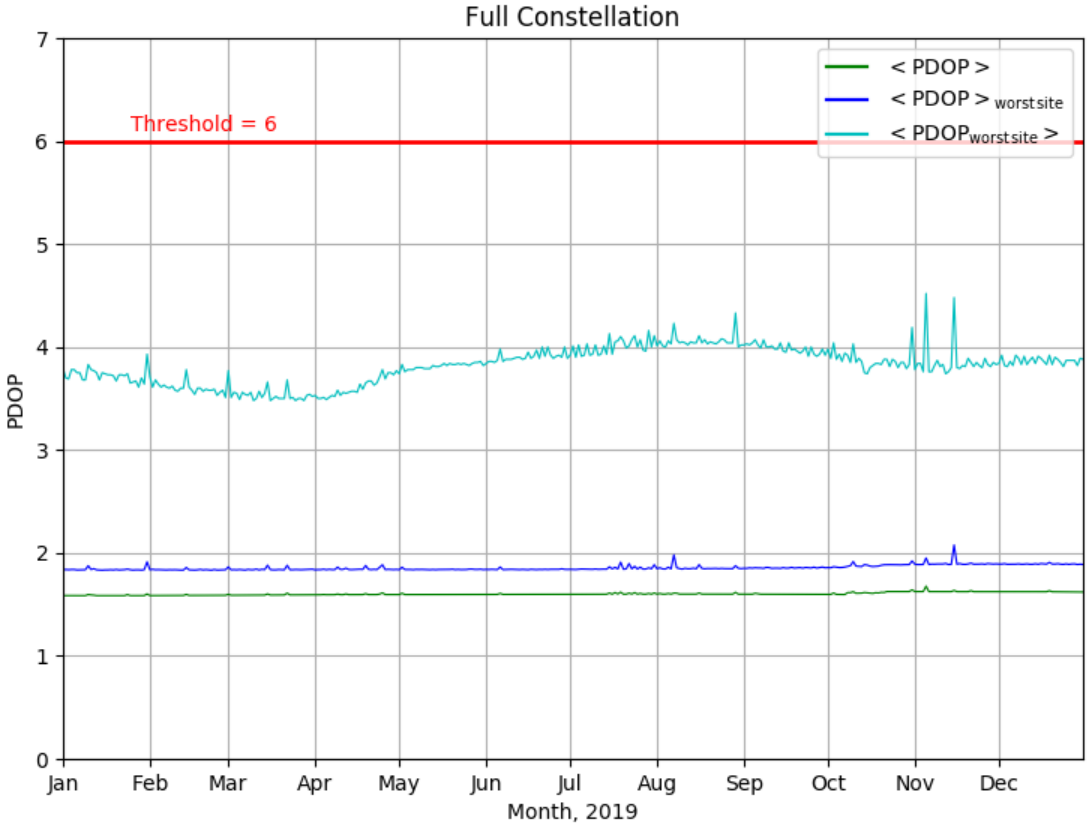

Figure 3.13: Daily PDOP Metrics Using All SVs for 2019

3.6.2 Position Service Availability

The positioning and timing availability standards are stated in Table 3.8-2 of SPSPS08 as follows:

- *"≥ 99% Horizontal Service Availability, average location"*
- *"≥ 99% Vertical Service Availability, average location"*
- *"≥ 90% Horizontal Service Availability, worst-case location"*
- *"≥ 90% Vertical Service Availability, worst-case location"*

The conditions and constraints associated with the standards include the specification of a 17 m horizontal 95$^{\text{th}}$ percentile threshold and a 37 m vertical 95$^{\text{th}}$ percentile threshold.

These are derived values as described in the sentence preceding SPSPS08 Table 3.8-2:

> *"The commitments for maintaining PDOP (Table 3.8-1) and SPS SIS URE accuracy (Table 3.4-1) result in support for position service availability standards as presented in Table 3.8-2."*

Because the commitments for PDOP and constellation SPS SIS URE have been met, this assertion in the SPSPS08 implies that the position and timing availability standards have also been fulfilled. A direct assessment of these metrics was not undertaken.

3.6.3 Position Accuracy

The positioning accuracy standards are stated in Table 3.8-3 of SPSPS08 as follows:

- *"≤ 9 m 95% Horizontal Error Global Average Position Domain Accuracy"*
- *"≤ 15 m 95% Vertical Error Global Average Position Domain Accuracy"*
- *"≤ 17 m 95% Horizontal Error Worst Site Position Domain Accuracy"*
- *"≤ 37 m 95% Vertical Error Worst Site Position Domain Accuracy"*

These are derived values as described in the sentence preceding SPSPS08 Table 3.8-3:

> *"The commitments for maintaining PDOP (Table 3.8-1) and SPS SIS URE accuracy (Table 3.4-1) result in support for position service availability standards as presented in Table 3.8-3."*

Because the commitments for PDOP and constellation SPS SIS URE have been met, the position and timing accuracy standards have also been fulfilled.

While this verifies the assertion has been fulfilled, it is useful to corroborate that finding through examination of empirical results. We do this by evaluating position solutions for a set of continuously operating stations from two networks (MSN and IGS). The process used by ARL:UT is described in Appendix B.4.

The process generates position solutions using both NGA and IGS observation data (see Figure 1.1) and using both a simplistic approach with no data editing and a receiver autonomous integrity monitoring (RAIM) approach.

We conducted the elevation angle processing with a 5° minimum elevation angle in agreement with the standard.

Once the solutions are computed, two sets of statistics were developed for each approach, yielding 4 sets of results. The first set is a set of daily average values across all stations. In the second set, the worst site is determined on a day-to-day basis and the worst site 95^{th} percentile values are computed.

These are empirical results and should not be construed to represent proof that the metrics presented in the standard have been met. Instead, they are presented as a means of corroboration that the standards have been met through the fulfillment of the more basic commitments of PDOP and SPS SIS URE.

3.6.3.1 Results for Daily Average

Using the approach outlined above, position solutions were computed at each 30 s interval for data from both the NGA and IGS stations. In the nominal case in which all stations are operating for a complete day, this yields 2880 solutions per station per day. Truth positions for the IGS stations were taken from the weekly Station Independent Exchange format (SINEX) files. Truth locations for the NGA stations were taken from station locations defined as part of the latest WGS 84 reference frame [12] with corrections for station velocities applied.

Residuals between estimated locations and the truth locations were computed in the form of North, East and Up components in meters. The horizontal residual was computed from the root sum square (RSS) of the North and East components, and the vertical residual was computed from the absolute value of the Up component. As a result, the residuals will have non-zero mean values. The statistics on the residuals were compiled across all stations in a set for a given day. Figures 3.14-3.17 show the daily average for the horizontal and vertical residuals corresponding to the four cases.

The statistics associated with the processing are provided in Table 3.16. The table contains the mean, median, maximum, and standard deviation of the daily values across 2019. The results are organized in this fashion to facilitate comparison of the same quantity across the various processing options. The results are expressed to the centimeter level of precision. This choice of precision is based on the fact that the truth station positions are known only at the few-centimeter level.

The following observations regarding the quality of the daily average position solutions may be drawn from the charts and the supporting statistics in Table 3.16:

- Outliers - Figure 3.15 shows a number of large outliers for the IGS averages computed with a simple pseudorange solution and no data editing. The outliers are distributed among several stations. These outliers are largely missing from Figure 3.14. This indicates the importance of conducting at least some level of data editing in the positioning process.

- Mean & Median values - The means and medians of the position residuals given in Table 3.16 are nearly identical for the NGA data sets, suggesting that if there are any 30 s position residual outliers, they are few in number and not too large. The means for the RAIM solutions from IGS are less than 5% higher than the medians. The means and medians for the IGS data set solutions with no data editing are significantly different. This is consistent with the outliers observed in Figure 3.14 and Figure 3.15 and with the maximum and standard deviation values for the IGS data set solutions with no editing. This suggests that there are some large 30 s position residuals in the epoch-by-epoch results for these data sets.

- Maximum values and Standard Deviation - The values shown in Table 3.16 for the IGS data sets are quite a bit larger than the corresponding values for the NGA data sets. Once again, this suggests that there are some large 30 s position residuals in the epoch-by-epoch results for these data sets.

- Differences between NGA and IGS results - The mean magnitude of the position residual as reported in Table 3.16 is slightly smaller for the NGA stations than for the IGS stations. There are a number of differences between the two station sets. The NGA station set is more homogeneous in that the same receiver model is used throughout the data processed for this analysis, the data are derived from full-code tracking, and a single organization prepared all the data sets using a single set of algorithms. By contrast, the IGS data sets come from a variety of receivers and were prepared and submitted by a variety of organizations. These differences likely account for the greater variability in the results derived from the IGS data sets.

Table 3.16: Daily Average Position Errors for 2019

Statistic	**Data Editing**	**Horizontal**		**Vertical**	
		IGS	**NGA**	**IGS**	**NGA**
Mean (m)	RAIM	1.24	1.09	2.12	1.45
	None	2.10	1.09	3.76	1.46
Median (m)	RAIM	1.23	1.09	2.09	1.45
	None	1.25	1.09	2.12	1.45
Maximum (m)	RAIM	2.17	1.23	3.46	1.61
	None	33.63	1.25	72.95	1.63
Std. Dev. (m)	RAIM	0.07	0.03	0.14	0.04
	None	3.60	0.03	6.71	0.05

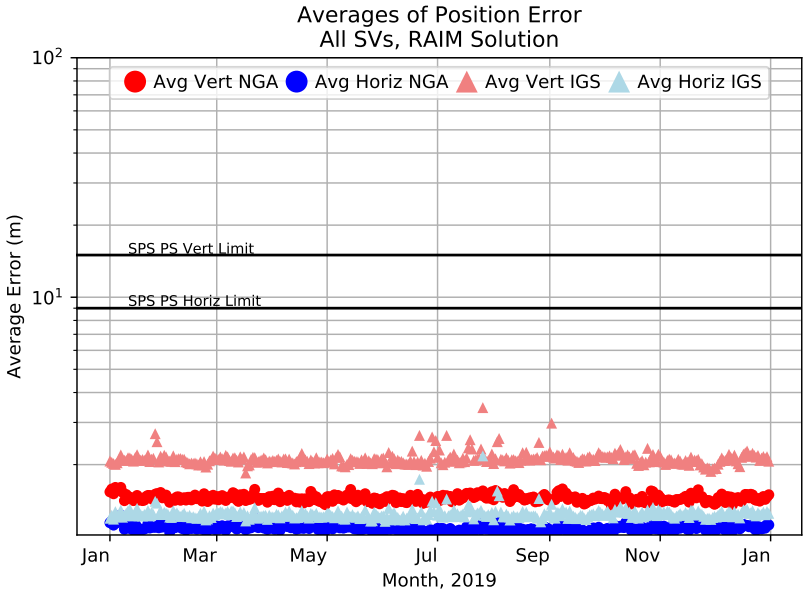

Figure 3.14: Daily Averaged Position Residuals Computed Using a RAIM Solution

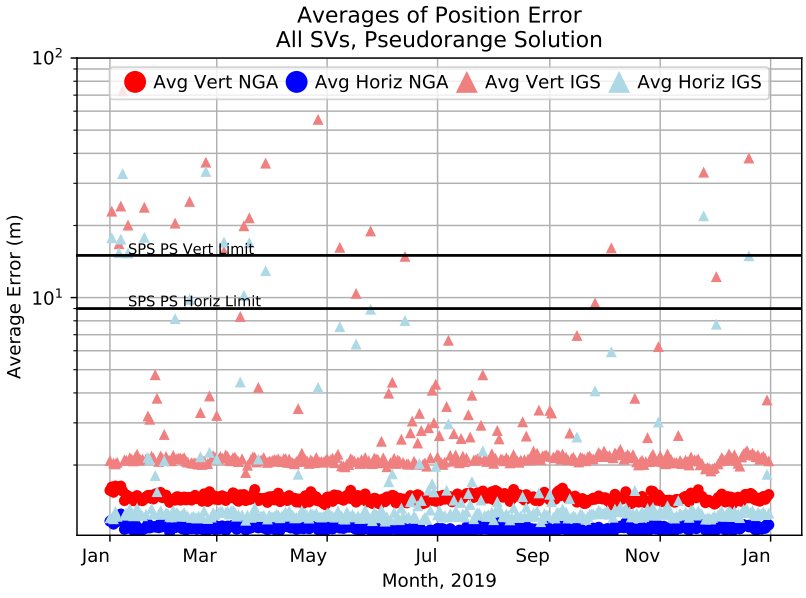

Figure 3.15: Daily Averaged Position Residuals Computed Using No Data Editing

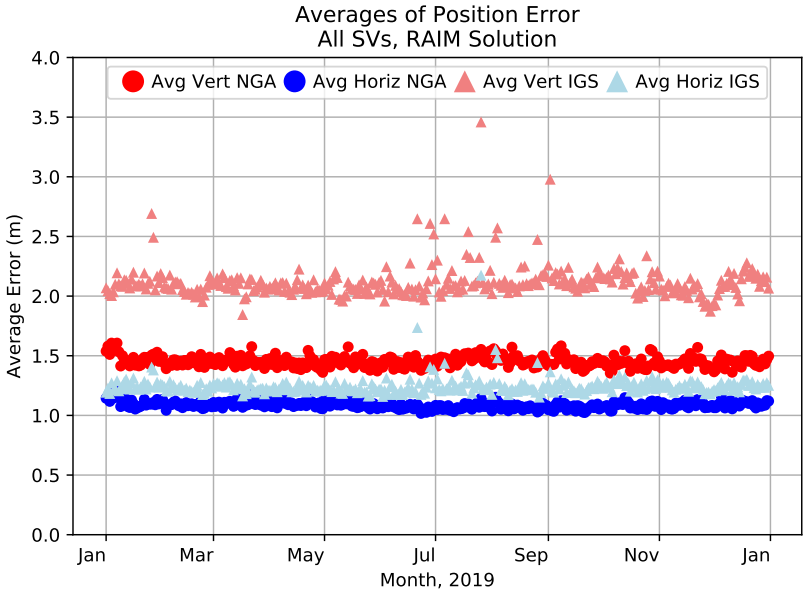

Figure 3.16: Daily Averaged Position Residuals Computed Using a RAIM Solution (enlarged)

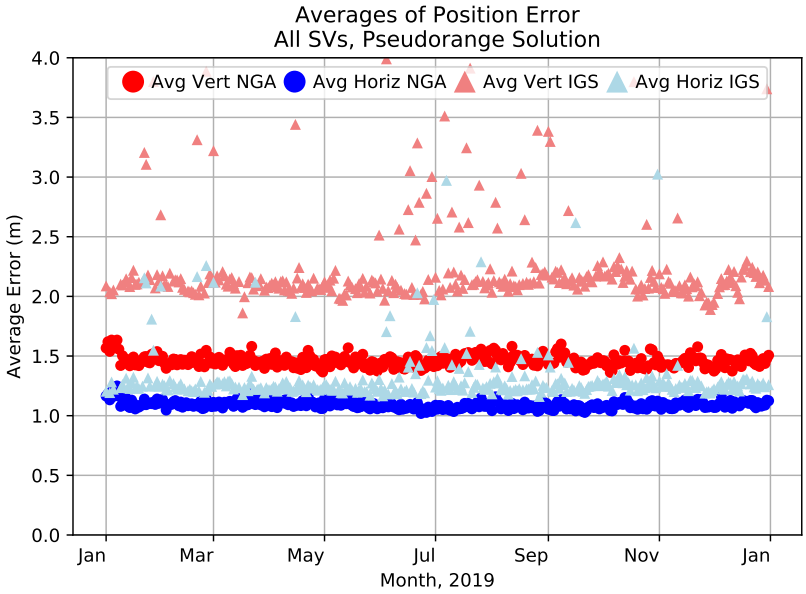

Figure 3.17: Daily Averaged Position Residuals Computed Using No Data Editing (enlarged)

3.6.3.2 Results for Worst Site 95th Percentile

The edited and non-edited 30 s position residuals were then independently processed to determine the worst site 95th percentile values. In this case, the 95th percentile was determined for each station in a given set, and the worst of these was used as the final 95th percentile value for that day. Figures 3.18-3.21 show these values for the various processing options described in the previous section. The plots are followed by a table of the statistics for the mean, median, maximum, and standard deviation of the daily worst site 95th percentile values. Some general observations on the results are included following the tables.

The statistics associated with the worst site 95th percentile values are provided in Table 3.17. As before, the results are organized in this fashion to facilitate comparison of the same quantity across the various processing options. Values are reported with a precision of one centimeter due to (a.) the magnitude of the standard deviation and (b.) the fact that the station positions are known only at the few-centimeter level.

Most of the observations from the daily averaged position residuals hold true in the case of the result from the worst site 95th percentile case. However, there are a few additional observations that can be drawn from Figures 3.18-3.21 and Table 3.17 regarding the worst site 95th percentile position solutions.

- Comparison to threshold - The values for both mean and median of the worst 95th percentile for both horizontal and vertical errors are well within the standard for both solutions. Compared to the thresholds of 17 m 95th percentile horizontal and 37 m 95th percentile vertical these results are outstanding.

- Comparison between processing options - For the NGA data sets, the statistics between the pseudorange and RAIM solutions are nearly identical. For the IGS data sets, a comparison of the solutions shows that the median is nearly the same while the mean is roughly a factor 2 smaller for the RAIM solutions. In addition, the maximum and standard deviation values are much smaller for the RAIM solution. Once again, this indicates that there are some large 30 s position residuals in the IGS results and illustrates the importance of data editing.

Table 3.17: Daily Worst Site 95th Percentile Position Errors for 2019

Statistic	Data Editing	Horizontal		Vertical	
		IGS	NGA	IGS	NGA
Mean (m)	RAIM	3.95	2.86	6.68	4.15
	None	8.36	2.88	8.82	4.18
Median (m)	RAIM	3.69	2.85	6.61	4.07
	None	3.77	2.87	6.65	4.10
Maximum (m)	RAIM	61.23	3.51	12.55	6.42
	None	160.71	3.94	437.25	6.40
Std. Dev. (m)	RAIM	3.09	0.12	0.67	0.43
	None	17.00	0.16	28.39	0.43

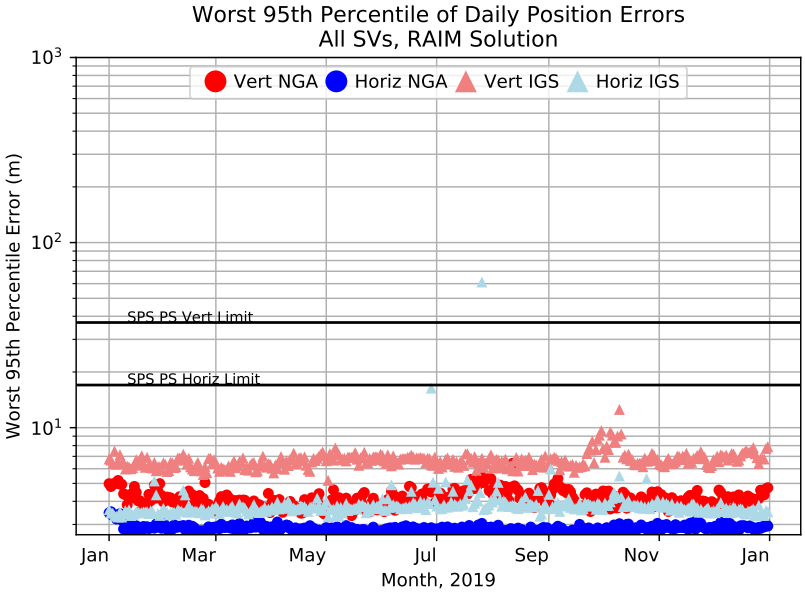

Figure 3.18: Worst Site 95$^{\text{th}}$ Daily Averaged Position Residuals Computed Using a RAIM Solution

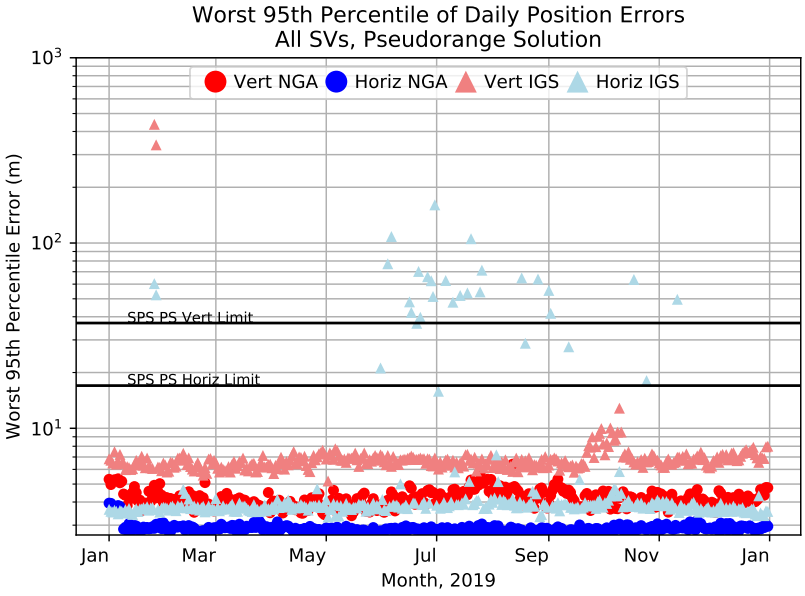

Figure 3.19: Worst Site 95$^{\text{th}}$ Daily Averaged Position Residuals Computed Using No Data Editing

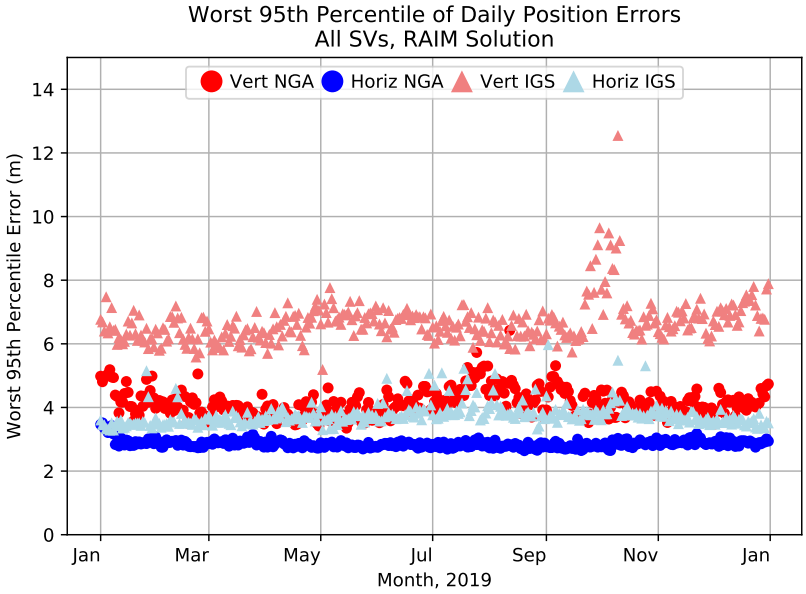

Figure 3.20: Worst Site 95th Daily Averaged Position Residuals Computed Using a RAIM Solution (enlarged)

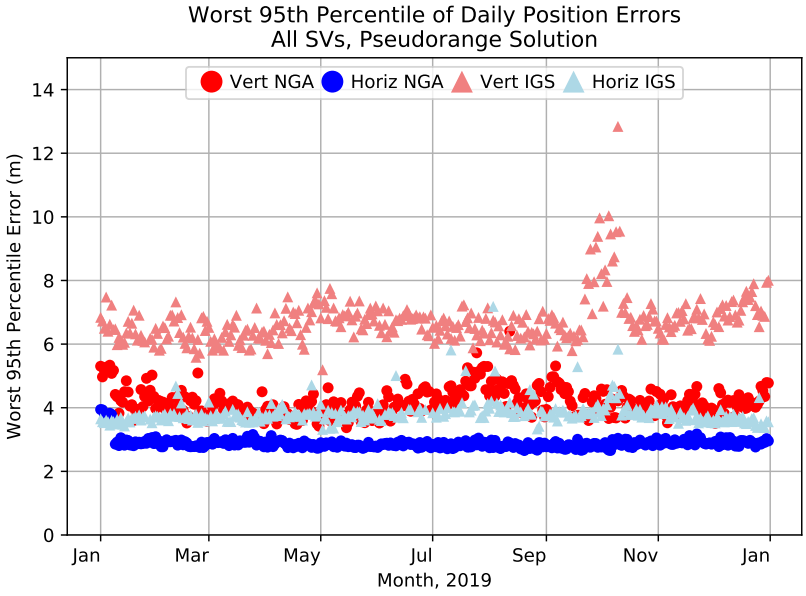

Figure 3.21: Worst Site 95th Daily Averaged Position Residuals Computed Using No Data Editing (enlarged)

3.6.4 Time Accuracy

The timing accuracy standard is stated in Table 3.8-3 of SPSPS08 as follows:

- *"≤ 40 nsec 95% Error Time Transfer Domain Accuracy"* (SIS only)

Conditions and Constraints:

- *Defined for a time transfer solution meeting the representative user conditions*
- *Standard based on a measurement interval of 24 hours averaged over all points in the service volume.*

The equation for time transfer accuracy relative to UTC(USNO) in GPS is found in the SPSPS08, Appendix B.2.2.

$$\text{UUTCE} = \sqrt{(\text{UERE} * \text{TTDOP}/c)^2 + (\text{UTCOE})^2)} \tag{3.6.1}$$

Time transfer dilution of precision (TTDOP) is $1/\sqrt{\text{N}}$, where N is the number is satellites visible to the user[1]. The User UTC(USNO) Error (UUTCE) calculation was performed for each day of the year.

This computation was done only for satellites that meet the criteria of: healthy, trackable, operational, and have no NANU at each given time. To meet the requirement of an average over all points in the service volume a worldwide grid with 425 points was created (see Figure 3.22). Because time transfer accuracy can be dependent on which SVs are in view of a given location, the grid was selected to provide a representative sampling of possible user locations around the world with a variety of possible SV combinations. The grid has 10° separation in latitude, and 10° separation in longitude at the equator. The longitude spacing for latitudes away from the equator was selected to be as close as possible to the distance between longitude points along the equator while maintaining an even number of intervals. This yields a spacing of roughly 1100 km.

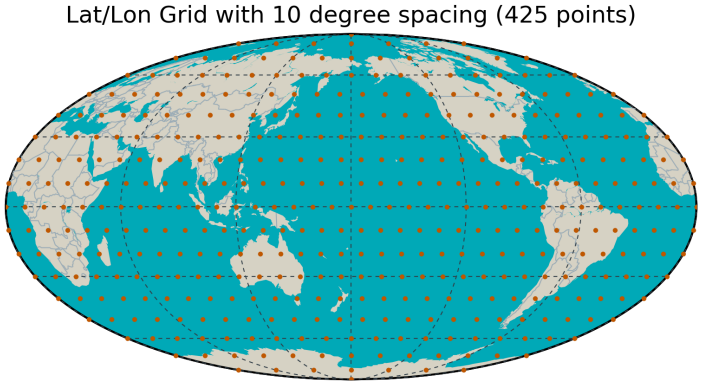

Figure 3.22: 10° Grid for UUTCE Calculation

[1] *as per conversation with Mr. Karl Kovach, author of the SPS PS, 31 August 2017*

Statistics were performed for each day over the grid of 425 points and time step of 15 minutes (96 time points), resulting in 40800 points to determine the 95th percentile UUTCE value.

The computation steps are:

1. Compute satellite positions for each time point in day using the broadcast ephemeris,
2. For each time and grid point,
   (a) find visible satellites (above 5° elevation) that meet the above criteria,
   (b) determine the appropriate UTCO data set (UTCO$_i$). The appropriate data set is the valid data set that has the latest reference time (t_{ot}) of all valid data sets received at that location at that time. Calculate UTCOE$_i$ = UTCO$_i$ - USNO, where USNO is the daily truth value,
   (c) get the Instantaneous SIS URE for each visible satellite, then take the mean of all values (UERE$_i$) and assign as the value for that time and grid point,
3. Calculate all 40800 UUTCE values for the day, find 95% containment of all values.

The daily UUTCE results over all grid points and times per day are shown in Figure 3.23. All of these results are well below 40 nsec. Therefore this assertion is met.

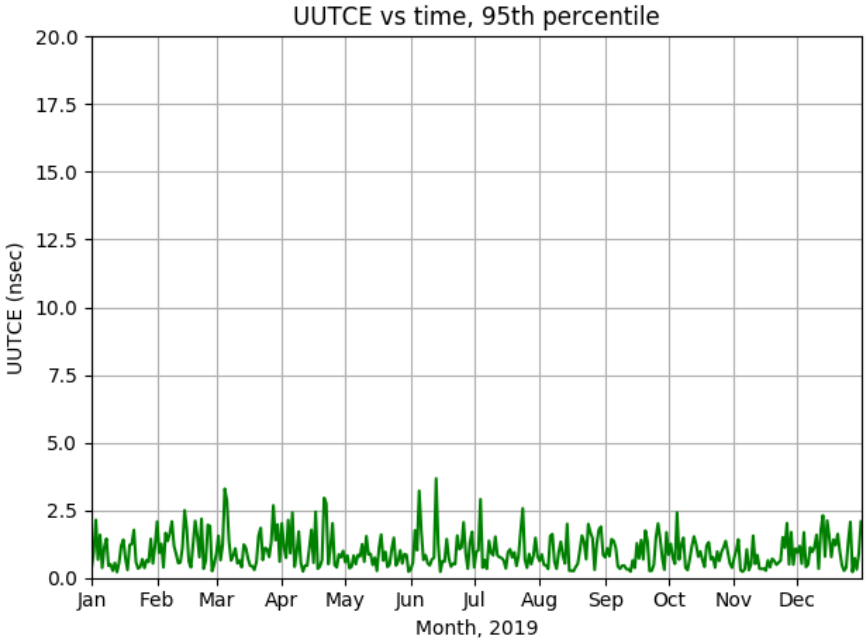

Figure 3.23: UUTCE 95th Percentile Values

Chapter 4

Additional Results of Interest

4.1 Health Values

Several of the assertions require examination of the health information transmitted by each SV. We have found it useful to examine the rate of occurrence for all possible combinations of the six health bits transmitted in subframe 1. We examined all unique navigation messages received in 2019. There are typically 13 unique message per day for each SV. This leads to approximately 4750 unique messages for each SV for the year. The total for SVN 34/PRN 18 was smaller as it was decommissioned in early October.

Table 4.1 presents a summary of health bit usage in the ephemerides broadcast during 2019. Each row in the table presents a summary for a specific SV. The summary across all SVs is shown at the bottom. The table contains the count of the number of times each unique health code was seen, the raw count of unique subframe 1 messages collected during the year, and the percentage of subframe 1 messages that contained specific health codes. Only two unique health settings were observed throughout 2019: binary 000000_2 (0x00) and binary 111111_2 (0x3F).

Table 4.1: Distribution of SV Health Values

SVN	PRN	Count by Health Code		Total # Subframe 1 Collected	% of Time by Health Code		Operational Days for 2019	Average # Subframe 1 per Operational Day
		0x3F	0x00		0x3F	0x00		
34	18	33	3647	3680	0.9	99.1	282	13.0
41	14	4	4751	4755	0.1	99.9	365	13.0
43	13	0	4749	4749	0.0	100.0	365	13.0
44	28	0	4803	4803	0.0	100.0	365	13.2
45	21	4	4753	4757	0.1	99.9	365	13.0
46	11	5	4750	4755	0.1	99.9	365	13.0
47	22	4	4749	4753	0.1	99.9	365	13.0
48	07	4	4754	4758	0.1	99.9	365	13.0
50	05	4	4751	4755	0.1	99.9	365	13.0
51	20	4	4747	4751	0.1	99.9	365	13.0
52	31	3	4751	4754	0.1	99.9	365	13.0
53	17	4	4757	4761	0.1	99.9	365	13.0
55	15	3	4750	4753	0.1	99.9	365	13.0
56	16	4	4744	4748	0.1	99.9	365	13.0
57	29	7	4745	4752	0.1	99.9	365	13.0
58	12	4	4757	4761	0.1	99.9	365	13.0
59	19	0	4753	4753	0.0	100.0	365	13.0
60	23	3	4749	4752	0.1	99.9	365	13.0
61	02	7	4746	4753	0.1	99.9	365	13.0
62	25	3	4754	4757	0.1	99.9	365	13.0
63	01	14	4746	4760	0.3	99.7	365	13.0
64	30	7	4748	4755	0.1	99.9	365	13.0
65	24	7	4846	4853	0.1	99.9	365	13.3
66	27	7	4751	4758	0.1	99.9	365	13.0
67	06	6	4752	4758	0.1	99.9	365	13.0
68	09	3	4760	4763	0.1	99.9	365	13.0
69	03	7	4749	4756	0.1	99.9	365	13.0
70	32	8	4752	4760	0.2	99.8	365	13.0
71	26	6	4748	4754	0.1	99.9	365	13.0
72	08	7	4776	4783	0.1	99.9	365	13.1
73	10	3	4749	4752	0.1	99.9	365	13.0
All SVs		175	146337	146512	0.1	99.9	365	401.4

4.2 Age of Data

The Age of Data (AOD) represents the elapsed time between the observations that were used to create the broadcast navigation message and the time when the contents of subframes 1, 2, and 3 became available to the user to estimate the position of a SV. The accuracy of GPS (at least for users that depend on the broadcast ephemeris) is indirectly tied to the AOD because the prediction accuracy degrades over time (see Section 3.2.2). This is especially true for the clock prediction. It has been recognized that reducing the AOD improves position, velocity, or time (PVT) solutions for autonomous users; however, there is an impact in terms of increased operations tempo at 2nd Space Operations Squadron (2SOPS).

Note that there is no need for a GPS receiver to refer to AOD in any PVT computation other than the optional application of the navigation message correction table (NMCT). (See IS-GPS-200 Section 20.3.3.5.1.9 for a description of the NMCT.) The AOD is computed here to validate that the operators at 2SOPS are not modifying the operational tempo to maintain the URE accuracy described in Section 3.2.

The daily average AOD throughout 2019 is shown in Table 4.2, along with values for the previous three years. Details on how AOD was computed are provided in Appendix B.3. The daily average AOD for the constellation, Block IIR/IIR-M, and Block IIF is illustrated in Figure 4.1. The single Block IIA SV, SVN 34/PRN 18, is not shown in Figure 4.1 as there were no other Block IIA SVs with which to conduct an average. In addition, this SV was subject of several NANUs prior to its decommissioning in October (see Tables 3.11, 3.9). The average AOD is generally constant throughout 2019, which indicates that any variations in the URE results discussed earlier are not due to changes in operations tempo at 2SOPS.

Table 4.2: Age of Data of the Navigation Message by SV Type

	Average Age of Data (hrs)			
	2016	**2017**	**2018**	**2019**
Full Constellation	11.9	12.1	12.1	12.0
Block II/IIA	11.7	–	11.9	12.0
Block IIR/IIR-M	11.9	12.1	12.1	12.0
Block IIF	11.8	12.1	12.1	12.0

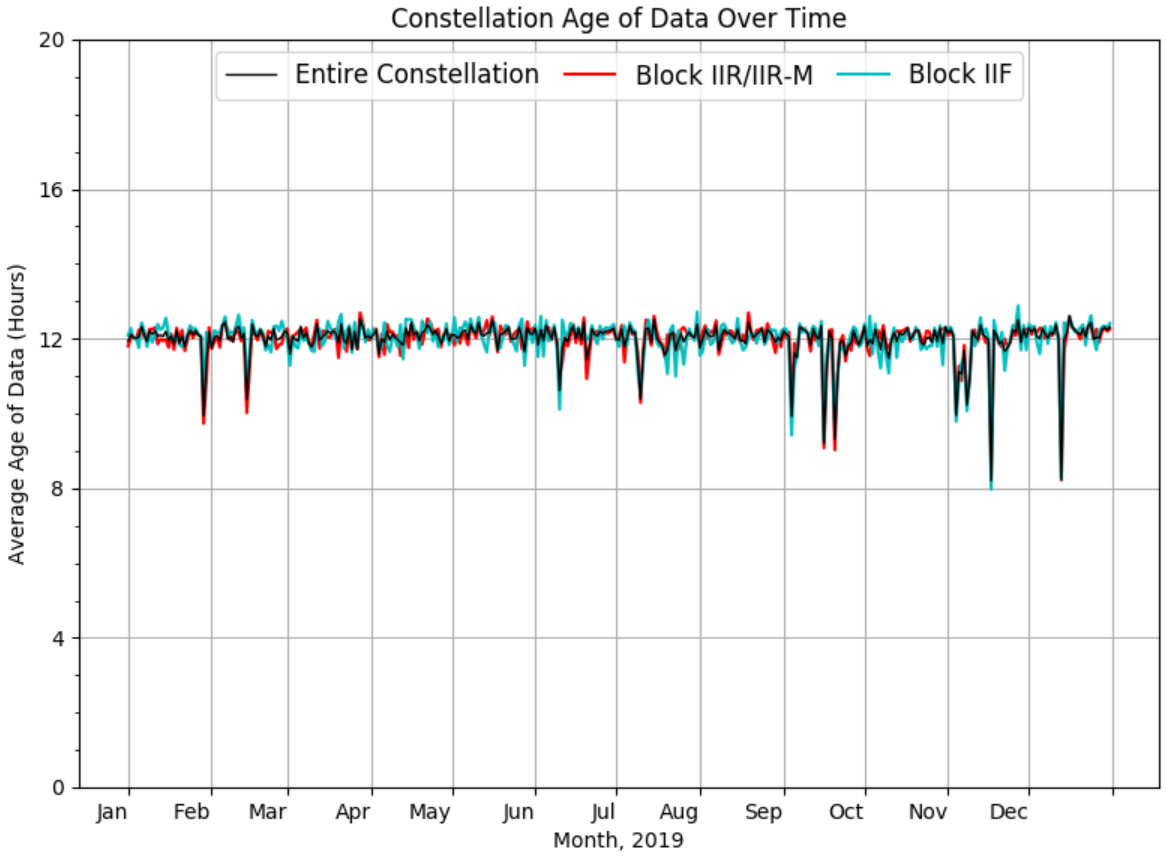

Figure 4.1: Constellation Age of Data for 2019

4.3 User Range Accuracy Index Values

Table 4.3 and Figure 4.2 present a summary of the analysis of the URA index values throughout 2019. The total number of navigation messages examined differs from the health summary in Section 4.1 as only URA index values corresponding to health settings of 0x00 are included in this analysis.

The vast majority of the values are 0, 1, or 2 (over 99.9%). Index values of 3 and 4 were very rare. No values over 4 were observed.

Table 4.3: Distribution of SV URA Index Values

SVN	PRN	URA Index						Total # Subframe 1 examined[a]	Average # Subframe 1 per Oper. Day[a]	Oper. Days for 2019
		5	4	3	2	1	0			
34	18				1	411	3235	3647	13.0	282
41	14		4	1	5	389	4352	4751	13.0	365
43	13					384	4365	4749	13.0	365
44	28			6	745	1178	2874	4803	13.2	365
45	21			5	2	250	4496	4753	13.0	365
46	11					342	4408	4750	13.0	365
47	22			2	6	70	4671	4749	13.0	365
48	07				4	375	4375	4754	13.0	365
50	05				6	73	4672	4751	13.0	365
51	20				1	71	4675	4747	13.0	365
52	31		6	1	8	438	4298	4751	13.0	365
53	17				1	684	4072	4757	13.0	365
55	15					151	4599	4750	13.0	365
56	16		1	5	2	296	4440	4744	13.0	365
57	29				7	703	4035	4745	13.0	365
58	12				3	295	4459	4757	13.0	365
59	19					346	4407	4753	13.0	365
60	23		2	4	5	179	4559	4749	13.0	365
61	02			1	5	385	4355	4746	13.0	365
62	25					324	4430	4754	13.0	365
63	01					200	4546	4746	13.0	365
64	30			5	5	351	4387	4748	13.0	365
65	24				90	1620	3136	4846	13.3	365
66	27			3	4	343	4401	4751	13.0	365
67	06		2	3	6	217	4524	4752	13.0	365
68	09					174	4586	4760	13.0	365
69	03		1	5	2	171	4570	4749	13.0	365
70	32		5	1	5	114	4627	4752	13.0	365
71	26				1	333	4414	4748	13.0	365
72	08				1	484	4291	4776	13.1	365
73	10					52	4697	4749	13.0	365
All SVs		0	21	42	915	11403	133956	146337	400.9	365

[a] *Only sets of SF 1,2,3 that include a healthy indication are included.*

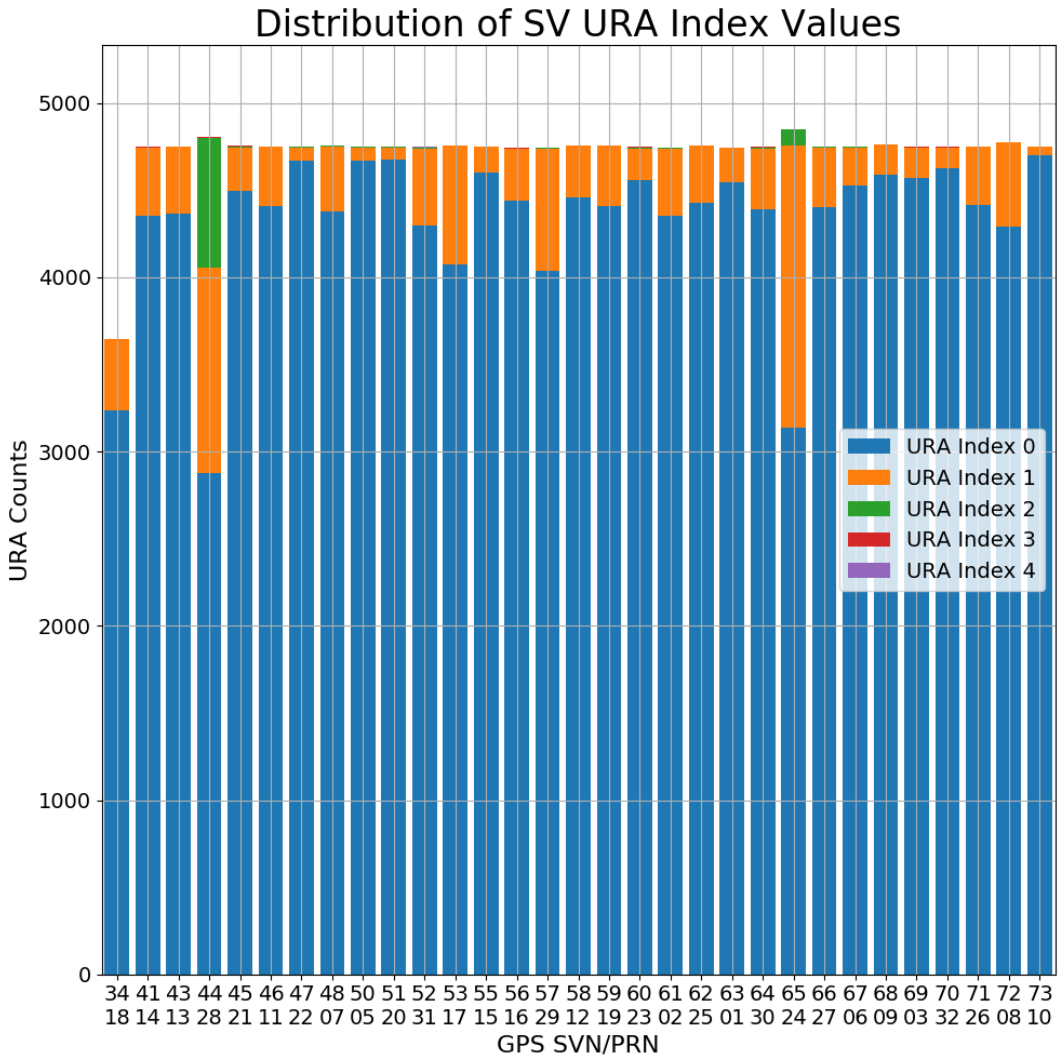

Figure 4.2: Stacked Bar Plot of SV URA Index Counts for 2019

4.4 Extended Mode Operations

IS-GPS-200 defines Normal Operations as the period of time when subframe 1, 2, and 3 data sets are transmitted by the SV for periods of two hours with a curve fit interval of four hours (IS-GPS-200 Section 20.3.4.4). This definition is taken to be the same as the definition of Normal Operations in SPSPS08 for the URE metrics. To determine if any SV operated in other than Normal Operations at any time in 2019, the broadcast ephemerides were examined to determine if any contained fit interval flags were set to 1. (See IS-GPS-200 20.3.3.4.3.1 for definition of the fit interval flag.)

The analysis found a total of 56 examples of extended operations for satellites set healthy. The examples were distributed across 42 days. The average time of an occurrence was 55 minutes. The minimum duration was 30 seconds and the maximum duration was 4 hours 4 minutes. These results are summarized in Table 4.4.

Given the relative rarity of occurrence, the URE values for the periods summarized in Table 4.4 are included in the statistics presented in Section 3.2.1, even though a strict interpretation of the SPSPS08 would suggest that they be removed. However, the SVs involved were still set healthy and (presumably) being used by user equipment, it is appropriate to include these results to reflect performance seen by the users.

Examination of the ephemerides from past years reveals that 2019 is not an anomaly. Such periods have been found in all years checked (back to 2005).

Past discussions with the operators have revealed several reasons for these occurrences. Some are associated with Alternate MCS (AMCS) testing. When operations are transitioned from the MCS to the AMCS (and reverse) it is possible that SVs nearing the end of their daily cycle may experience a longer-than-normal upload cycle. Other occurrences may be caused by delays due to ground antenna maintenance or due to operator concentration on higher-priority issues with the constellation at the time.

Table 4.4: Summary of Occurrences of Extended Mode Operations

SVN	PRN	# of Occurrences		Duration (minutes)	
		Healthy	Unhealthy	Healthy	Unhealthy
41	14	1	0	27	0
44	28	4	0	75	0
47	22	2	0	21	0
50	05	3	0	211	0
51	20	1	0	120	0
52	31	5	0	399	0
53	17	1	0	69	0
55	15	3	0	20	0
57	29	1	0	244	0
58	12	4	0	334	0
59	19	1	0	44	0
61	02	1	0	34	0
62	25	1	0	84	0
63	01	1	0	77	0
64	30	3	0	69	0
65	24	1	0	0	0
66	27	4	0	245	0
67	06	3	0	181	0
68	09	1	0	77	0
69	03	4	0	75	0
70	32	3	0	179	0
71	26	4	0	87	0
72	08	3	0	161	0
73	10	1	0	103	0
Totals		56	0	2936	0

Appendix A

URE as a Function of AOD

This appendix contains supporting information for the results presented in Section 3.2.2. Charts of SIS RMS URE vs. AOD similar to Figures 3.4-3.7 are presented for each GPS SV. The charts are organized by SV block and by ascending SVN within each block.

These charts are based on the same set of 30 s Instantaneous RMS SIS URE values used in Section 3.2.1. For each SV, the entire year of 30 s URE values was grouped by AOD in bins of 15 minutes each. The URE values in each bin were sorted and the 95^{th} percentile was determined. Since GPS SVs are typically uploaded daily, bins beyond 24 hours of AOD are sparsely populated. Bins with few points tend to be dominated by occasional high-value outliers; which can lead to erroneous conclusions about behavior. Therefore, bins containing fewer than 10% of points relative to the maximum populated bin were dropped before plotting.

The figures on the following pages each show two curves:

- Blue: 95^{th} percentile SIS RMS URE vs. AOD (in hours)
- Green: the count of points in each bin as a function of AOD

Note that for most SVs, the green curve has a well-defined horizontal plateau that begins near zero AOD, continues for roughly 24 hours, and then drops quickly toward zero. The location of the right-hand drop of the green curve toward zero provides an estimate of the typical upload period for the SV. In cases where the SV is uploaded more frequently, the shape of the green curve will vary reflecting that difference.

A.1 Block IIA SVs

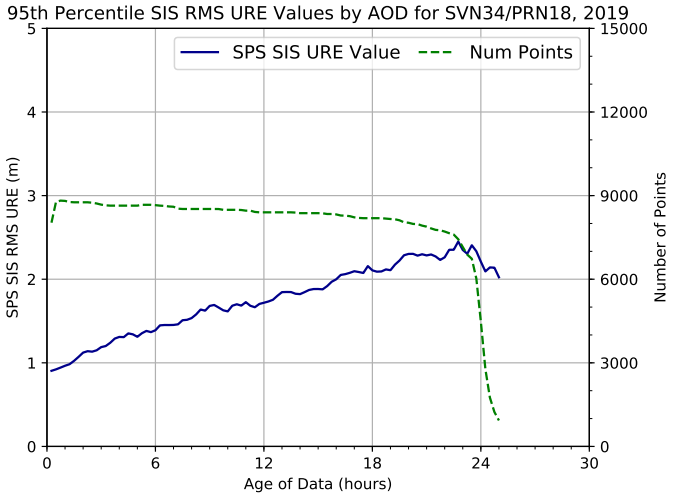

A.2 Block IIR SVs

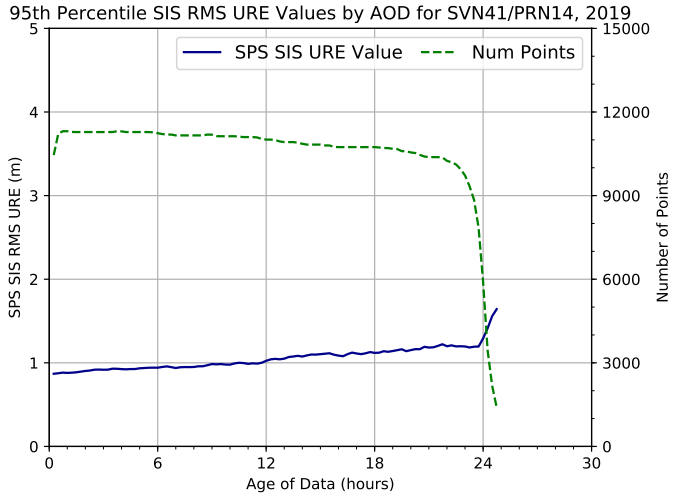

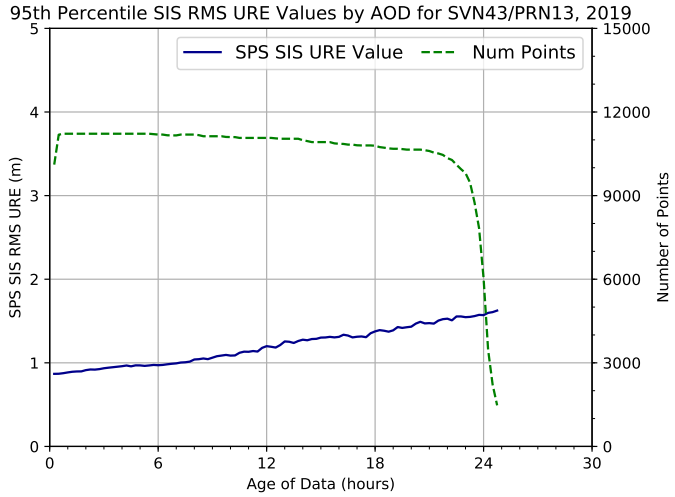

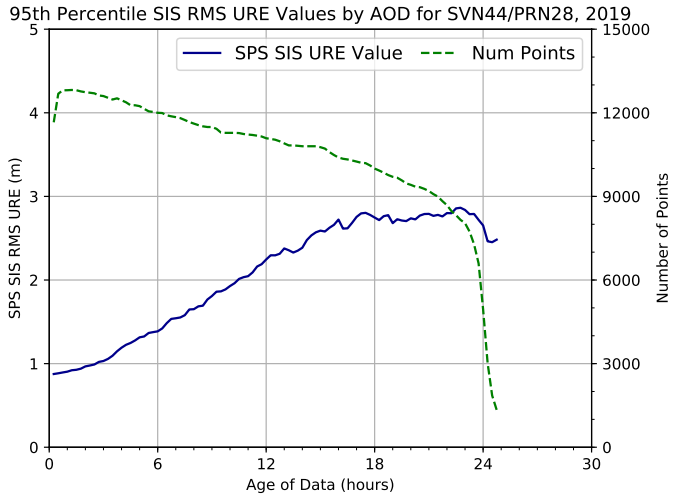

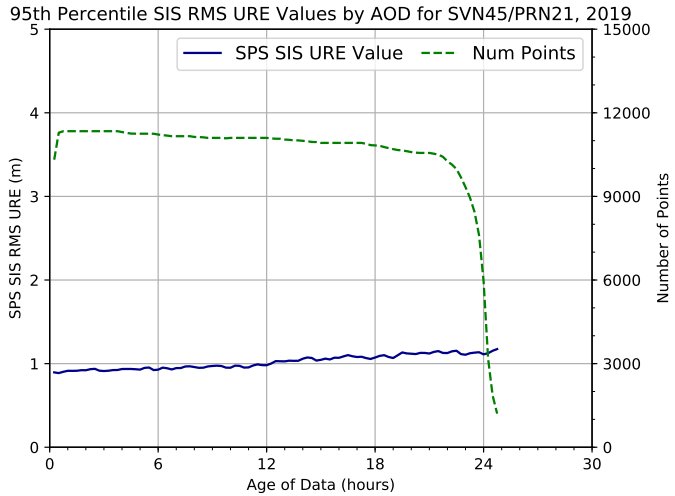

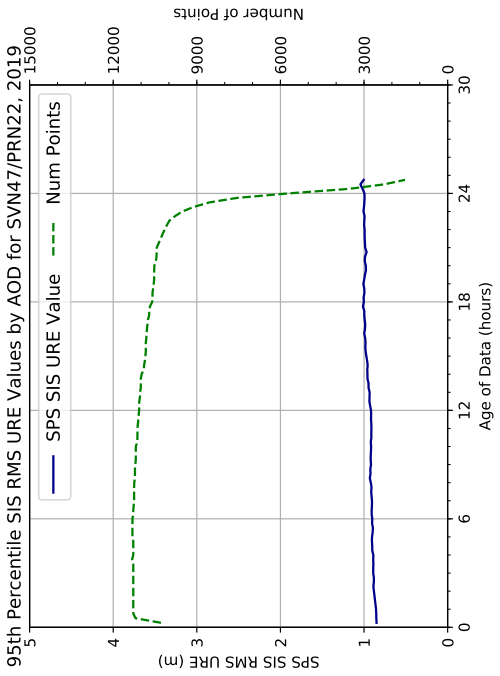
95th Percentile SIS RMS URE Values by AOD for SVN47/PRN22, 2019
SPS SIS URE Value
Num Points
SPS SIS RMS URE (m)
Number of Points
Age of Data (hours)

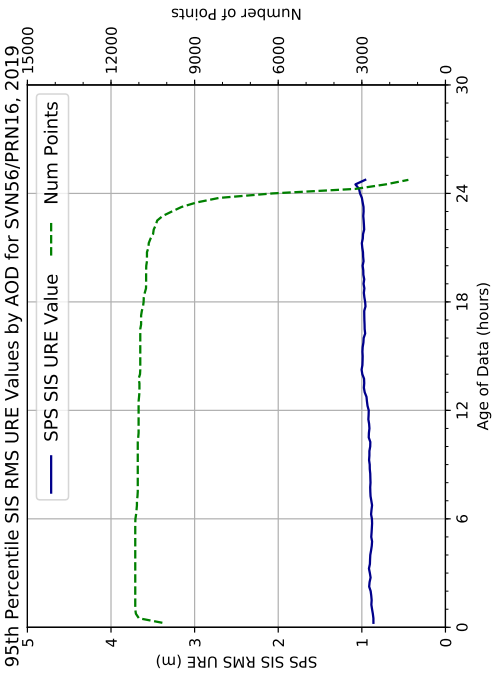
95th Percentile SIS RMS URE Values by AOD for SVN56/PRN16, 2019
SPS SIS URE Value
Num Points
SPS SIS RMS URE (m)
Number of Points
Age of Data (hours)

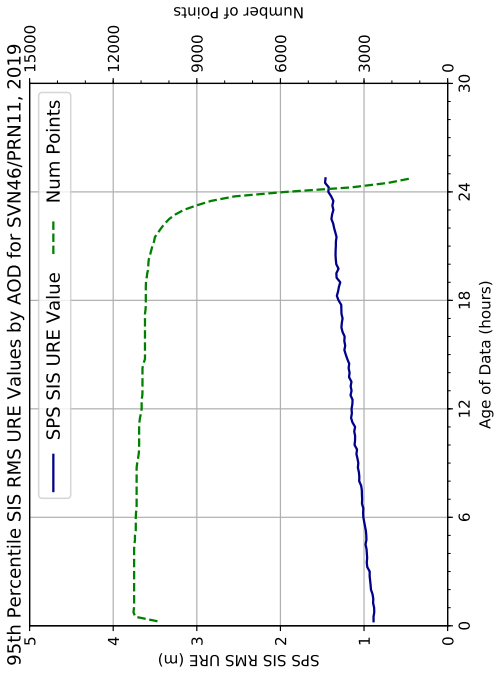
95th Percentile SIS RMS URE Values by AOD for SVN46/PRN11, 2019
SPS SIS URE Value
Num Points
SPS SIS RMS URE (m)
Number of Points
Age of Data (hours)

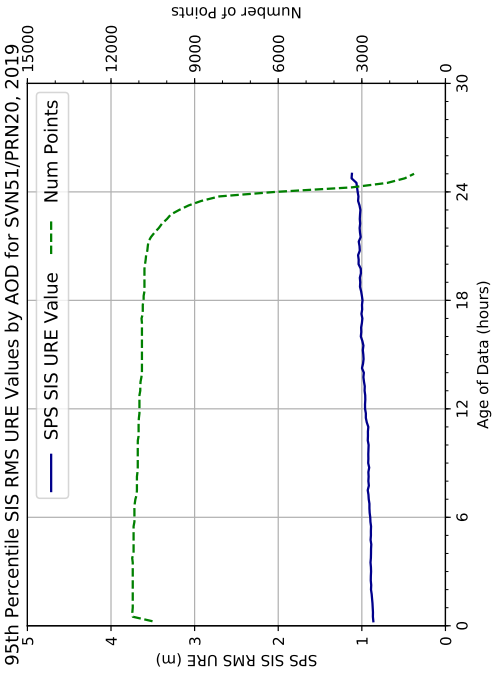
95th Percentile SIS RMS URE Values by AOD for SVN51/PRN20, 2019
SPS SIS URE Value
Num Points
SPS SIS RMS URE (m)
Number of Points
Age of Data (hours)

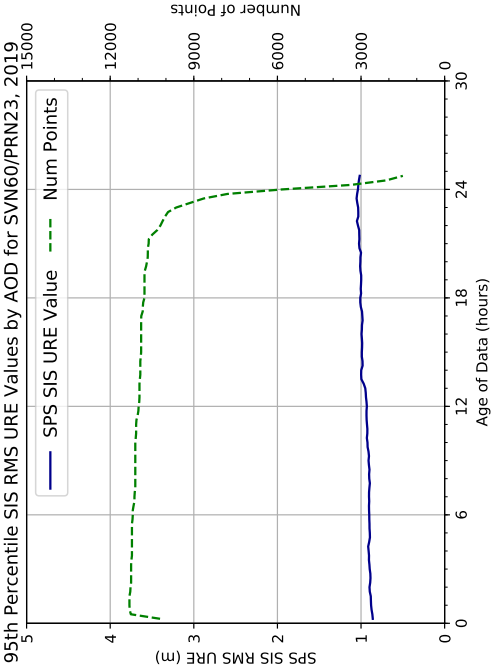
95th Percentile SIS RMS URE Values by AOD for SVN60/PRN23, 2019
SPS SIS URE Value
Num Points
SPS SIS RMS URE (m)
Number of Points
Age of Data (hours)

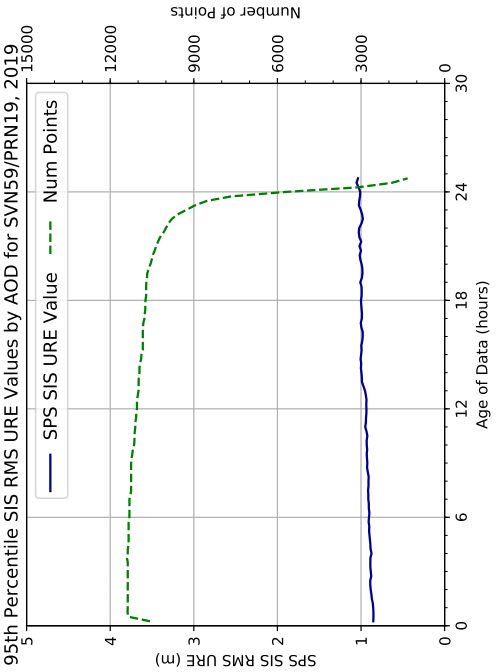
95th Percentile SIS RMS URE Values by AOD for SVN59/PRN19, 2019
SPS SIS URE Value
Num Points
SPS SIS RMS URE (m)
Number of Points
Age of Data (hours)

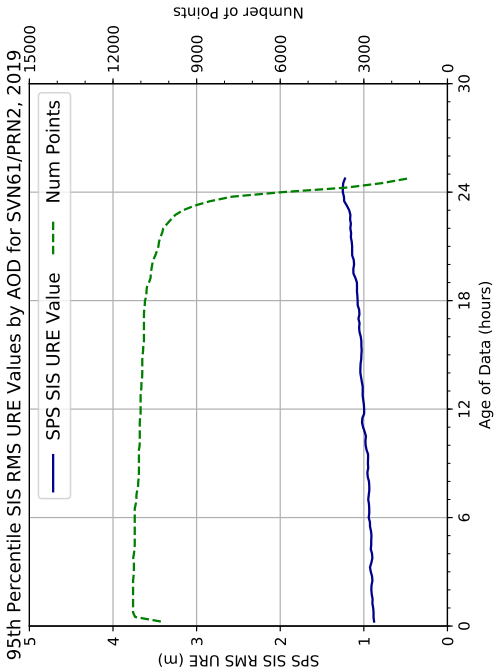
95th Percentile SIS RMS URE Values by AOD for SVN61/PRN2, 2019
SPS SIS URE Value
Num Points
SPS SIS RMS URE (m)
Number of Points
Age of Data (hours)

A.3 Block IIR-M SVs

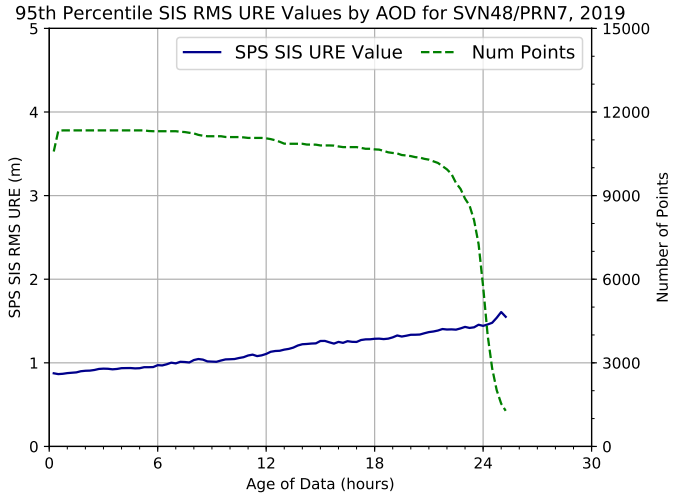

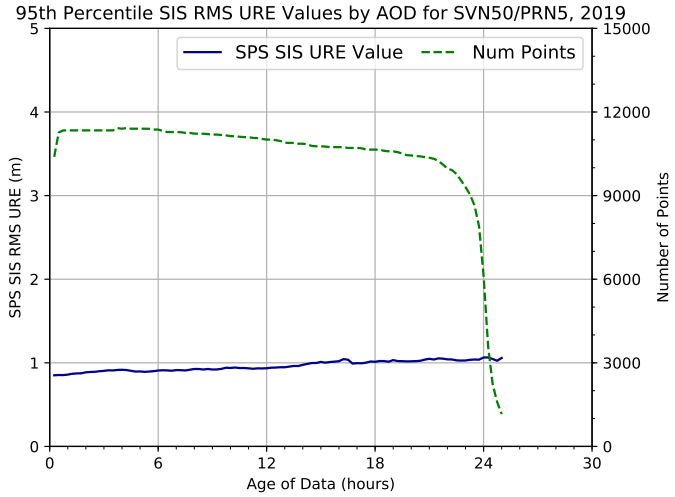

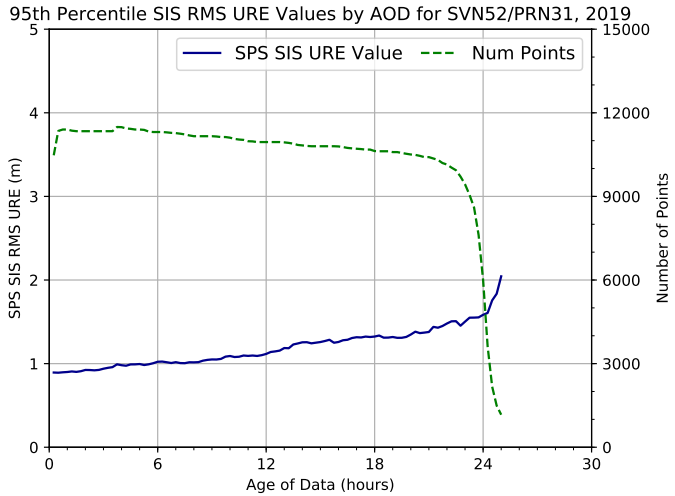

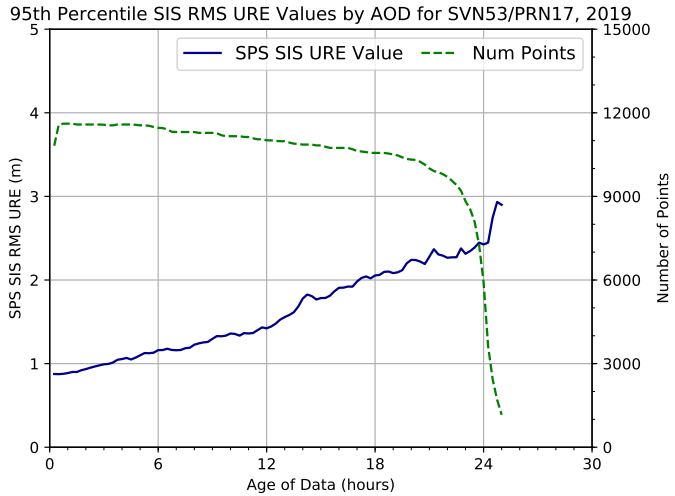

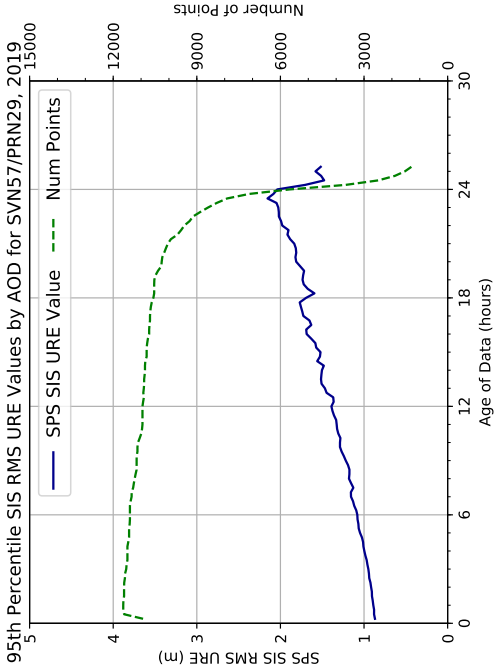
95th Percentile SIS RMS URE Values by AOD for SVN57/PRN29, 2019
SPS SIS URE Value
Num Points
SPS SIS RMS URE (m)
Number of Points
Age of Data (hours)

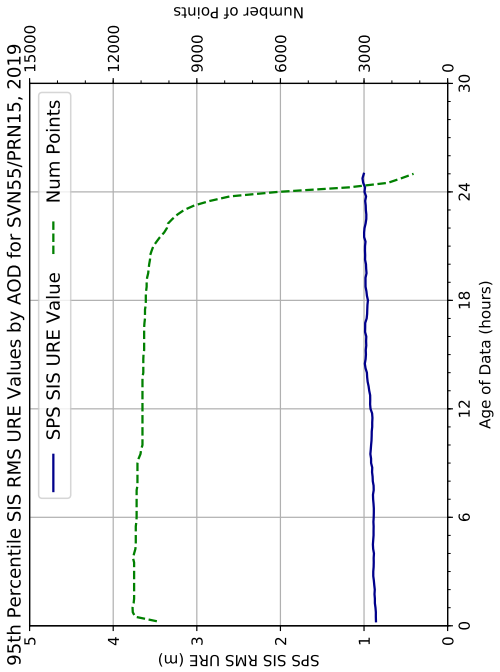
95th Percentile SIS RMS URE Values by AOD for SVN55/PRN15, 2019
SPS SIS URE Value
Num Points
SPS SIS RMS URE (m)
Number of Points
Age of Data (hours)

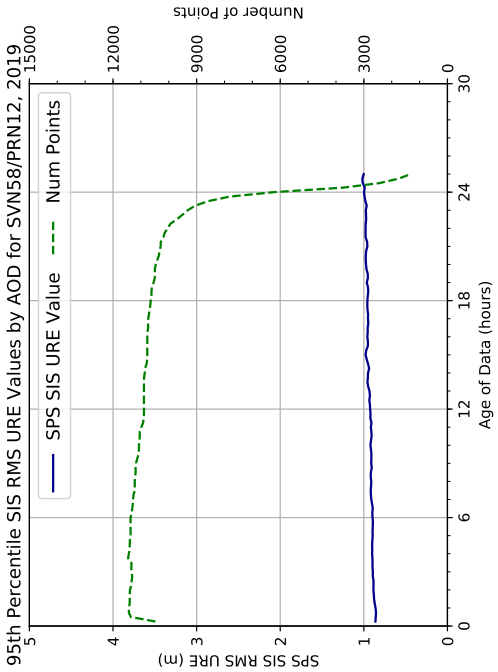
95th Percentile SIS RMS URE Values by AOD for SVN58/PRN12, 2019
SPS SIS URE Value
Num Points
SPS SIS RMS URE (m)
Number of Points
Age of Data (hours)

A.4 Block IIF SVs

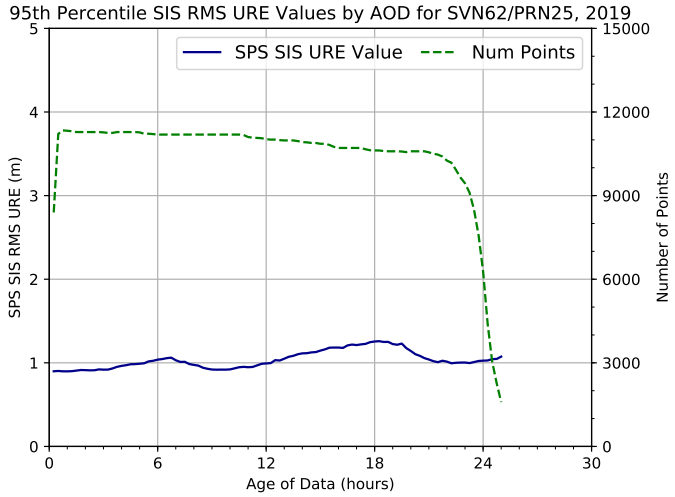

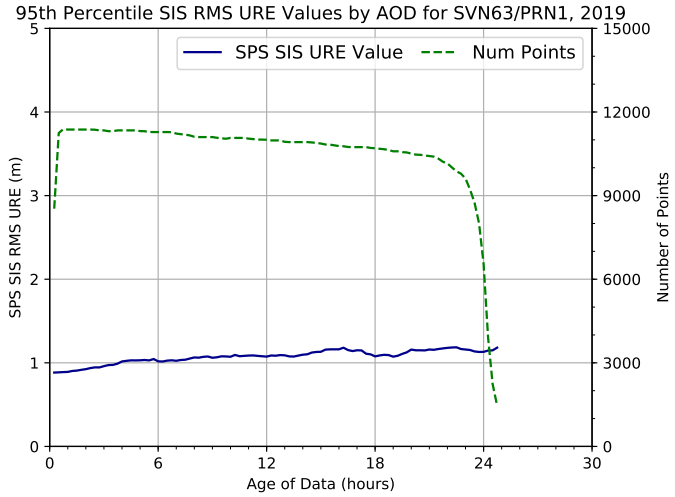

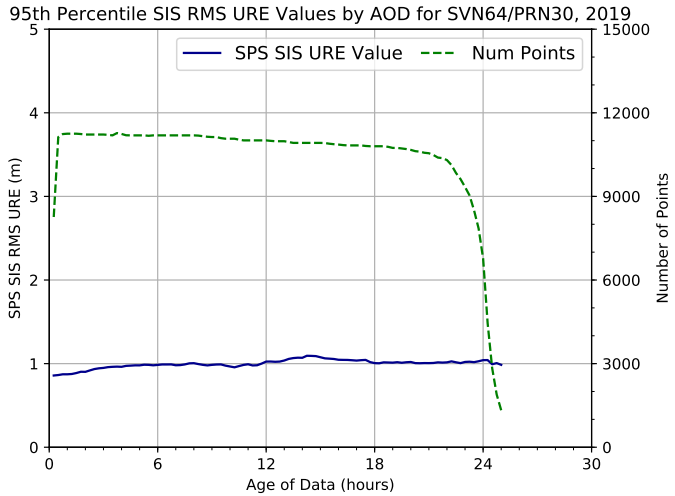

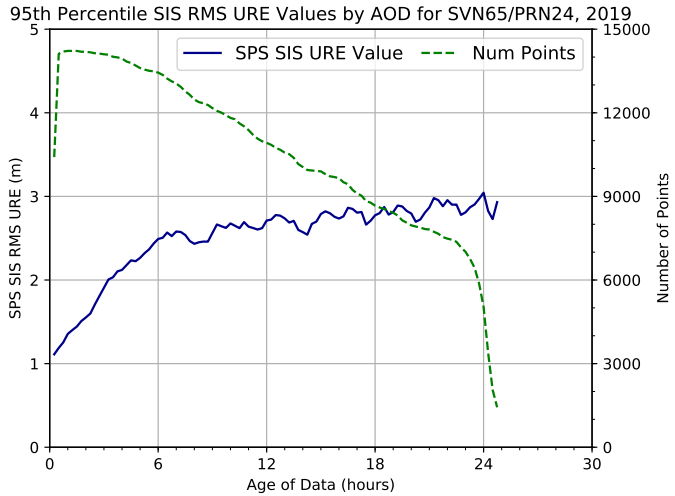

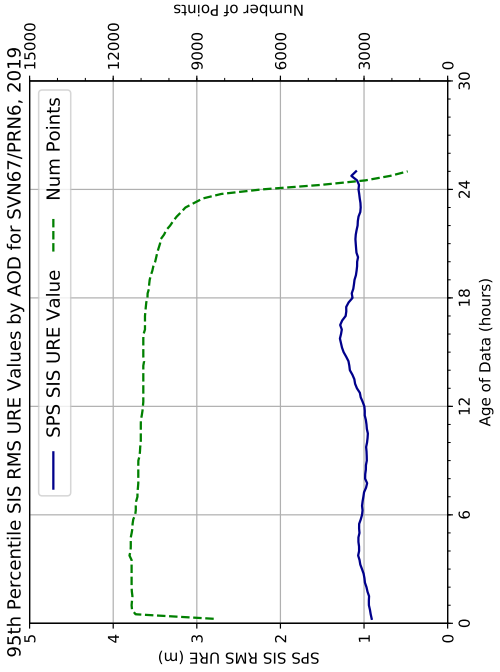
95th Percentile SIS RMS URE Values by AOD for SVN67/PRN6, 2019
SPS SIS URE Value
Num Points
SPS SIS RMS URE (m)
Number of Points
Age of Data (hours)

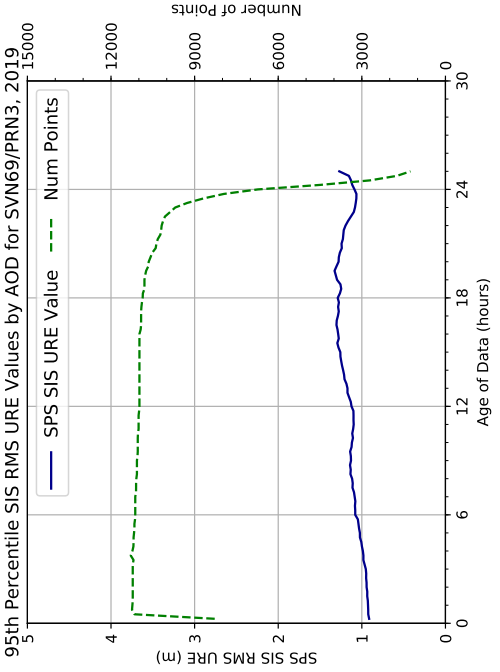
95th Percentile SIS RMS URE Values by AOD for SVN69/PRN3, 2019
SPS SIS URE Value
Num Points
SPS SIS RMS URE (m)
Number of Points
Age of Data (hours)

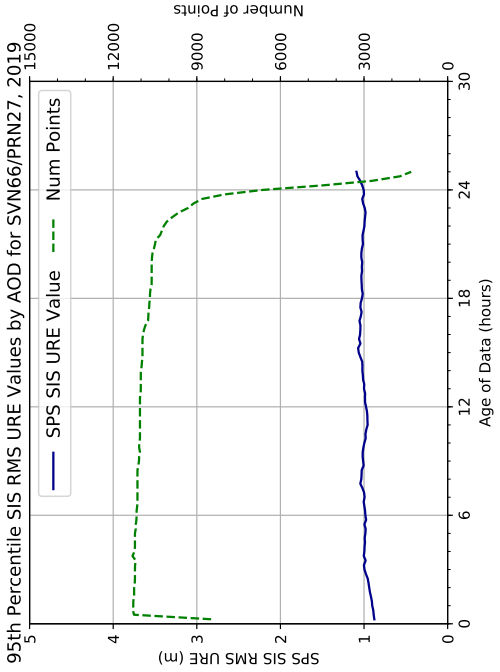
95th Percentile SIS RMS URE Values by AOD for SVN66/PRN27, 2019
SPS SIS URE Value
Num Points
SPS SIS RMS URE (m)
Number of Points
Age of Data (hours)

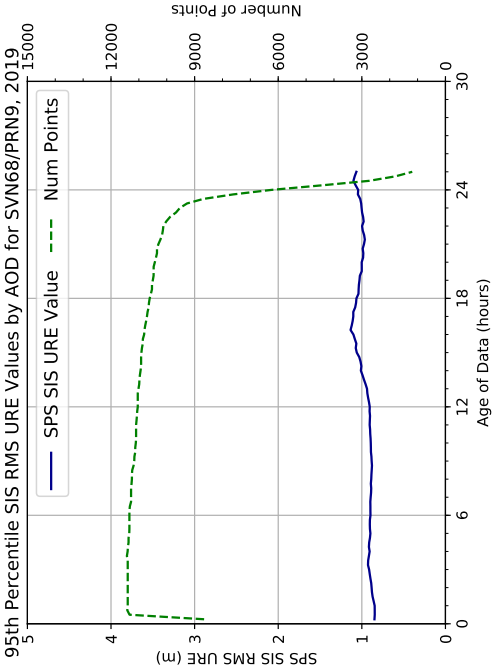
95th Percentile SIS RMS URE Values by AOD for SVN68/PRN9, 2019
SPS SIS URE Value
Num Points
SPS SIS RMS URE (m)
Number of Points
Age of Data (hours)

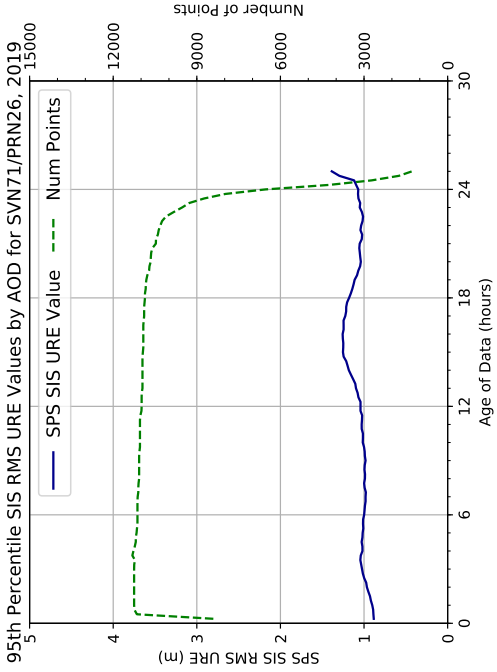
95th Percentile SIS RMS URE Values by AOD for SVN71/PRN26, 2019
SPS SIS URE Value
Num Points
SPS SIS RMS URE (m)
Number of Points
Age of Data (hours)

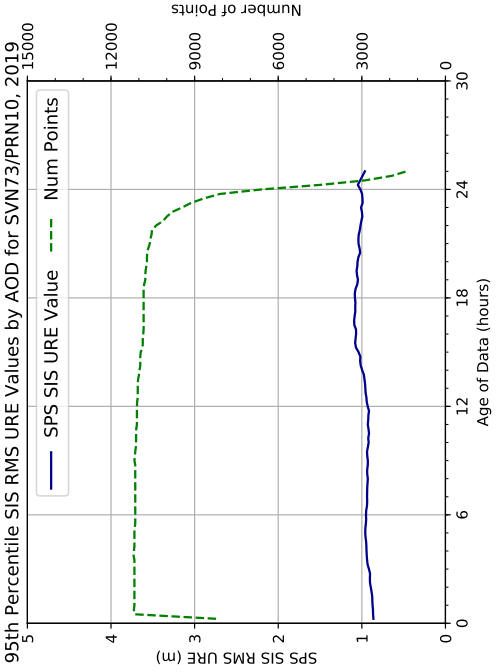
95th Percentile SIS RMS URE Values by AOD for SVN73/PRN10, 2019
SPS SIS URE Value
Num Points
SPS SIS RMS URE (m)
Number of Points
Age of Data (hours)

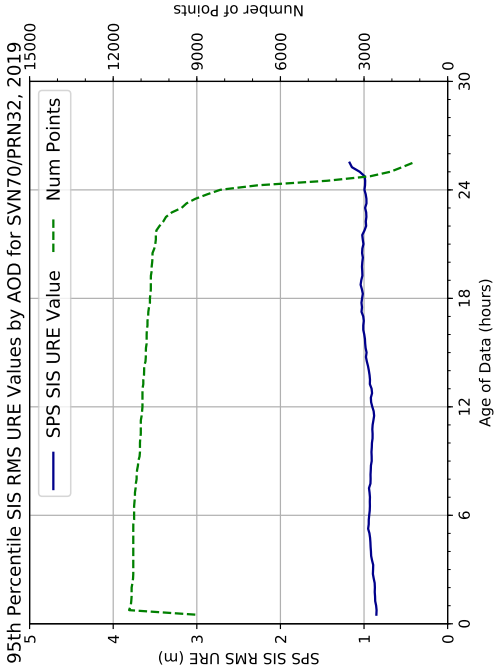
95th Percentile SIS RMS URE Values by AOD for SVN70/PRN32, 2019
SPS SIS URE Value
Num Points
SPS SIS RMS URE (m)
Number of Points
Age of Data (hours)

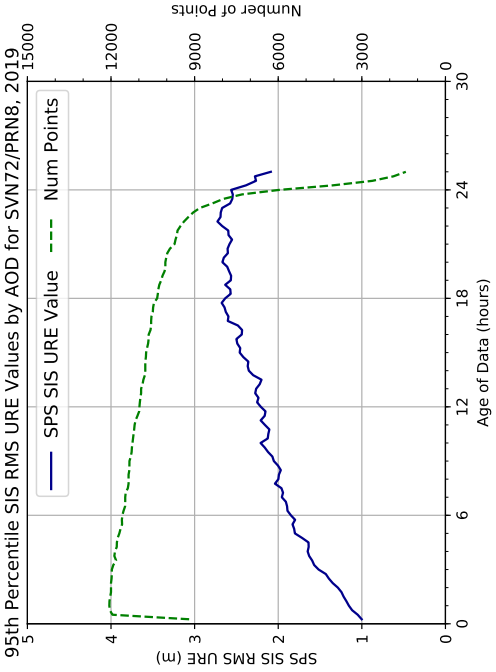
95th Percentile SIS RMS URE Values by AOD for SVN72/PRN8, 2019
SPS SIS URE Value
Num Points
SPS SIS RMS URE (m)
Number of Points
Age of Data (hours)

Appendix B

Analysis Details

B.1 URE Methodology

User range error (URE) represents the accuracy of the broadcast navigation message. There are a number of error sources that affect the URE, including errors in broadcast ephemeris and timing.

This report provides two methods for URE analysis. The first method (Section B.1.2) uses separate statistical processes over space and time to arrive at a URE. The second method (Section B.1.3) derives the URE by a single statistical process but is more computationally demanding. Both methods are valid interpretations of the information provided in Appendix A.4.12 of SPSPS08. We perform both methods to confirm the two agree.

B.1.1 Clock and Position Values for Broadcast and Truth

The URE values in this report are derived by comparison of the space vehicle (SV) clock and position representations as computed from the broadcast clock and position (BCP) as transmitted in the GPS legacy navigation (LNAV) message against the SV truth clock and position data (TCP) provided by a precise orbit calculated after the time of interest.

The broadcast LNAV message data used in the calculations were collected by the National Geospatial-Intelligence Agency (NGA) Monitor Station Network (MSN) (Section B.2). The broadcast LNAV messages provide a set of parameters for an equation which can be evaluated at any time for which the parameters are valid. Our process evaluates the parameters at either a 30 s or 5 min cadence (depending on the setup options).

The TCP values are computed from the archived NGA products. The NGA products used in the calculations are the antenna phase center (APC) precise ephemeris (PE) files available from the NGA public website [13]. The NGA product is published in tabular SP3 format, with positions and clocks provided at a 5 min cadence. For 30 s cadence analysis, Lagrange interpolation is sufficient for SV position, using the five points prior to and after the desired epoch; linear interpolation is sufficient for clock values.

B.1.2 95th Percentile Global Average in the SPS PS

The SPSPS08 specifications for URE suggest averaging across the service volume visible to a GPS SV at any specified point in time. The process is illustrated in Figure B.1.

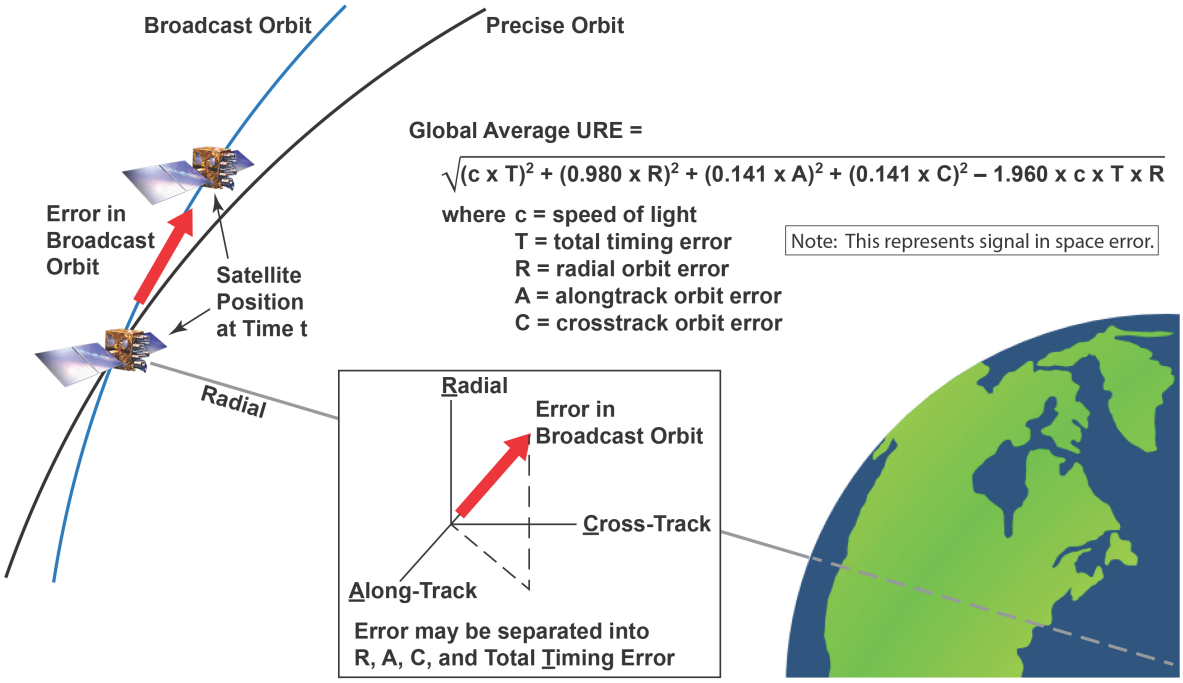

Figure B.1: Global Average URE as defined in SPS PS

The equation shown in Figure B.1 is Equation A-1 of SPSPS08 Section A.4.11. This expression allows the computation of the URE from known errors. Based on the coefficients of this equation, the URE is calculated for a surface corresponding to the WGS 84 radius of the Earth.

For purposes of this report, the Instantaneous RMS SIS URE values were generated at 30 s intervals for all of 2019. The URE was formed by differencing the BCP and TCP to obtain the radial, along-track, cross-track, and time errors at each epoch. These errors were used as inputs to the SPSPS08 Equation A-1.

After the Instantaneous RMS SIS URE values were computed, values for periods when each SV was unhealthy or not broadcasting were discarded. The remaining values were then grouped by monthly period for each SV and sorted; the 95th percentile values within a given month were identified for each SV. This is the basis for Table 3.2. The monthly grouping corresponds closely to the 30 day period suggested in Note 2 of SPSPS08 Section 3.4, while being more intuitive to the reader.

B.1.3 An Alternate Method

The previous method computes an SIS Instantaneous RMS URE (an average over space) for a given SV at a 30 s cadence over a month, then selects a 95^{th} percentile value from that set. That is to say, two different statistical processes are combined.

An alternate method is to compute the SIS Instantaneous URE for a large number of locations at each time point and store those results. For each SV, this is done for a series of time points at a 5 min cadence. At each time point, the components of the URE (i.e., the radial, along-track, cross-track, and clock offset errors) are projected along the line of sight to each location to form a SIS Instantaneous URE value. The collection of SIS Instantaneous URE values at each time point are stored. Once the values for all the time points for a month have been computed, the absolute values of SIS Instantaneous URE values for all time points are gathered together in a monthly set. The 95^{th} percentile value is selected from that set.

This method uses an approximation of an equidistant grid over the portion of the Earth visible to the SV with a spacing of roughly 550 km (5° latitude on the surface of the Earth). Considering those points at or above a 5° elevation angle with respect to the SV, this yields a set of 577 SIS Instantaneous URE values for each SV for each evaluation time. Figure B.2 illustrates this set of grid points for a particular SV-time shown as a projection onto the surface of the Earth.

This was done at a cadence of 5 min for each SV for all of 2019 and all 577 values were stored for all time points. Sets of values corresponding to each month were extracted (approximately 5 million values per SV-month). The absolute values and 95^{th} percentile values for each month were selected as the result for the SV-month. This is the basis for Table 3.3.

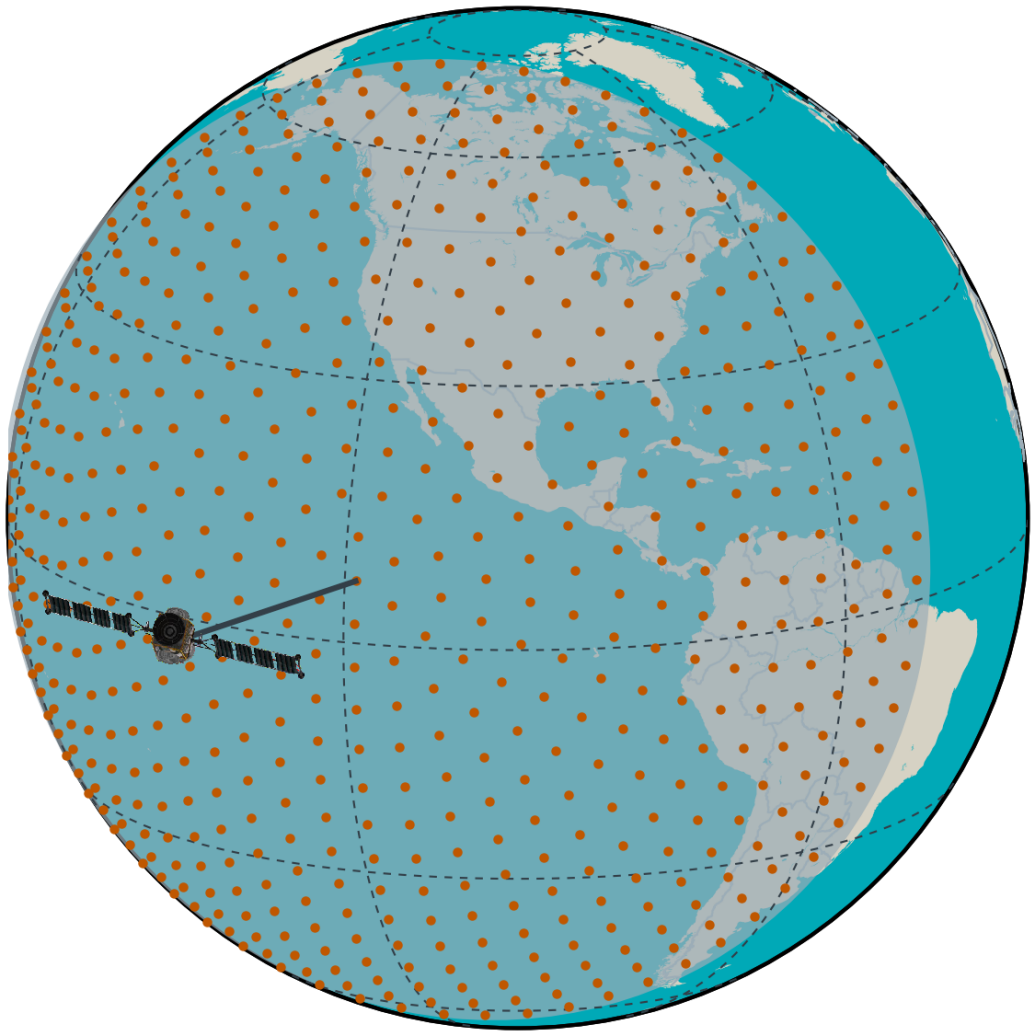

Figure B.2: Illustration of the 577 Point Grid

B.1.4 Limitations of URE Analysis

The methods described in Sections B.1.1-B.1.3 work well when the estimated URE accuracy is below the required thresholds, as it verifies that the system is operating as expected. However, experience has shown that when an actual problem arises, the use of this procedure, without other cross-check mechanisms, can create some issues and may lead to incorrect results. Consider the following two cases.

- The precision with which we can identify the time at which the URE values for an SV exceed a given threshold is limited by the cadence at which the UREs are calculated. We use a cadence of 30 s for the method described in Section B.1.2, which is a satisfactory granularity for nearly all cases. We use a cadence of 5 min for the method described in Section B.1.3, which may require additional examination of the results to determine the 30 s epoch at which a threshold was exceeded.
- When an SV is set unhealthy or cannot be tracked, the PE may provide misleading results. The analyst preparing the PE has several options for handling discontinuities that occur during outages. Therefore, the URE values generated near such events may be incorrect. As a result, it is necessary to avoid accepting UREs into the statistical process under conditions in which the SV could not be tracked or was set unhealthy. This has been done for all the results presented here.

In all cases, when an apparent violation of the URE limits is encountered, we chose to reconcile the analysis described above with the behavior of ORDs formed from the data collected at NGA and IGS sites. Because the observational data used is collected at a 30 s cadence, we obtain a much higher resolution insight into the details of the actual event than we do with the interpolated PE.

B.2 Selection of Broadcast Navigation Message Data

Several of the processes used in deriving the results in this report are dependent on the broadcast navigation message data. In most cases the data needed are the clock, ephemeris, and integrity data (CEI data) contained in subframes 1, 2, and 3 of the GPS LNAV message. A CEI data set is the CEI data broadcast by a given SV at a moment in time. For LNAV, the CEI data set nominally changes every two hours. The position and the health status of the transmitting SV are derived from the CEI data.

The goal in selecting a CEI data for a given SV at a given time of interest is to reproduce what the user would have experienced had they been collecting data from that SV at that time. To accomplish this, the process must have access to a complete time-history of navigation message data and it must properly select specific sets of CEI data from that time-history.

The CEI data sets supporting this analysis were collected from the NGA MSN, which has complete dual-station visibility to all GPS SVs (and generally much better). The MSN data collection process captures the earliest transmission of each unique CEI data set. We investigated any gaps in the CEI data set time-history and filled such gaps if practical. The result is a time-history of the unique CEI data sets transmitted by each SV.

Wherever the analysis process requires CEI data for a given SV at a given time, it selects the CEI data set from the archive that corresponds to what was being transmitted from the SV at that time. During periods in which new data is being transmitted (data set cutovers), the preceding CEI data set is used until the time the new CEI data set had been completely transmitted and available to the user.

It must be recognized that this may be an inexact reproduction of the experience of any given user. Users may experience delays in the receipt of newly transmitted navigation message data due to obstructions, atmospheric issues, or receiver problems. However, our process is deterministic and reproducible.

B.3 AOD Methodology

The AOD was calculated by finding the upload times based on the t_{oe} offsets as defined in IS-GPS-200 Section 20.3.4.5 and then examining the t_{nmct} under the following assumptions:

- A complete set of the subframe 1, 2, and 3 data broadcast by all SVs of interest is available throughout the time period of interest.
- The term t_{nmct} defined in IS-GPS-200 Section 20.3.3.4.4 represents the time of the Kalman state used to derive the corresponding navigation message.

Given these assumptions, the AOD at any point in time can be determined by the following process:

- Working backward from the time of interest to finding the time when the most recent preceding upload was first broadcast
- Finding the AOD offset (AODO) of the associated subframe 2
- Subtracting the AODO from the t_{oe} (as described in IS-GPS-200 20.3.3.4.4) to determine the time of the Kalman state parameters
- Calculating the difference between the time of interest and the Kalman state parameter time

The search for the preceding upload is necessary because the AODO has a limited range and is not sufficient to maintain an accurate count for a complete upload cycle.

The results of this algorithm are generally consistent with the results provided by MCS analysis. The first assumption is fulfilled by the NGA MSN archive. The remaining assumptions were discussed with systems engineers supporting 2SOPS and are believed to be valid.

The exception to this process is PRN 32. PRN 32 does not have the AODO term described due to limitations in the navigation message format. As a result, we cannot directly derive the AOD for PRN 32.

For purposes of this report we examined all upload cutovers through 2019 for all SVs except SVN 70/PRN 32. For each upload cutover we computed the AOD at the time of the upload cutover. We then computed the mean of these samples to determine an average AOD at the time of the upload cutover. There were 11554 samples with an average AOD of 916 sec (about 15 minutes). We assumed this average holds true for SVN 70/PRN 32 and conducted the analysis accordingly.

Note that there is no need for a GPS receiver to calculate AOD. The URE as a function of AOD is one of the metrics evaluated for this report, but is not a concern for a real-time user.

B.4 Position Methodology

Section 2.4.5 of SPSPS08 provides usage assumptions for the SPS PS, and some of the notes in Section 2.4.5 are relevant to the question of position determination. The following is quoted from Section 2.4.5:

The performance standards in Section 3 of this SPS PS do not take into consideration any error source that is not under direct control of the Space Segment or Control Segment. Specifically excluded errors include those due to the effects of:

- *Signal distortions caused by ionospheric and/or tropospheric scintillation*
- *Residual receiver ionospheric delay compensation errors*
- *Residual receiver tropospheric delay compensation errors*
- *Receiver noise (including received signal power and interference power) and resolution*
- *Multipath and receiver multipath mitigation*
- *User antenna effects*
- *Operator (user) error*

In addition, at the beginning of Section 3.8, the SPSPS08 explains that in addition to the error exclusions listed in Section 2.4.5, the following assumptions are made regarding the SPS receiver:

The use of a representative SPS receiver that:

- *is designed in accordance with IS-GPS-200.*
- *is tracking the SPS SIS from all satellites in view above a 5° mask angle... It is assumed the receiver is operating in a nominal noise environment...*
- *accomplishes satellite position and geometric range computations in the most current realization of the WGS 84 Earth-Centered, Earth-Fixed (ECEF) coordinate system.*
- *generates a position and time solution from data broadcast by all satellites in view.*
- *compensates for dynamic Doppler shift effects on nominal SPS ranging signal carrier phase and C/A-code measurements.*
- *processes the health-related information in the SIS and excludes marginal and unhealthy SIS from the position solution.*
- *ensures the use of up-to-date and internally consistent ephemeris and clock data for all satellites it is using in its position solution.*
- *loses track in the event a GPS satellite stops transmitting a trackable SIS.*
- *is operating at a surveyed location (for a time transfer receiver).*

To address these assumptions, we adopted the following approach for computing a set of accuracy statistics:

1. 30 s GPS observations were collected from the NGA GPS monitor station network and a similar set of 31 IGS stations. This decision addressed the following concerns:
   (a) All stations selected collect dual-frequency observations. Therefore the first-order ionospheric effects can be eliminated from the results.
   (b) All stations selected collect weather observations. The program that generates the positions uses the weather data to eliminate first order tropospheric effects.
   (c) The receiver thermal noise will not be eliminated, but both the NGA and IGS stations are equipped with the best available equipment, so effects will be limited.
   (d) Similarly, multipath cannot be eliminated, but both networks use antennas designed for multipath reduction, and station sites were chosen to avoid the introduction of excessive multipath.
   (e) Antenna phase center locations for such stations are precisely surveyed. Therefore, position truth is readily available.
   (f) Despite the similarities, the two networks are processed separately for a variety of reasons.
      i. The NGA GPS network uses receivers capable of tracking the Y-code. As a result, the individual observations have somewhat better SNR than the observations from the IGS stations.
      ii. By contrast, the IGS stations are tracking L1 C/A and L2 codeless, then averaging their observations over 30 s in order to reduce noise on the data.
      iii. The NGA GPS network uses a single receiver which limits the number of receiver-specific traits but leaves open the possibility that a systemic problem could affect all receivers. The IGS network uses a variety of receivers, which is some proof against systemic problems from a single receiver, but requires that the processing address a variety of receiver-specific traits.
      iv. The NGA network is operated and maintained by a single organization. Changes are rare and well-controlled. The IGS network is cooperative in nature. While policies are in place to encourage operational standards, changes in station behavior are not as well-coordinated.
2. Process the data using a comprehensive set of broadcast ephemerides collected as described in Appendix B.2.

3. Process the collected observations using the PRSOLVE program of the ARL:UT-hosted open source GPS Toolkit (GPSTk)[14]. Note:

   (a) PRSOLVE meets the relevant requirements listed above. For example, SV positions are derived in accordance with IS-GPS-200, the elevation mask is configurable, weather data is used to estimate tropospheric effects, and WGS 84 [12] conventions are used. Data from unhealthy SVs were removed from PRSOLVE using an option to exclude specific satellites.

   (b) PRSOLVE is highly configurable. Several of the items in the preceding list of assumptions are configuration parameters to PRSOLVE.

   (c) Any other organization that wishes to reproduce the results should be able to do so. (Both the algorithm and the data are publicly available.)

4. Process the collected 30 s observations in two ways:

   (a) Use all SVs in view without data editing in an autonomous pseudorange solution to generate 30 s position residuals at all sites.

   (b) Use a receiver autonomous integrity monitoring (RAIM) algorithm (another PRSOLVE option) to remove outlier pseudorange measurements from which a "clean" set of 30 s position residuals is generated at all sites. The RAIM algorithm used by PRSOLVE is dependent on several parameters, the two most important of which are the RMS limit on the post-fit residuals (default: 3.0 m) and the number of SVs that can be eliminated in the RAIM process (default: unlimited). This analysis was conducted using the default values.

5. Compute statistics on each set of data independently.

Appendix C

PRN to SVN Mapping for 2019

Throughout the report, SVs have been referred to by both PRN and SVN. The PRN to SVN mapping is time dependent as PRN assignments change. Keeping track of this relationship has become more challenging over the past few years as the number of operational SVs is typically very close to the number of available PRNs. Therefore it is useful to have a summary of the PRN to SVN mapping as a function of time. Figure C.1 presents that mapping for 2019. SVNs on the right vertical axis appear in the order in which they were assigned the PRN values in 2019. Colored bars indicate the range of time each relationship was in effect. Start and end times of relationships are indicated by the dates at the top of the chart.

These data are assembled by ARL:UT from the NANUs and the operational advisories, and confirmed by discussion with The Aerospace Corporation staff supporting 2SOPS.

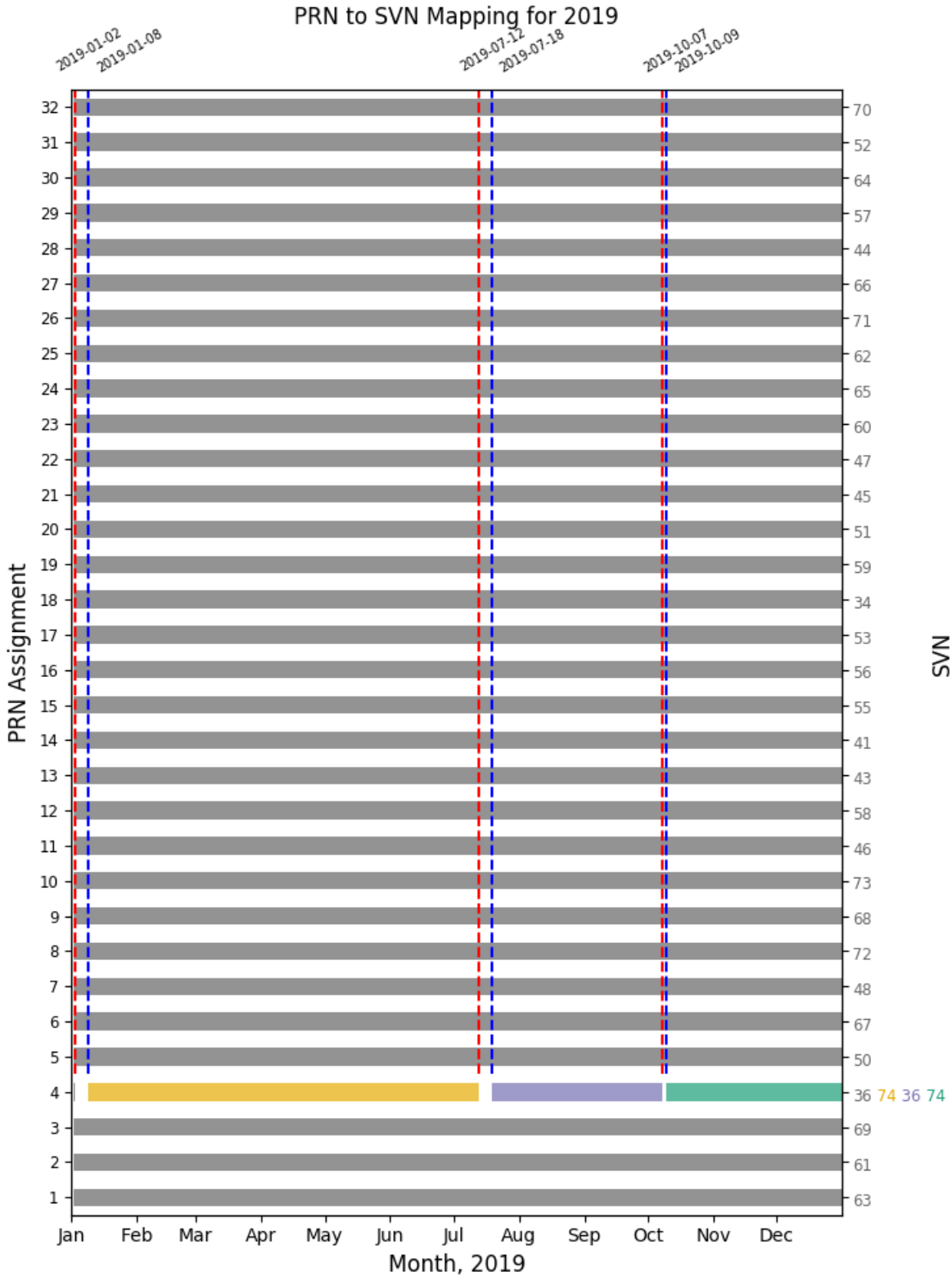

Figure C.1: PRN to SVN Mapping for 2019

Appendix D

NANU Activity in 2019

Several sections in the report make use of NANUs. It is useful to have a time history of the relevant NANUs sorted by SVN. This makes it convenient to determine which NANU(s) should be examined if an anomaly is observed for a particular satellite at a particular time.

Figure D.1 presents a plot of the NANU activity in 2019. Blue bars represent scheduled outages and red bars represent unscheduled outages. Gray bars represent SVs that were decommissioned in 2019. Teal bars represent SVs after launch prior to a NANU declaring initial usability. Yellow bars indicate scheduled outages with notice of less than 48 hours. There were no such events in 2019. NANU numbers are indicated next to each bar. In the event there is more than one NANU for an outage, the last NANU number is displayed.

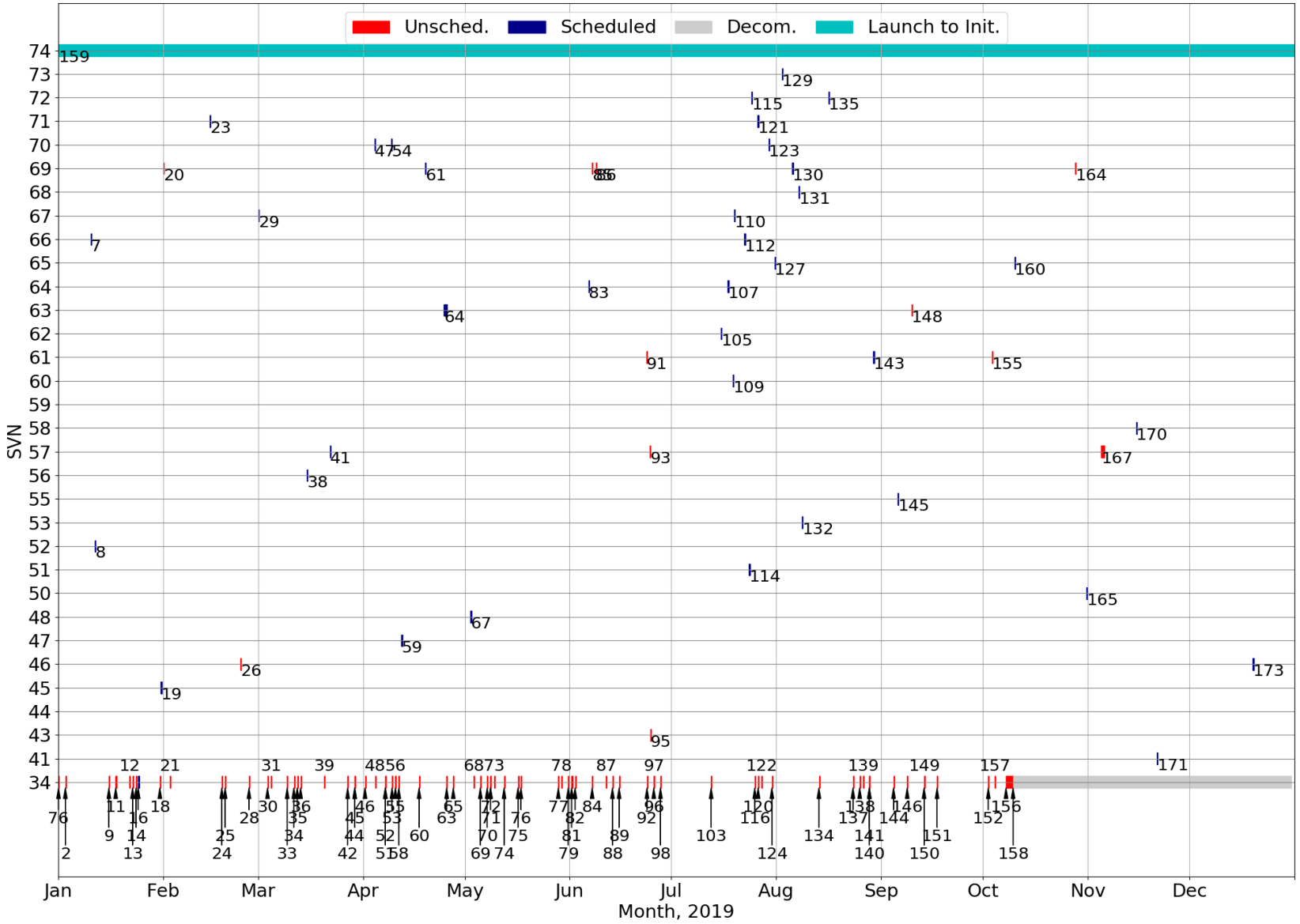

Figure D.1: Plot of NANU Activity for 2019

Appendix E

SVN to Plane-Slot Mapping for 2019

Several assertions are related to the performance of the constellation as defined by the plane-slot arrangement specified in the performance standard. The standard defines six planes lettered A-F. Each plane contains four slots numbered 1-4. For planes B, D, and F, one slot in each plane may be expanded into a pair of locations designated by the addition of the letters F (fore) or A (aft). The possible plane-slot designators appear on the vertical axis of Figure E.1. Evalution of these assertions requires information on the plane-slot occupancy during the year.

The constellation definition located in Section 3.2 of the SPSPS08 that provides the plane-slot definitions is an ideal model in the sense that it assumes all SVs have zero eccentricity and nominal inclination. Slots within a plane are defined by the Groundtrack Equatorial Crossing (GEC) value (also known as the Geographic Longitude of the Ascending Node (GLAN) value). In the real world, discrepancies in orbit insertion lead to a situation in which some SVs are less well-positioned than others. The operators manage the SV locations within the constellation in order to achieve the desired coverage (DOP) as documented in Section 3.6. In some cases, this means assigning plane-slot identifiers to SVs that are fulfilling the responsibility of a particular plane-slot but may not be strictly within the slot as defined by GEC (GLAN). This makes independent verification of plane-slot assignments a challenge.

Information on plane-slot assignment appears in the operational advisory (OA) provided by 2SOPS to the USCG Navigation Center, defined in ICD-GPS-240. However, the format does not permit clarity for expanded slots: there is no provision for "fore/aft" designation. Also, designations for plane/slot contain numbers greater than the number of designated slots. The operators define these "slots of convenience" without fixed meaning for constellation position. As a result, OA interpretation can be challenging.

During 2019, the Navigation Center also posted a graphic depicting the SV locations in terms of plane and slot. This graphic shows the status at a particular epoch.

For the past several years, the plane-slot assignments have been provided to ARL:UT by The Aerospace Corporation analysts supporting 2SOPS. The assignments are provided as a set of daily plane-slot relationships. This information source is not publicly available.

Both of these sources are limited in that only a single satellite may be designated as being present in a slot at a given moment. In fact, as satellites are moved within the constellation, there exists occasional periods when more than one SV may be present within the defined boundaries of a slot. From the user's point of view, the slot should be counted as occupied if a satellite transmitting a healthy signal, or a combination of multiple satellites each transmitting a healthy signal, cover the area visible from the designated primary slot locations.

Figure E.1 provides a graphical illustration of the plane-slot relationships throughout 2019. The contents of Figure E.1 are primarily drawn from the information provided by The Aerospace Corporation and cross-checked against the operational advisories. In the cases where an SV is decommissioned or a new SV is launched, the appropriate NANUs were also checked to confirm dates. The dates when satellites are judged to be present in a slot location are noted only when a change occurs in the plane-slot during the year. This allows the reader to determine when multiple satellites occupied the same slot.

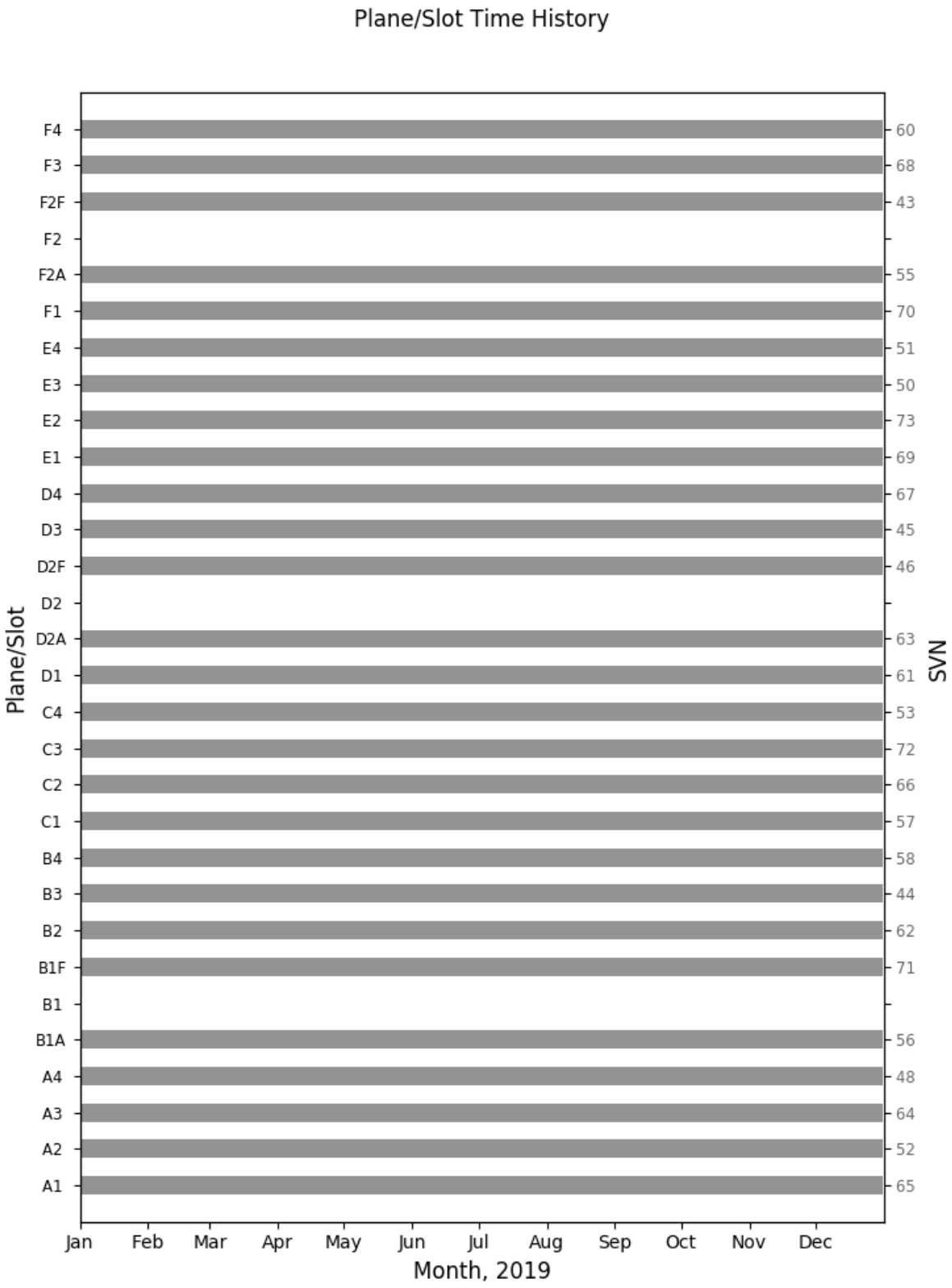

Figure E.1: Time History of Satellite Plane-Slots for 2019

Appendix F

Translation of URE Statistics Among Signals

The URE processes described in Appendix B are based on the data broadcast in subframes 1, 2, and 3 of the navigation message and the NGA PE. Both estimates of the satellite orbits and clock offsets are referenced to the dual-frequency P(Y)-code signal. Therefore, the URE results are directly related to the Precise Positioning Service (PPS) dual-frequency performance. This appendix explains how these results have been interpreted to apply to the SPS assertions.

The PPS dual-frequency results may be mapped to SPS equivalent results by considering the effects of both the group delay differential and the intersignal bias (ISB) between the P(Y)-code and the C/A-code on L1.

F.1 Group Delay Differential

As described in IS-GPS-200 Section 3.3.1.7, the group delay through the satellite transmission hardware is accounted for in the satellite clock offset. However, there remains a group delay differential effect that comes about due to the fact that the signals passing through the different frequency chains experience slightly different delays. An estimate of the group delay differential is transmitted to the users in the navigation message using the group delay differential (T_{GD}) term in subframe 1. Note that T_{GD} is not the group delay differential but the group delay differential scaled to account for the difference between a dual-frequency observation and a single-frequency observation. This is described in IS-GPS-200 Section 20.3.3.3.3.2. This distinction will be relevant below when comparisons to other estimates are discussed.

IS-GPS-200 Section 3.3.1.7.2 states that the random plus non-random variations about the mean of the differential delay shall not exceed 3.0 nsec (95% probability). While this establishes an upper bound on the uncertainty, it does not represent actual performance. The quantization in the T_{GD} term is 0.5 nsec. Therefore, even with perfect estimation, the floor on the uncertainty would be on the order of 0.25 nsec.

If one assumes that T_{GD} is correct and that the user equipment properly applies the correction, then the single-frequency results would be aligned with the dual-frequency results to within that quantization error. However, once the satellite is on orbit it is not possible to directly observe T_{GD}. Instead it must be estimated, and the estimates are subject to a variety of factors including receiver group delay differential effects and ionospheric dispersion. This uncertainty has the effect of inflating the PPS dual-frequency results when these results are interpreted in terms of the PPS single-frequency or SPS services. In fact, because the errors are not directly observable, the best that can be done is to examine the repeatability in the estimate or the agreement between independent estimates and consider these as proxies for the actual uncertainty.

Since 1999, the T_{GD} values have been estimated by Jet Propulsion Laboratory (JPL) and provided to 2SOPS on a quarterly basis. Shortly before this process was instituted there was a study of the proposed estimation process and a comparison of the estimates to those independently developed by two other sources [15]. The day-to-day uncertainty in the JPL estimates appeared to be about 0.3 nsec and the RMS of the differences between the three processes (after removal of a bias) was between 0.2 nsec and 0.7 nsec.

The Center For Orbit Determination Europe (CODE) at the University of Bern estimates the P1-P2 bias [16]. CODE provides a group delay differential estimate for each SV every month. All sets of monthly values exhibit a zero mean, from which it may be inferred the estimation process includes a constraint that the group differential delay is zero when averaged over the constellation.

An ARL:UT comparison of the CODE estimates and the broadcast T_{GD} values (scaled by the group differential delay values) shows a $\sim$5 nsec bias between the estimates. This bias can be removed as we are comparing mean-removed vs non-mean removed values. After the bias across the constellation is removed, the level of agreement between the scaled T_{GD} values and the monthly CODE estimates is between 0.1 nsec and 0.8 nsec RMS.

Considering all these factors, for the purpose of this analysis the uncertainty in each T_{GD} is assumed to be 0.5 nsec RMS.

F.2 Intersignal Bias

The ISB represents the difference between two signals on the same frequency. This bias is due to differences in the signal generation chain coupled with dispersive effects in the transmitter due to the differing signal bandwidths. It is not possible to observe these effects directly. When examining the signal structure at the nanosecond level the chip edges are not instantaneous transitions with perfectly vertical edges but exhibit rise times that vary by signal. Therefore, measuring the biases requires assumptions about the levels at which one decides a transition is in progress. These assumptions will vary between receivers.

There is no estimate of the ISB provided in the GPS legacy navigation message. However, CODE estimates the bias between the L1 P(Y)-code and the L1 C/A-code [16]. An estimate is provided for each SV every month. When this adjustment process was developed, these estimates were examined for each month in 2013. The monthly mean across all SVs is zero, suggesting the estimation process is artificially enforcing a constraint. The RMS of the monthly values across the constellation is 1.2 nsec for each month. Because there is no estimate of the ISB, this RMS value represents an estimate of the error C/A users experience due to the ISB.

F.3 Adjusting PPS Dual-Frequency Results for SPS

The PPS dual-frequency and SPS cases are based on different code-carrier combinations: PPS uses the dual-frequency P(Y)-code, while SPS uses L1 C/A-code. Therefore, the uncertainties in both T_{GD} and ISB must be considered. The PPS dual-frequency URE results are all stated as 95^{th} percentile (2-sigma) values. This means that the RMS errors estimated in Sections F.1 and F.2 must be multiplied by 1.96 (effectively 2, given that the amount of uncertainty in the values).

If it is assumed that these errors are uncorrelated, the total error may be estimated as:

$$\begin{aligned} \text{Total error} &= \sqrt{((2 * \text{T}_{\text{GD}} \text{ uncertainty})^2 + (2 * \text{ISB uncertainty})^2)} \\ &= \sqrt{((2 * 0.5 \text{ nsec})^2 + (2 * 1.2 \text{ nsec})^2)} \\ &= \sqrt{(1 \text{ nsec}^2 + 5.76 \text{ nsec}^2)} \\ &= 2.6 \text{ nsec} \end{aligned} \tag{F.3.1}$$

Converted to equivalent range at the speed of light and given only a single significant digit is justified, the total error is about 0.8 m. This adjustment may then be combined with the PPS dual-frequency result in a root-sum-square manner.

Appendix G

Acronyms and Abbreviations

Table G.1: List of Acronyms and Abbreviations

2SOPS	2nd Space Operations Squadron
AMCS	Alternate Master Control Station
AOD	Age of Data
AODO	Age of Data Offset
ARL:UT	Applied Research Laboratories, The University of Texas at Austin
BCP	Broadcast Clock and Position
CEI	Clock, Ephemeris, and Integrity
CMPS	Civil Monitoring Performance Specification
CODE	Center For Orbit Determination Europe
DECOM	Decommission (NANU Type)
DOP	Dilution of Precision
ECEF	Earth-Centered, Earth-Fixed
FAA	Federal Aviation Administration
FCSTDV	Forecast Delta-V (NANU Type)
FCSTEXTD	Forecast Extension (NANU Type)
FCSTMX	Forecast Maintenance (NANU Type)
FCSTRESCD	Forecast Rescheduled (NANU Type)
FCSTUUFN	Forecast Unusable Until Further Notice (NANU Type)

GEC	Groundtrack Equatorial Crossing
GLAN	Geographic Longitude of the Ascending Node
GNSS	Global Navigation Satellite System
GPS	Global Positioning System
GPSTk	GPS Toolkit
HDOP	Horizontal Dilution Of Precision
IGS	International GNSS Service
IODC	Issue of Data, Clock
IODE	Issue of Data, Ephemeris
ISB	Intersignal Bias
JPL	Jet Propulsion Laboratory
LNAV	Legacy Navigation Message
LSB	Least Significant Bit
MCS	Master Control Station
MSB	Most Significant Bit
MSI	Misleading Signal Information
MSN	Monitor Station Network
NANU	Notice Advisory to Navstar Users
NAV	Navigation Message
NGA	National Geospatial-Intelligence Agency
NMCT	Navigation Message Correction Table
NTE	Not to Exceed
OA	Operational Advisory
ORD	Observed Range Deviation
PDOP	Position Dilution of Precision
PE	Precise Ephemeris
PNT	Position, Navigation, and Timing

PPS	Precise Positioning Service
PRN	Pseudo-Random Noise
PVT	Position, Velocity, and Time
RAIM	Receiver Autonomous Integrity Monitoring
RINEX	Receiver Independent Exchange Format
RMS	Root Mean Square
RSS	Root Sum Square
SINEX	Station Independent Exchange Format
SIS	Signal-in-Space
SMC	Space and Missile Systems Center
SNR	Signal-to-Noise Ratio
SP3	Standard Product 3
SPS	Standard Positioning Service
SPS PS (SPSPS08)	2008 Standard Positioning Service Performance Standard
SV	Space Vehicle
SVN	Space Vehicle Number
TCP	Truth Clock and Position
T_{GD}	Group Delay Differential
UERRE	User-Equivalent Range Rate Error
UNUNOREF	Unusable with No Reference (NANU Type)
UNUSUFN	Unusable Until Further Notice (NANU Type)
URA	User Range Accuracy
URAE	User Range Acceleration Error
URE	User Range Error
URRE	User Range Rate Error
USCG	United States Coast Guard
USNO	U.S. Naval Observatory

USSF	U.S. Space Force
USSF/SMC/ZAC-PNT	Capability Integration Division for PNT Mission Integration
UTC	Coordinated Universal Time
UTCOE	UTC Offset Error
UUTCE	User UTC(USNO) Error
WGS 84	World Geodetic System 1984
ZAOD	Zero Age of Data

Bibliography

[1] U.S. Department of Defense. Standard Positioning Service Performance Standard, 4th Edition. https://www.gps.gov/technical/ps/2008-SPS-performance-standard.pdf, 2008.

[2] U.S. Department of Defense. Navstar GPS Space Segment/Navigation User Interfaces, IS-GPS-200, Revision K. https://www.gps.gov/technical/icwg/IS-GPS-200K.pdf, March 2019.

[3] John M. Dow, R.E. Neilan, and C. Rizos. The International GNSS Service in a changing landscape of Global Navigation Satellite Systems. *Journal of Geodesy*, 2009.

[4] B. Renfro, D. Munton, R. Mach, and R. Taylor. Around the World for 26 Years - A Brief History of the NGA Monitor Station Network. In *Proceedings of the Institute of Navigation International Technical Meeting*, Newport Beach, CA, 2012.

[5] U.S. Coast Guard. GPS Constellation Status. https://www.navcen.uscg.gov/?Do=constellationStatus.

[6] U.S. Naval Observatory. Satellite Information. ftp://tycho.usno.navy.mil/pub/gps/gpstd.txt, January 2017.

[7] U.S. Naval Observatory. Daily GPS-UTC Comparison data. ftp://tycho.usno.navy.mil/pub/gps/gps15m/gps_utc_1day.hist.

[8] W. Gurtner and L. Estey. RINEX: The Receiver Independent Exchange Format Version 2.11, 2006.

[9] U.S. Department of Defense. Navstar GPS Control Segment to User Support Community Interfaces, ICD-GPS-240, Revision C, March 2019.

[10] U.S. Department of Transportation. Global Positiong System (GPS) Civil Monitoring Performance Specification, DOT-VNTSC-FAA-09-08, April 2009.

[11] P. Misra and P. Enge. *Global Positioning System: Signals, Measurements, and Performance*. Ganga-Jamuna Press, revised second edition, 2012.

[12] National Geospatial-Intelligence Agency. Department of Defense World Geodetic System 1984, Its Definition and Relationships With Local Geodetic Systems, Version 1.0.0, NGA.STND.0036_1.0.0_WGS84, July 2014.

[13] National Geospatial-Intelligence Agency. NGA Antenna Phase Center Precise Ephemeris products. `ftp://ftp.nga.mil/pub2/gps/pedata`.

[14] B. Tolman et al. The GPS Toolkit - Open Source GPS Software. In *Proceedings of the 17th International Technical Meeting of the Satellite Division of the Institute of Navigation (ION GNSS 2004)*, Long Beach, CA, 2004.

[15] Colleen H. Yinger, William A. Feess, Ray Di Esposti, The Aerospace Corporation, Andy Chasko, Barbara Cosentino, Dave Syse, Holloman Air Force Base, Brian Wilson, Jet Propulsion Laboratory, Maj. Barbara Wheaton, and SMC/CZUT. GPS Satellite Interfrequency Biases, June 1999.

[16] Center for Orbit Determination Europe. GPS satellite bias estimates for 2013. `ftp://ftp.aiub.unibe.ch/CODE/2013`, 2013.